# Assessment of Dynamic Collapse of Container Ship Subjected to Whipping


## Nwe Nwe Soe


**Master Thesis**

presented in partial fulfillment
of the requirements for the double degree:
“Advanced Master in Naval Architecture” conferred by University of Liege
"Master of Sciences in Applied Mechanics, specialization in Hydrodynamics, Energetics and Propulsion”
conferred by Ecole Centrale de Nantes

developed at University of Rostock, Rostock
in the framework of the

**“EMSHIP”**
**Erasmus Mundus Master Course**
**in “Integrated Advanced Ship Design”**
EMJMD 159652 – Grant Agreement 2015-1687

Supervisor: Dr.-Ing. Thomas Lindemann, University of Rostock.

Internship Supervisor: Mr.Ionel Darie Dipl.-Ing, DNV GL SE, Hamburg.

Reviewer: Prof. Hervé Le Sourne, ICAM.

Rostock, February 2018

*This page was left intentionally blank.*

## DECLARATION OF AUTHORSHIP

I declare that this thesis and the work presented in it are my own and has been generated by me as the result of my own original research.

Where I have consulted the published work of others, this is always clearly attributed.

Where I have quoted from the work of others, the source is always given. With the exception of such quotations, this thesis is entirely my own work.

I have acknowledged all main sources of help.

Where the thesis is based on work done by myself jointly with others, I have made clear exactly what was done by others and what I have contributed myself.

This thesis contains no material that has been submitted previously, in whole or in part, for the award of any other academic degree or diploma.

I cede copyright of the thesis in favour of the University of Rostock

Date: Signature

*This page was left intentionally blank.*

# Table of Contents

# LIST OF FIGURES

# LIST OF TABLES

# Abbreviations

LSTC : Livermore Software Technology Corporation

FEA : Finite Element Analysis

FE : Finite Element

FEM : Finite Element Method

DOF : Degree of Freedom

HGUS : Hull Girder Ultimate Strength

TEU : Twenty-foot Equivalent Unit (standard unit to count containers on board of a ship)

UF : Usage Factor

SR : Strain Rate

# Nomenclature

$\Upsilon_S$ : partial safety factor for the still water bending moment

$M_{SW}$ : permissible still water bending moment

$M_{WV}$ : vertical wave bending moment

$\Upsilon_W$ : partial safety factor for vertical wave bending moment

$\Upsilon_{WH}$ : partial safety factor for the additional whipping contribution

$\Upsilon_{dU}$ : partial safety factor reducing the effectiveness of whipping during collapse

$M_U$ : vertical hull girder ultimate bending capacity from quasi-static loading

$\Upsilon_R$ : partial safety factor for the vertical hull girder ultimate bending capacity

$\Upsilon_M$ : partial safety factor for the vertical hull girder ultimate bending capacity, covering material, geometric and strength prediction uncertainties

$\Upsilon_{DB}$ : partial safety factor for the vertical hull girder ultimate bending capacity, covering the effect of double bottom bending

M : mass matrix

C : damping matrix

K : stiffness matrix

$F_{ext}$ : external forces vector

$F_{int}$ : internal forces vector

u : displacement vector

$\dot{u}$ : velocity vector

ü : acceleration vector

$\delta_{plate}$ : initial deflection of the plate

$\delta_{stiffener}$ : initial deflection of the stiffener

b : stiffener spacing

a : frame spacing

$\varepsilon$ : strain of material

$\dot{\varepsilon}$ : strain rate of material

$l_0$ : original length of geometry

$l$ : length of geometry after deformed

$\sigma'_y$ : dynamic yield stress

$\sigma_y$ , $\sigma_0$ : initial yield stress

C,p : Cowper-Symonds constants

*This page was left intentionally blank.*

# ABSTRACT

Nowadays the demand for larger container ships has increased dramatically as world trade continues to grow and with the marine industry requirement for more energy efficient ships. Springing and whipping phenomena are critical for the design and operation of these large containers. Nowadays the interest on the whipping and springing stress on the hull girder loadings has increased more and more. Based on the MOL Comfort, structural analysis concerned with the dynamic effects on the hull girder loading are especially done. Wave impact loads are important in the structural design and wave impact causes both local and global effects. One of the critical issues on global effects for large container ships is the vibration of the hull girder due to wave impact which leads to excitation of whipping responses of the ship's hull girder. Time domain whipping analyses were carried out for a large container ship by using a computational tool.

In this thesis, the dynamic collapse of the container ship will be performed using the cargo hold model of 14000TEU container ship when the model is subjected to the whipping load and without whipping load. In dynamic analysis, the analysed model is imposed with the material strain rate and we will analyse whether the material strain rate influence the strength capacity. In this thesis, we will also investigate whether an increase in the hull girder capacity strength can be found for the case including whipping load compared to the case without. My thesis is aimed to implement the structure and fulfill some of the requirements for container ship.

*This page was left intentionally blank.*

# 1 INTRODUCTION

## 1.1 Background and Motivation

Nowadays container ships are in an important role for transportation of goods and others. MSC Napoli accident in 2007 and recently incident of MOL Comfort in 2013 made all the classification societies and researchers much attention. In this case, there are many reports of MOL Comfort accident by researchers and the whipping loads are assumed as one of the concerns that lead to the failure of the ship structure of MSC Napoli and MOL Comfort. Recently, classification societies and many researchers consider and focus on the whipping loads on the extreme hull girder of the container ships.

What is “whipping”?

Whipping is usually defined as transient hydro elastic ship structural response due to impulsive loading such as slamming, underwater explosion, etc. One example of the typical whipping event is shown in Figure 1[1]. This figure represents the time evolution of the vertical bending moment, following severe slamming event at the midship of the relatively small container ship. Whipping is especially important in container ships because the container ships have to carry very large capacity of loads and they mostly experience the accidents on the sea due to the extreme unbalance of upward loads and download loads, that lead to structural failure. When the container ships are subjected to whipping mode, the typical period of the typical container ship is in the range from 1 to 2 seconds compared to the wave periods of 8 to 12 seconds. Whipping contribution to the overall vertical bending moment is not only very important but it also last for a relatively long time due to the low structural damping. There are several reasons why the whipping is likely to be more important for the large container ships. Large ship size reduces the natural frequency. High whipping responses are usually driven by large bow flare angles, high ship speed, and a low draught in association with flat bottom. Stern slamming also lead to whipping. Ship whipping may contribute to the structural failure of the hull girders of the ship as the consequence of the wave impact on the hull.
Nowadays the demand for larger container ships has increased dramatically. To fulfil the various aspects like economic and safe voyage, it is quite challenging. Here, we will try to assess the enough strength of the hull girder of the container ships to avoid structural failure when it is subjected to whipping.

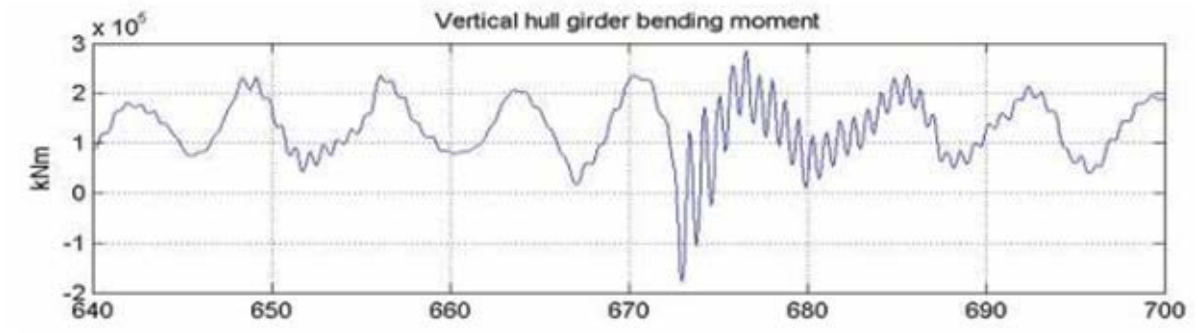


**Figure 1 Typical Whipping Event**
[Figure from [1]]

## 1.2 Objectives

The main objectives of this master thesis are

- to study and access the dynamic collapse force of the container ships induced by whipping load by using the finite element code of LS-DYNA
- to assess the ultimate strength of a container ship structure with and without whipping load
- to investigate the influence of material strain rate using the Cowper-Symonds relations.
- to investigate whether an increase in the hull girder capacity strength can be found for the case including whipping load compared to the case without.

## 1.3 Scope of Thesis

Scope of this thesis is to access "$\Upsilon_{dU}$ ,partial safety factor reducing the effectiveness of whipping during collapse" to check the ultimate hull girder strength of container ship according to DNV GL class guideline code-0153.[4] This parameter will be determined through dynamic collapse analysis.

Ultimate strength check including the effect of whipping and applicable for both, hogging and sagging is described by DNV GL class guideline as below:

$$\Upsilon_S M_{SW} + M_{WV} (\Upsilon_W + (\Upsilon_{WH} - \Upsilon_W) \Upsilon_{dU}) \leq M_U/\Upsilon_R \quad (1)$$

where,

$\Upsilon_S$ = partial safety factor for the still water bending moment

$M_{SW}$ = permissible still water bending moment, in kNm, in still water condition at the hull transverse section considered

$M_{WV}$ = vertical wave bending moment in kNm, in seagoing condition at the hull transverse section considered

$\Upsilon_W$ = partial safety factor for vertical wave bending moment

$\Upsilon_{WH}$ = partial safety factor for the additional whipping contribution and defined as

$$\Upsilon_{WH} \geq \max \{ \Upsilon_W ; \frac{MD}{MWV} \} \geq 1$$

$\Upsilon_{dU}$ = partial safety factor reducing the effectiveness of whipping during collapse (dynamic collapse effect)

$M_U$ = vertical hull girder ultimate bending capacity from quasi-static loading, in kNm, at the hull transverse section considered

$\Upsilon_R$ = partial safety factor for the vertical hull girder ultimate bending capacity ,

$$\Upsilon_R = \Upsilon_M \times \Upsilon_{DB}$$

$\Upsilon_M$ = partial safety factor for the vertical hull girder ultimate bending capacity, covering material, geometric and strength prediction uncertainties,

$\Upsilon_{DB}$ = partial safety factor for the vertical hull girder ultimate bending capacity, covering the effect of double bottom bending,

Here, the safety factor can be defined as follows [4][5]:

$\Upsilon_W$ = 1.2

$\Upsilon_S$ = 1.0

$\Upsilon_{dU}$ = 0.9 [recommended by DNV-GL class guideline]

$\Upsilon_M$ = 1.05

$\Upsilon_{DB}$ = 1.15

## 1.4 Methodology

It is proposed to subject a three cargo holds FE model to low frequent and superimposed low- and high frequent vertical bending loads in time domain:

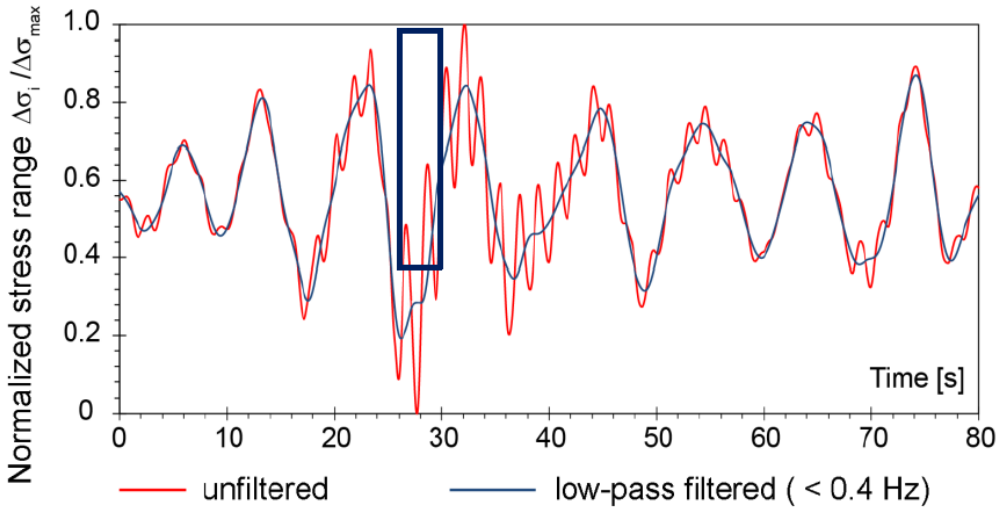


**Figure 2** Normalized Stress Range in Time Domain [6]

Parts of time histories from full-scale measurements could be used for the analysis as highlighted by the rectangle in Figure 2 which shows the enlarge part of the stress history within 30-minute time series measured onboard of the container ship. Full scale measurement can clearly show the magnification of stress history in moderate sea. This guarantees a realistic ratio of wave and vibration frequencies and amplitudes [6].

FE models appropriate for HGUS assessment will be available [7]. Dynamic analysis of the cargo hold model (the midship part) of the container ship will be performed. Structural FE analysis using an explicit solver (LS-DYNA) will be performed. The numerical simulations will take into account material strain rate effects using the Cowper-Symonds expression to solve the dynamic yield stress behaviour. To reach the collapse point in the analyses, it is expected that the load histories need to be scaled iteratively. Therefore, several runs may need to be performed. For a preliminary investigation the local loads (lateral loads, container forces) will be ignored in the numerical simulations.

# 2. LITERATURE REVIEW

## 2.1 History of Container Ship

Nowadays transportation in shipping are widely used because it is the cheapest way and also economic. And container ships are in important role in shipping transportation. We need to make the safe and timely voyage to deliver the cargos. Therefore we have to be design and build container ships more and more to withstand the rough weather and internal and external effect (for instance, whipping, springing, etc). Over the years, the evolution of the container ships are improved and modified as shown in Figure 3.

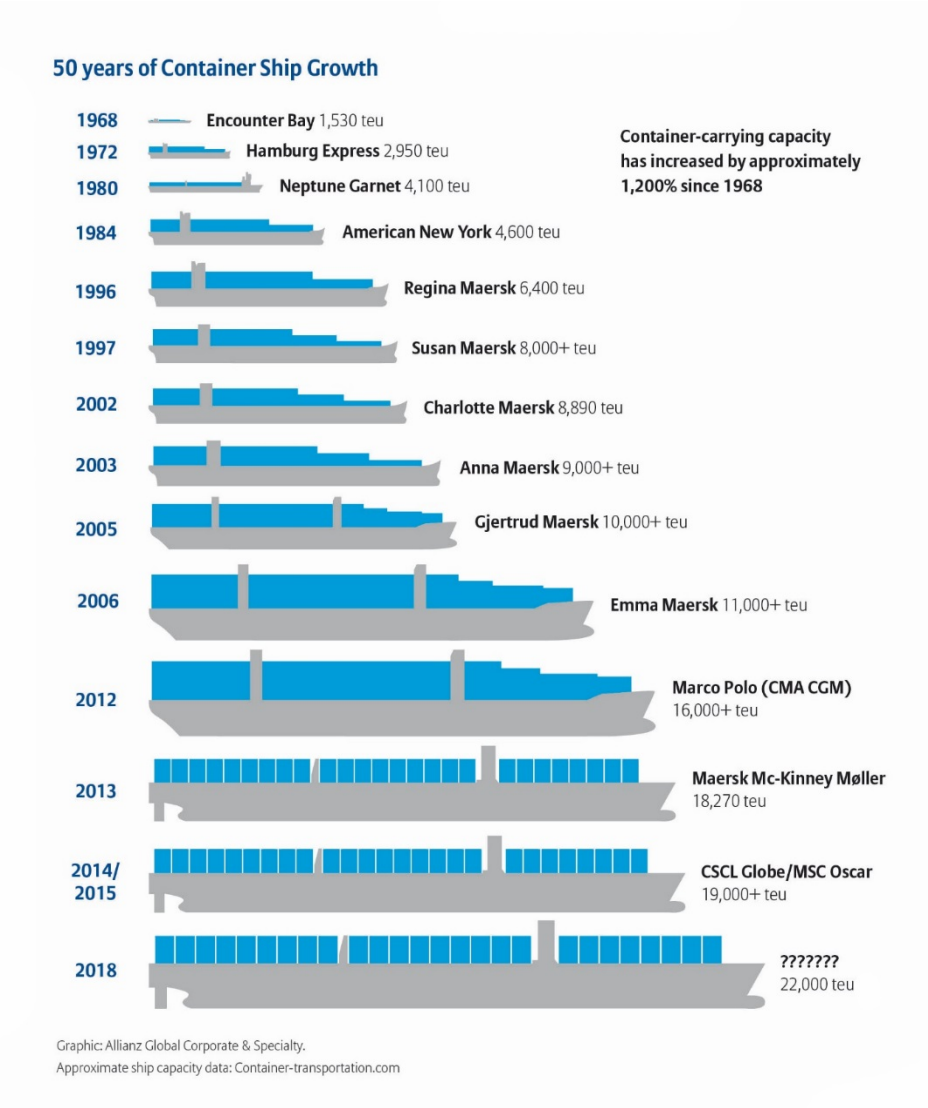


**Figure 3 Evolution of Container Ship over Years**
**[https://www.clydemarinetraining.com/content/50-years-containership-growth]**

## 2.2 Collapse of Container Ships

Container ships become more and more large and typically can carry the large amount of loads. There is the buoyant force that carry and support the loads. The downward loading is evenly distributed along the length of the ship while the upward thrust (buoyancy) is more concentrated around the middle part of the ship because most of the ships encounter with the moderate amount of hogging. The difference between the downward load and the upward thrust of buoyancy of the water creates the bending stress. The ships may break up depending on the amount of this bending stress. Therefore ships are designed to handle these stresses. Here is the recently example of the collapse of the MOL Comfort due to these stresses such a shock as shown in Figure 4.


**Figure 4 MOL Comfort Accident**
[https://goo.gl//velqiC]

On June 2013, 8111 TEU container ship (MOL Comfort) split into two halves during the voyage from Singapore to Jeddash (Saudi Arabia). After this recently accident, many researchers in marine industry become more interested in this case and many researches are done. From the investigations, the two most obvious answers for MOL Comfort accident are a structural flaw in the ship's hull girder and improper loading of container cargoes. The attention of the collapse of hull girder of container ship and importance of the whipping stress on the extreme hull girder loading has significantly increased. An investigation has found that a fractured hull girder caused the break-up and sinking of container ship MOL Comfort in June 2013[8].
The other failure of a container ship's hull structure occurred in 1997 and 2007.In 1997, MSC Carla broke into two parts in the North Atlantic while she was carrying 1600 containers on board. Her forward section sank after five days and the aft part was towed to the port. When

the aft part was investigated, inspection indicated that the manufacturing defects (welding defects) and design defects caused the structural failure. The forward part and aft part of MSC Carla after the accident are as in Figure 5 and Figure 6[9].

**Figure 5 Aft part of Carla**
[http://media.greenpeace.org/archive/MSC-Carla-Accident-27MZIF2SJUKF.html]

**Figure 6 Forward part of Carla**

[http://www.shipstructure.org/case_studies/carla/]

Similar accident of MSC Napoli also occurred in 2007. [The DNV assessment identified the mode of failure on the hull structure of MSC Napoli as a localized plate bulking. The failure mechanism started as elastic buckling of the hull shell plating in the bilge area, which progressed into the bottom, double bottom and up into the ship's side.][10]

**Figure 7 Napoli**
[Figure from [10] ]

Researcher indicated that whipping is also one of major concerns of these ship collapses. We should also take into account this effect to reduce the structural failure of the container ships.

# 3 THEORECTICAL BACKGROUND

## 3.1 Finite Element Theory

### 3.1.1 General Equation

FE Structural analysis LS DYNA software will be performed in this thesis. LS-DYNA is an advanced general-purpose simulation software package developed by the Livermore Software Technology Corporation (LSTC). Its origins and core-competency lie in highly nonlinear transient dynamic finite element analysis (FEA) using explicit time integration. Nonlinearities in FE analysis is considered based on the description of the problem to get the reliable and accurate result. General Equation of the FEM is described as:

$$\boldsymbol{M\ddot{u}\,(t) + C\,\dot{u}\,(t) + Ku(t) = F_{ext}\,(t)} \qquad (2)$$

Here,

M = Mass Matrix,

C = Damping Matrix,

K = Stiffness Matrix,

$F_{ext}$ =External Forces Vector,

u = Displacement Vector,
$\dot{u}$ = Velocity Vector,
$\ddot{u}$ = Acceleration Vector

The above Equation can be applied for explicit and implicit methods. Solution of each step requires the iterations to establish the equilibrium within a certain tolerance in implicit method while no iterations is required in explicit method as the nodal accelerations are solved directly. Explicit method is computationally fast but conditionally stable. Implicit method is unconditionally stable independent of time step size. In this thesis, explicit method will be performed taking account the material strain rate effects. Explicit analysis handles nonlinearities with relative ease as compared to implicit analysis. This would include treatment of contact and material nonlinearities. Explicit method is mainly used when dynamic analyses are intensive and high level of non-linearity, friction and rupture processes are taking part in ship collision.

### 3.1.2 Implicit and Explicit Scheme of LS-DYNA (FEM)

LS-DYNA is one of the finite element codes for analysing the large deformation of the static and dynamic response of the structures coupled to fluids. In static analysis, there is no effect of mass and inertia while mass (inertia) and damping are important in dynamic analysis. Static analysis can be done using implicit solver code of LS-DYNA and explicit dynamics analysis can be done using the explicit solver or implicit solver.

In Implicit Analysis,

Solution of each step require iterations to reach the equilibrium within a certain tolerance. Memory is important in this analysis because the stiffness matrix requires lots of memory as shown in the below equation:

$$\boldsymbol{K\,u(t) = F_{ext}(t) - F_{int}(t)} \tag{3}$$

Where,

K = Stiffness Matrix,

u = Displacement Vector,

$F_{ext}$ =External Forces Vector,

$F_{int}$ =Internal Forces Vector.

In this solver, firstly compute mass and the internal and external forces and then from these forces, get the new displacement and loop the process until the convergence occurs.

In Explicit Analysis,

This type of analysis is applied to determine the dynamic response of a structure due to whipping or impact or rapidly changing time-dependent loads. In an explicit dynamics analysis, the time step is constrained to maintain the stability and consistency and time is important. Explicit scheme can be described as below:

$$\boldsymbol{M\,\ddot{u}\,(t) = F_{ext}(t) - F_{int}(t) - C\,\dot{u}\,(t)} \tag{4}$$

Here,

M = Mass Matrix,

ü = Acceleration Vector,

$F_{ext}$ =External Forces Vector,

$F_{int}$ =Internal Forces Vector,

C = Damping Matrix,

u̇ = Velocity Vector

Time integration Loop of the simulation spiral in LS-DYNA can be described as in Figure 8.

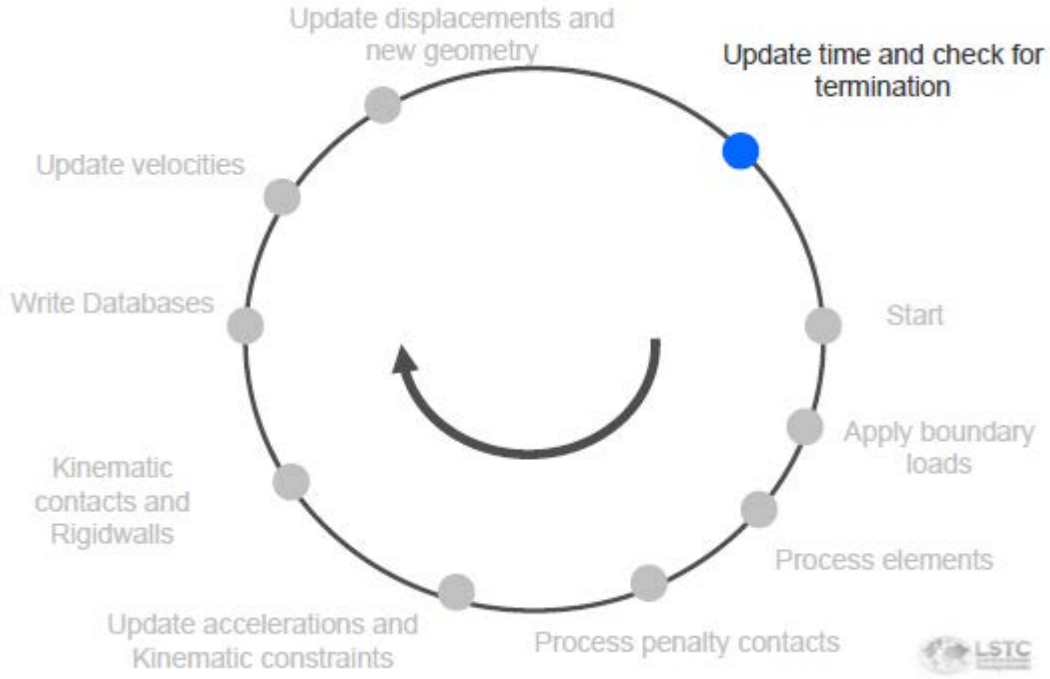


**Figure 8 Time Integration Loop**

[Figure from [11]]

The benefit of using LS-DYNA LSTC

- Conduct sophisticated explicit dynamic analysis with easy and high fidelity
- Have access to the material library that offers constitutive material models of virtually all materials that may need to be modelled with an explicit solver

## 3.2 Dynamic Collapse Analysis

### 3.2.1 General

**Initial Imperfection**

It is generally introduced in the model for post buckling. Initial Imperfection has the significant influence on the case of buckling of the ship structure. In our case, we will consider only geometric initial imperfection. And there are many ways to consider and define the imperfection. Here, we will impose initial imperfection to our model by using mathematical equations defined by DNV GL. And the maximum amplitude of the imperfection of the plate and stiffeners can be expressed as follows:

$$\delta_{plate} = \frac{b}{200}$$

$$\delta_{stiff:web} = \frac{a}{1000}$$

where,

b = stiffener spacing or unsupported length of patch in Y direction, “m”.
a = frame spacing or unsupported length of patch in X direction, “m”.

**Strain Rate**

Strain rate is the change in strain of material with respect to time and can be expressed as follow:

$$\dot{\varepsilon} = \frac{d\varepsilon}{dt} = \frac{d(l-lo)}{dt\ .\ lo} \tag{5}$$

Where,
ε =strain, and defined as follow:

$$\varepsilon = \frac{l-lo}{lo} \tag{6}$$

$l$ - $l_o$ = change in length
$l_o$ = original length of material geometry

Each type of ship has inherent structural design characteristics which affect the strain rate experience by the hull strain.
The yield stress of steel is effected directly by the rate of straining. The greater the speed of straining, the higher the yield stress tends to become until the limit when the ultimate load is reached without yielding.
A wide range strain rate of the material may be experienced when the materials were subjected to the dynamic loads such as whipping or high velocity impact, ect. The dynamic and static material properties may be different depending on the strain effect, temperature and pressure. Therefore, when we consider the collapse of the material, the strain, strain rate, temperature and pressure are primarily important. The material plastic strain rate is the key parameter to

assess the dynamic collapse effect of the ship's structure and to predict accurately the effect of dynamic collapse. Tensile test are normally performed to obtain the plastic behavior of a material. From the literature review, carbon steel is more sensitive to the high strain rates then the other materials. In carbon steel, mild steel is more sensitive than the high tensile steel. The dynamic material properties of steels have a highly non-linear behavior. And the dynamic sensitivity of the material is introduced by using Cowper-Symonds equation as below :

$$\sigma' = \sigma_y \left[1 + \left(\frac{\dot{\varepsilon}}{C}\right)^{\frac{1}{p}}\right] \quad (7)$$

$\sigma'_y$ = dynamic yield stress,
$\sigma_y$ = initial yield stress,
$\dot{\varepsilon}$ = material strain rate,
C and p = Cowper-Symonds Constants.

For Cowper-Symonds Constants, many researcher made researches and recommended the different values of C and P. Among them, we chose the valves of C and P recommended by the researchers, Paik and Lim.

In the present study, Cowper-Symonds constants for the material strain rate will be applied using the recommendations of the researchers as shown in the below table [15].

| | Value of C | | Value of p | |
|---|---|---|---|---|
| Researchers' Name | Mild steel | High Tensile Steel | Mild steel | High Tensile Steel |
| Paik | 40.4 (≈40) | 3200 | 5 | |
| Lim(2005) | $92000\times\exp(\frac{\sigma o}{364})$-193779 for $\sigma_o$ >271MPa<br>40 for $\sigma_o \leq$271MPa<br>*Here, $\sigma_o$ = initial yield stress of steel* | | 5 | |

**Table 1 Cowper-Symonds Constants**

The Cowper-Symonds dynamic scale factor for the percent increase in yield stress of various materials is shown in Figure 9 [16]:

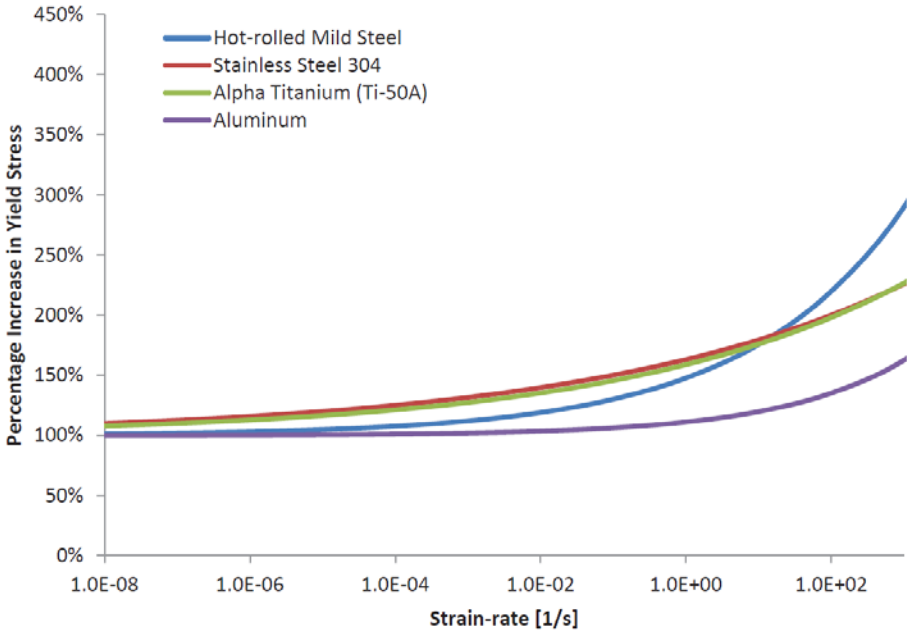


**Figure 9 Behaviour of Material Strain Rate**
[Figure from [16]]

From the above Figure 9, hot-rolled mild is the most sensitive to the strain rate among the other materials while the aluminium is the least sensitive material to the strain rate.

### 3.2.2 Dynamic Analysis (Explicit Solver)

Explicit solver is used to determine the dynamic structural response due to stress wave and time-dependent loads. This types of analysis are applied for many different types of nonlinearities involving the hyper elasticity, plasticity, large strain rates and large deformations, etc. The analysis with high frequency within short time are efficiently simulated with this type of solver. The time step in this analysis is constrained to maintain stability and consistency. The time increment is also dependent on the mesh quality of the element. Time increment in this type of analysis is normally on the order of microsecond and thousands of computational cycles are required to get the required solutions.

In LS-DYNA, all nodes, parts and element have connection each other and we have to define the material properties and curve of the material behaviour and properties. To define the finite element model, we have to create parts and define material using the keywords. The detail information can be seen in the LS-DYNA keyword user manual [17]. Basic knowledge for the organization of the keywords and the example of explicit analysis keyword file of aluminium cube can be described as shown in Figure 10 and Figure 11:

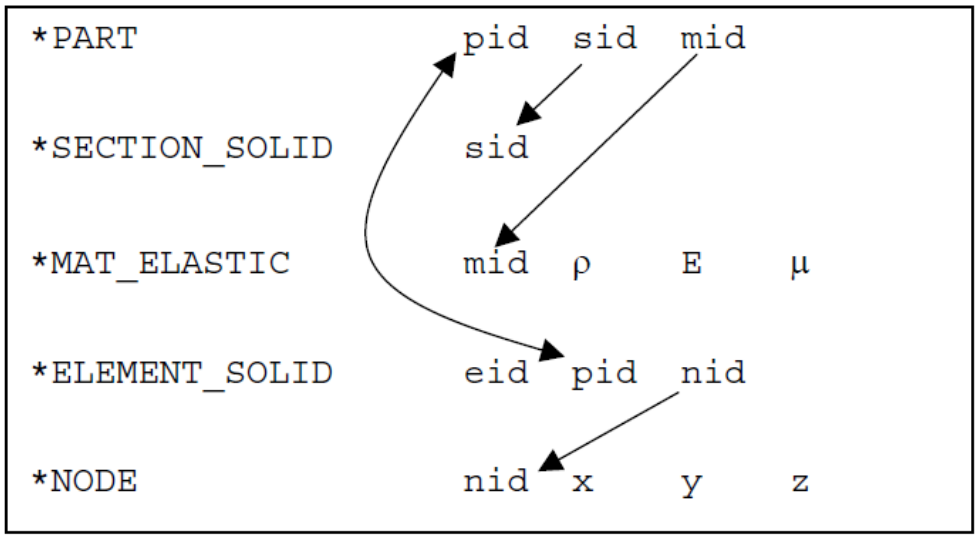


**Figure 10 Organization of Keywords in LS-DYNA [20]**

**Example 4-1 Aluminum cube deformation, explicit method (file: ex01.k)**

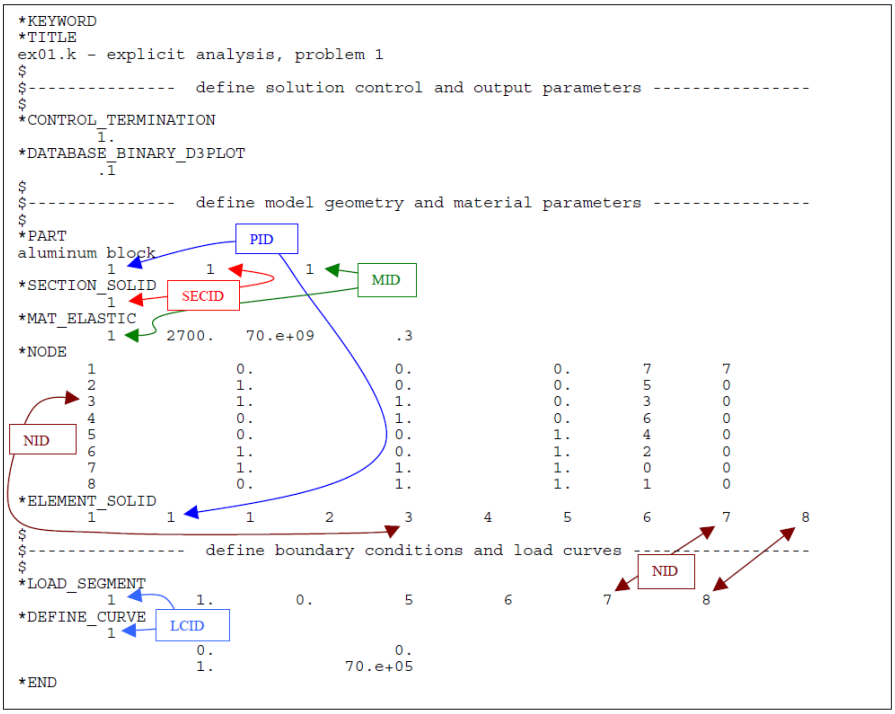


**Figure 11 Example of Keywords File [20]**

# 4 FINITE ELEMENT SIMULATION

## 4.1 General for LS-DYNA Simulation Procedure

For all simulations, LS-DYNA implicit and explicit finite element codes are applied. In this section, we will analyse the dynamic collapse of three different finite element models as follows:

1. Plate with stiffeners (Only stiffened panel)
2. Double bottom of the container ship(14000TEU container ship)
3. Cargo hold of the container ship ( TEU container ship)

All finite element models are available. Simulation procedure is as follow:

Simulation Procedure for

i. Create the desired model from the whole finite element model of cargo hold.
ii. Impose initial and boundary conditions.
iii. Impose Strain Rate for different materials.
And all simulations are looped for all desired simulation time as shown in Figure 12:

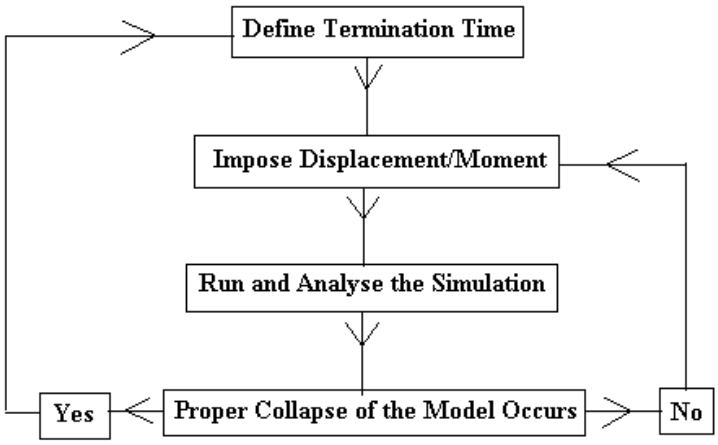


**Figure 12 Simulation Spiral**

(i) Creating the Desired Model

Here, the finite element model of the whole cargo hold and stiffened panel are available. And the finite element model of the double bottom is created by modifying the model of the cargo hold. Then the nodes sets are created to impose the boundary conditions. For all models, materials of modified piecewise linear plasticity are used. The material load curves are also defined for all steels in the models, which has different strength. After that, we define and apply the material strain rate by using the Cowper-Symonds equation.

(ii) & (iii) Initial and Boundary Conditions and Strain Rate

Initial and boundary condition of each model and strain rate will be described in detail in each model simulation.

## 4.2 Simulation Results with Model of Stiffened Panel

The model of the plate with stiffeners is as in Figure 13 and the size of the plate and stiffeners are as follows:

| | |
|---|---|
| Plate: | 3445 x 1800 x14 mm |
| Stiffener: | L 250/10 + 90/15 mm |
| Stiffener spacing: | 860 mm |

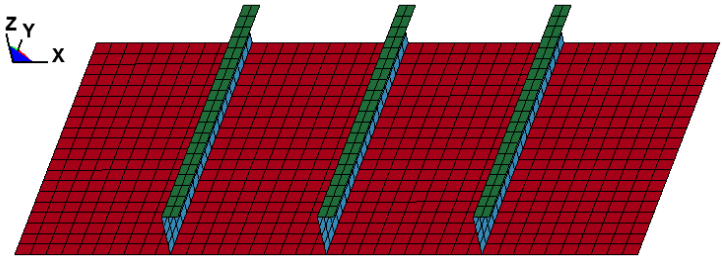


**Figure 13 Model of Stiffened Panel**

Damping should be considered in the dynamic analysis and numerical damping is imposed to avoid huge inertia effect in this stiffened panel. By specifying the structural damping coefficients, we can apply the damping force which are proportional to the displacements (strains). In this case, the model is imposed with 1% of damping (0.01) for all parts (plate, flange and web of stiffeners).

Boundary Condition

- Two ends of the stiffened panel are fixed in **x and z translational** and also in **y and z rotational DOFs** as shown in Figure 14.
- One side of the stiffened panel is fixed in **all six degree of freedom (6 DOFs)** as shown inFigure 15.
- The other side of the panel is imposed with the displacement of **4.5 mm** in y direction and fixed in x and z translational DOFs and also x-rotational DOF as in Figure 16.

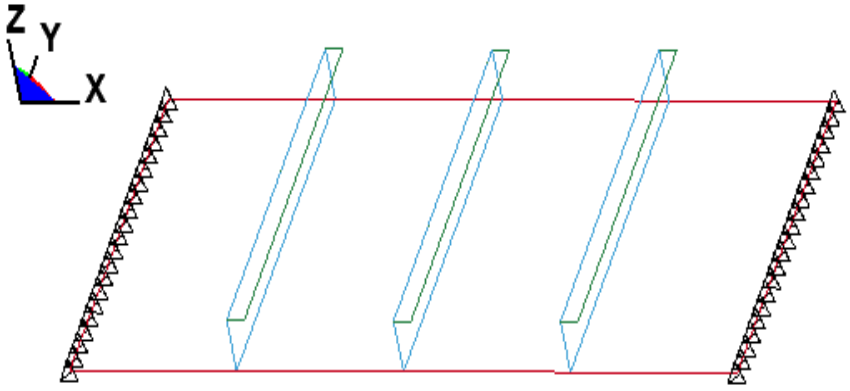


**Figure 14 Application of Symmetric Boundary Condition**

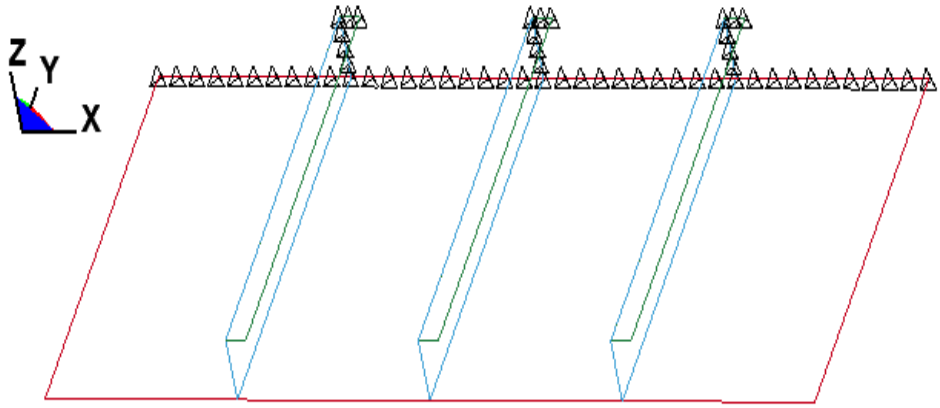


**Figure 15 Application of fixed boundary condition**

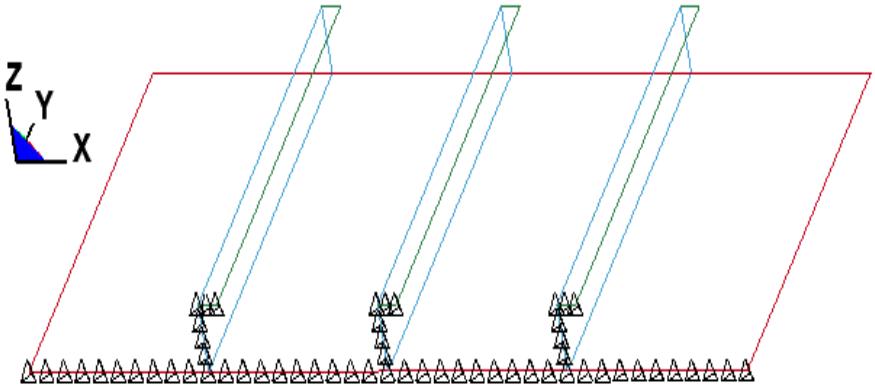


**Figure 16 Stiffened panel imposed with displacement as load**

For this model, we will analyse the collapse of three different conditions for mild steel (245MPa) and high tensile steel (315MPa) as:

1. Static condition (By using the implicit finite element code of LS-DYNA)
2. Dynamic condition without material strain rate imposed by Cowper-Symonds constants (By using the explicit finite element codes of LS-DYNA), and
3. Dynamic condition with the consideration of material strain rate imposed by Cowper-Symonds constants (By using the explicit finite element codes of LS-DYNA).

In the dynamic conditions (explicit analysis), the influence of time (low frequency and high frequency) will be studied by applying the different simulation time (different frequencies). And the collapse force at the design frequency of the container ship will be also determined for all the models. The design frequency of collapse of the container ship is measured by using red rectangle part of the full-scale measurement data as shown in Figure 2. From the full scale measurement, the design frequency of collapse of the container ship subjected to whipping is 0.54Hz (1.85sec).

### 4.2.1 Static Condition

Implicit finite element code of the LS-DYNA is applied to the mode using **the material of mild steel**. Collapse occurs when the resultant force reaches the maximum of 23.26MN and stress reaches the minimum of 262.58MPa and the displacement of 2.27mm. And the strain rate for static condition is zero. The result can be summarized as in Table 2. Variation of the force with respect to the displacement can be seen in Figure 17.

| Items | Value | Unit |
|---|---|---|
| Collapse Force | 23,26 | MN |
| Stress | 262,58 | MPa |
| Collapse displacement | 2,27 | mm |

**Table 2 Summary of Simulation Result**

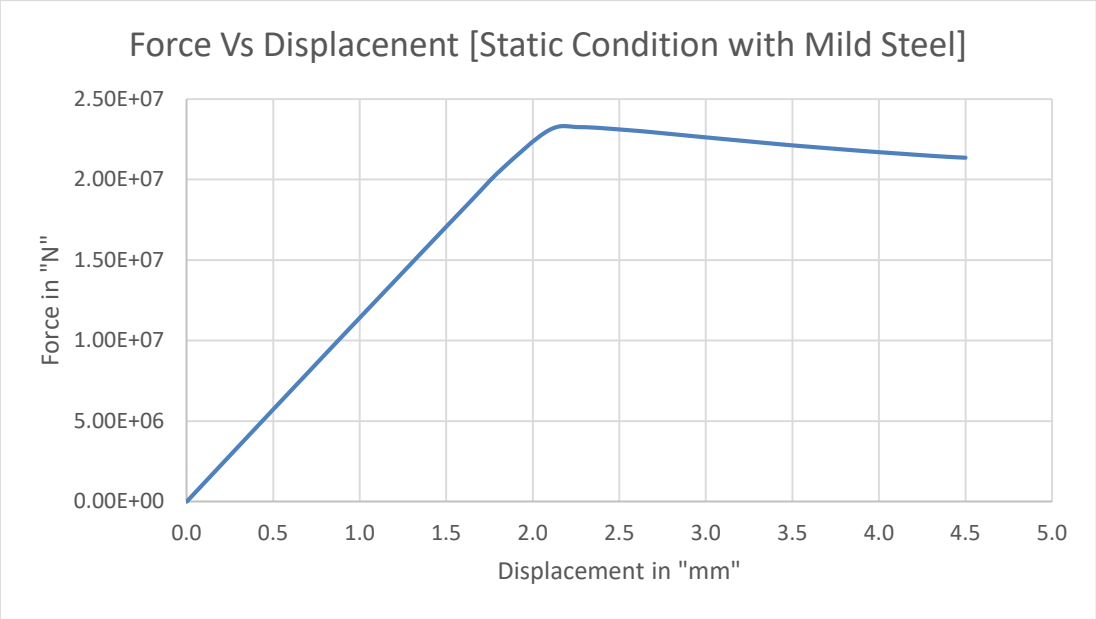


**Figure 17 Collapse Force Curve**

**In case of high tensile steel**, collapse occurs when the resultant force reaches the maximum of 29.38MN and stress reaches the minimum of 331.67MPa and displacement of 2.71mm. And the strain rate for static condition is zero. And the result can be described as in Table 3 The behaviour of the force and displacement is shown in Figure 18.

| Items | Value | Unit |
|---|---|---|
| Collapse Force | 29,38 | MN |
| Stress | 331,67 | MPa |
| Collapse displacement | 2,71 | mm |

**Table 3 Summary of Simulation Result**

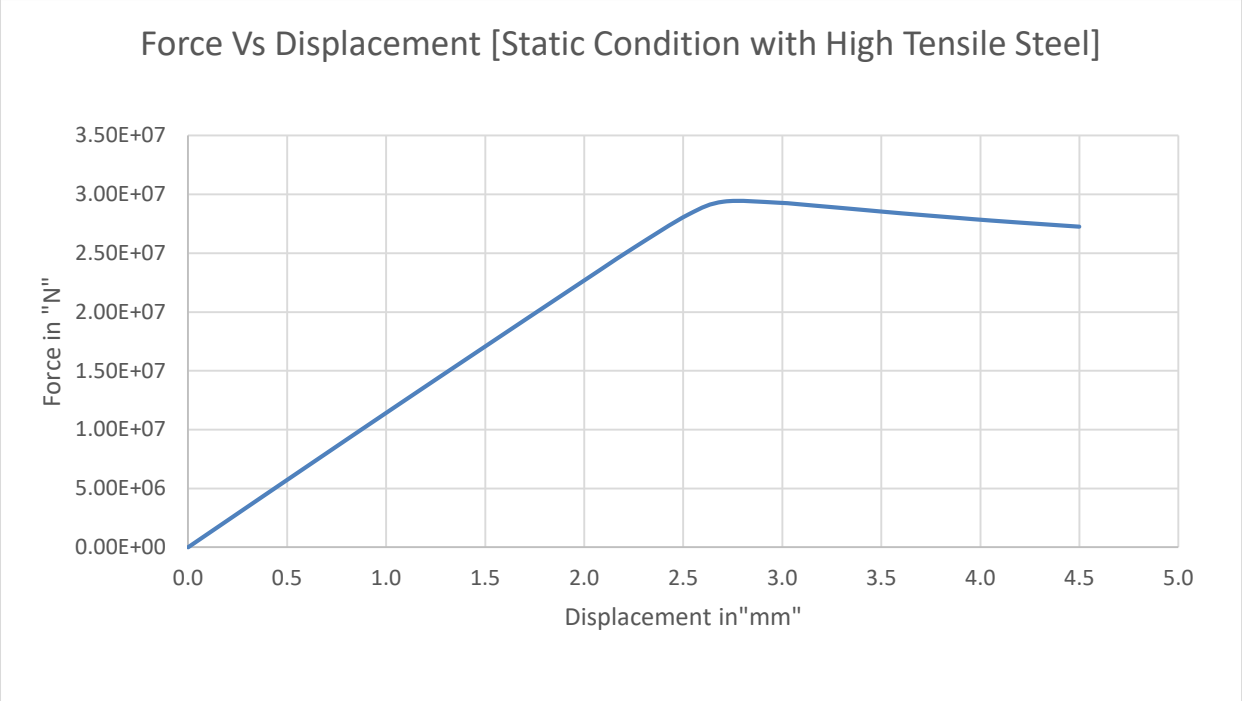


**Figure 18 Collapse Force Curve**

When the static analysis of the stiffened plate model for different materials is concluded, the collapse force of model with height tensile steel is much greater than that of the model with mild steel as shown in Figure 19. It is clear that the higher the material strength of the model, the greater the force that can make the model collapse.

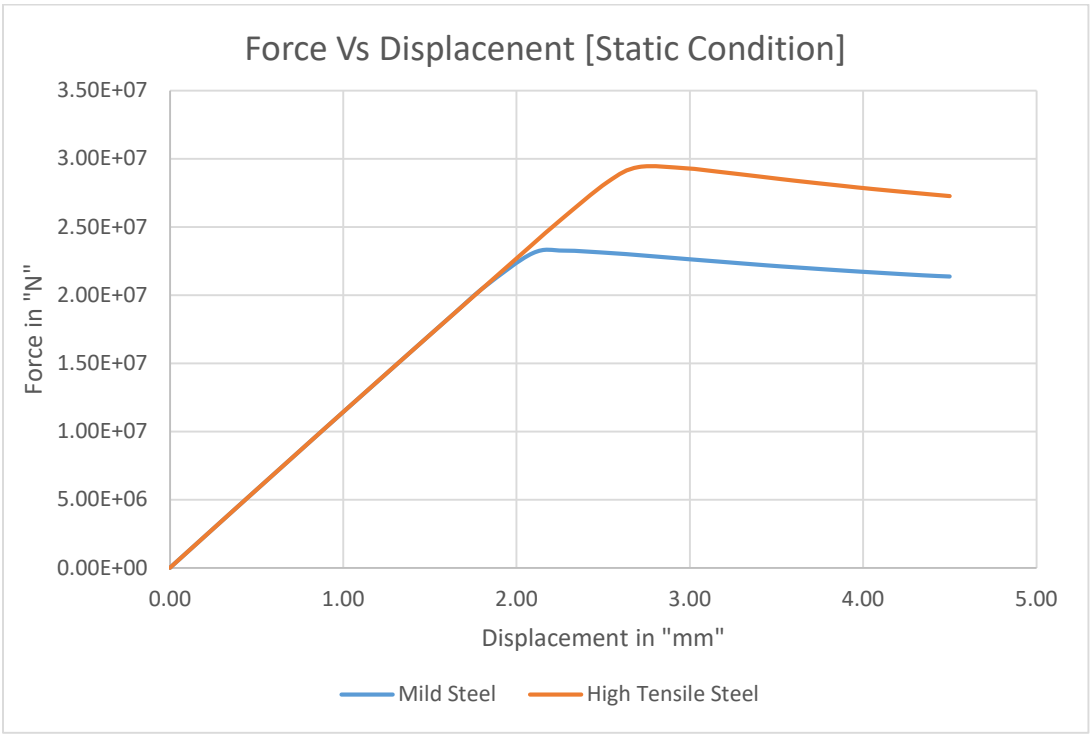


**Figure 19 Collapse Force Curve**

### 4.2.2 Dynamic Condition without Strain Rate Imposed by Cowper-Symonds Constants

For the dynamic analysis, explicit finite element code of LS-DYNA is applied and simulations are done for simulation times of 0.1s, 1s, 2s, 5s,10s and guess the simulation time to get the desired frequency of the collapse mode of the model and loop the simulations until we get the desired collapse mode of the model.

#### 4.2.2.1 Simulation Result of the Stiffened Panel with Mild Steel

From the simulation results, dynamic collapse force, collapse time and collapse displacement of the model are directly read. For readings of stress and strain rate, one element (element number 400) is taken and read the values. Then the collapse force and stress are compare the results of static simulation( force ratio = Dynamic collapse force/ static collapse force).The results can be summarized as shown in Table 4.The behaviour of the collapse force of the model with respect to displacement can be plotted as shown in Figure 20 and the results at design frequency of the collapse mode (0.54Hz) are highlighted in green.

| Simulation Time | Collapse Time[sec] | Collapse Frequency [Hz] | Dynamic Collapse force [MN] | Stress [MPa] | Force Ratio | Stress Ratio | Strain Rate | Displacement [mm] |
|---|---|---|---|---|---|---|---|---|
| 0,1sec | 0,05 | 20,00 | 23,25 | 261 | 1,00 | 1,03 | 1,98E-02 | 2,25 |
| 1sec | 0,50 | 2,00 | 23,24 | 261 | 1,00 | 1,03 | 2,62E-03 | 2,25 |
| 2sec | 1,00 | 1,00 | 23,24 | 261 | 1,00 | 1,03 | 1,25E-03 | 2,25 |
| 3sec | 1,85 | 0,54 | 23,25 | 261 | 1,00 | 1,03 | 7,17E-04 | 2,25 |
| 5sec | 2,55 | 0,39 | 23,24 | 262 | 1,00 | 1,03 | 5,26E-04 | 2,29 |
| 10sec | 5,10 | 0,20 | 23,24 | 262 | 1,00 | 1,03 | 2,59E-04 | 2,29 |

**Table 4 Summary of Simulation Result**

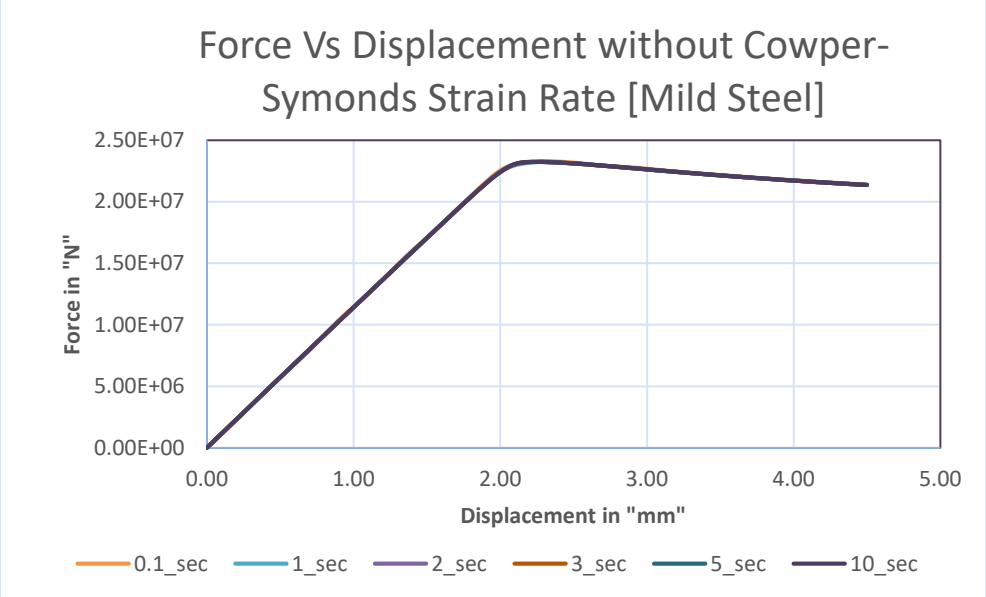


**Figure 20 Collapse Force Curve**

### 4.2.2.2 Simulation Result of the Stiffened Panel with High Tensile Steel

The results are read as explained in sec 4.2.2.1. The simulation result of the stiffened panel with high tensile steel can be summarized as shown in Figure 21 and in Table 5.

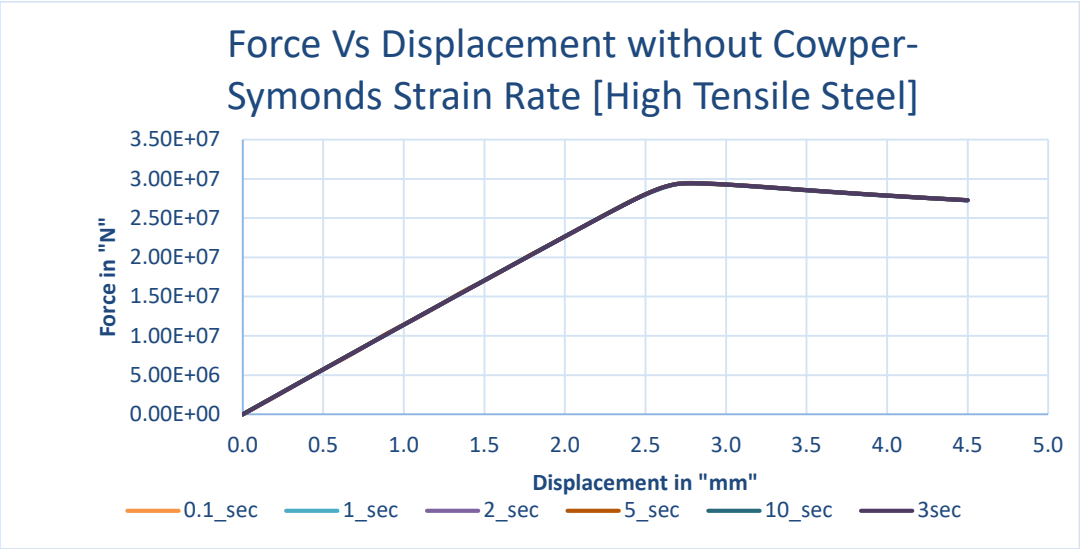


**Figure 21 Collapse Force Curve**

| Simulation Time | Collapse Time[sec] | Collapse Frequency [Hz] | Dynamic Collapse force [MN] | Stress [MPa] | Force Ratio | Stress Ratio | Strain Rate | Displacement [mm] |
|---|---|---|---|---|---|---|---|---|
| 0,1sec | 0,06 | 16,67 | 29,39 | 329,00 | 1,00 | 1,03 | 3,00E-02 | 2,70 |
| 1sec | 0,65 | 1,54 | 29,35 | 330,43 | 1,00 | 1,04 | 2,60E-03 | 2,92 |
| 2sec | 1,25 | 0,80 | 29,42 | 330,43 | 1,00 | 1,04 | 1,29E-03 | 2,81 |
| 3sec | 1,85 | 0,54 | 29,42 | 330,02 | 1,00 | 1,03 | 8,41E-04 | 2,78 |
| 5sec | 3,1 | 0,32 | 29,42 | 330,02 | 1,00 | 1,03 | 5,27E-04 | 2,79 |
| 10sec | 6,25 | 0,16 | 29,42 | 330,45 | 1,00 | 1,04 | 2,53E-04 | 2,81 |

**Table 5 Summary of Simulation Result**

Here we can see obviously that there is no significant change in dynamic force and stress with respect to simulation time if the material strain rate imposed with Cowper-Symonds constants is not considered for the dynamic analysis. It means that for the dynamic analysis, material strain rate is the one of the important parameters that we have to take account in our analysis. For the analysis of the stiffened panel with mild steel, all data that will occur dynamic collapse for different simulation times are summarized in Figure 20and Table 4 and for the model with high tensile steel are in Figure 21 and Table 5. From the full-scale measurements, we can measure the frequency of the model of 1.85 seconds (frequency of 0.54Hz). The detailed

dynamic data that cause the collapse at the frequency of 0.54Hz, are highlighted in green in Table 4 and Table 5 for the realistic collapse mode of the model.
The stiffened panel of mild steel collapses when the resultant force reaches the maximum of 23.25MN and stress reaches the minimum of 261MPa and displacement of 2.25mm while the panel of high tensile steel collapse when the resultant force reaches the maximum of 29.42 MN and stress reaches the minimum of 330MPa and displacement of 2.78 mm. And the overview of the force and displacement for the analysis of the stiffened model with dynamic condition without considering strain rate imposed by Cowper-Symonds constants for different steels can be seen in Figure 22. The collapse force of high tensile steel is 26 percent greater than that of mild steel. Here, we can see that the collapse force increases when the strength of the material become high.

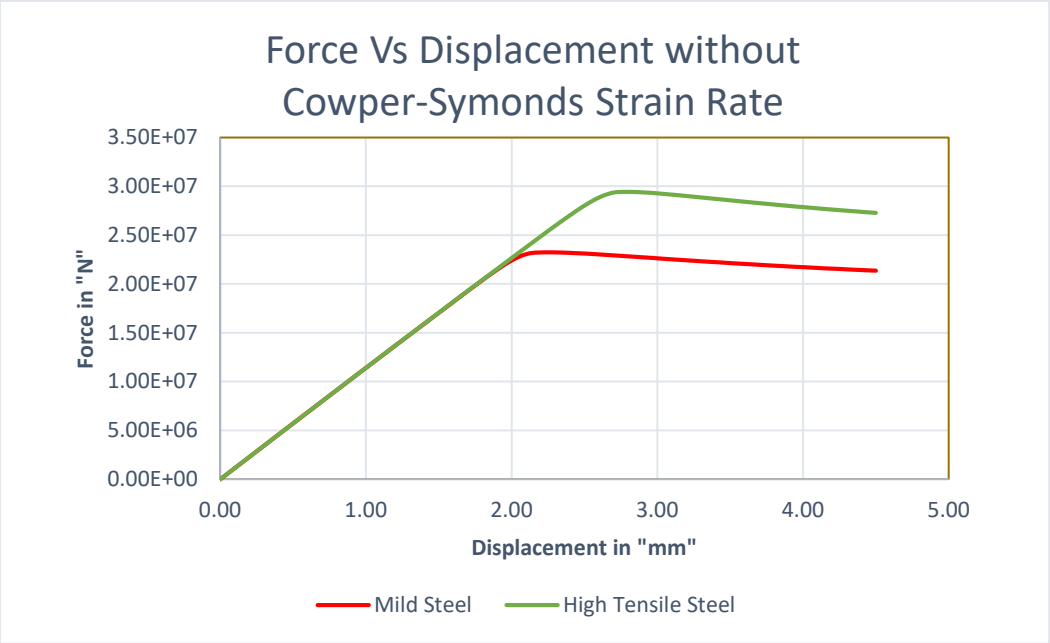


**Figure 22 Collapse Force Curve**

### 4.2.3 Dynamic Condition with Strain Rate imposed with Cowper-Symonds Constants

In this case, material strain rate is taken into account by using the Cowper-Symonds regression equation as described in section 3.2.1. Cowper-Symonds constants for different strengths of steel recommended by the researchers are as shown in Table 6:

| | Value of C | | Value of p | |
|---|---|---|---|---|
| Researchers' Name | Mild steel | High Tensile Steel | Mild steel | High Tensile Steel |
| Lim (2005) | 40 | 24806 | 5 | |
| Paik | 40.4 | 3200 | 5 | |

**Table 6 Cowper-Symonds Constants**

### 4.2.3.1 Simulation Result of the Stiffened Panel with Mild Steel

For Mild Steel, Cowper-Symonds constants recommended by Lim 2005 and Paik are same. By using the Cowper-Symonds constants given by Lim 2005 and Paik (C= 40.4,P=5), dynamic collapse for the panel of mild steel are analysed for different simulation times and dynamic collapse force, collapse time, collapse displacement and strain rate are directly from the FE analysis as explained in sec 4.2.2.1. The results are summarized as shown in Table 7.

.

| Simulation Time | Collapse Time[sec] | Collapse Frequency [Hz] | Dynamic Collapse force [MN] | Stress [MPa] | Force Ratio | Stress Ratio | Strain Rate | Displacement [mm] |
|---|---|---|---|---|---|---|---|---|
| 0,1sec | 0,065 | 15,38 | 30,08 | 336 | 1,29 | 1,33 | 2,46E-02 | 2,92 |
| 1sec | 0,6 | 1,67 | 28,03 | 315 | 1,21 | 1,24 | 2,77E-03 | 2,7 |
| 2sec | 1,25 | 0,80 | 27,58 | 310 | 1,19 | 1,22 | 1,26E-03 | 2,81 |
| 3,1sec | 1,85 | 0,54 | 27,3 | 306 | 1,17 | 1,21 | 8,10E-04 | 2,69 |
| 5sec | 3 | 0,33 | 27,01 | 304 | 1,16 | 1,20 | 5,68E-04 | 2,7 |
| 10sec | 5,9 | 0,17 | 26,63 | 300 | 1,14 | 1,18 | 2,66E-04 | 2,65 |

**Table 7 Summary of Simulation Result**

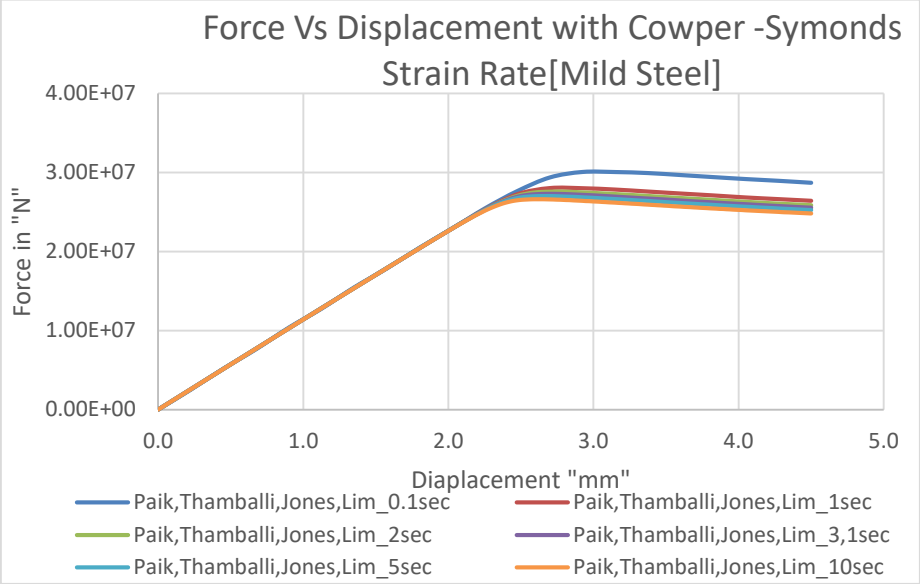


**Figure 23 Collapse Force Curve**

Figure 23 represents the collapse behaviour of the stiffened panel for different simulation times, taking into account the material strain rate impose by Cowper-Symonds constants. When this material strain rate is imposed to the model, we can see clearly that the material strain rate has significant influence on the dynamic yield stress ratio based on the duration times we impose. And we can also clearly see the dynamic effect of the model. If the displacement is imposed to the model to collapse within the very short time, the dynamic collapse force and strain rate increase significantly and we can see the dynamic behaviour of the model. It means the greater the frequency of the model, the higher dynamic yield stress ratio and the strain rate.

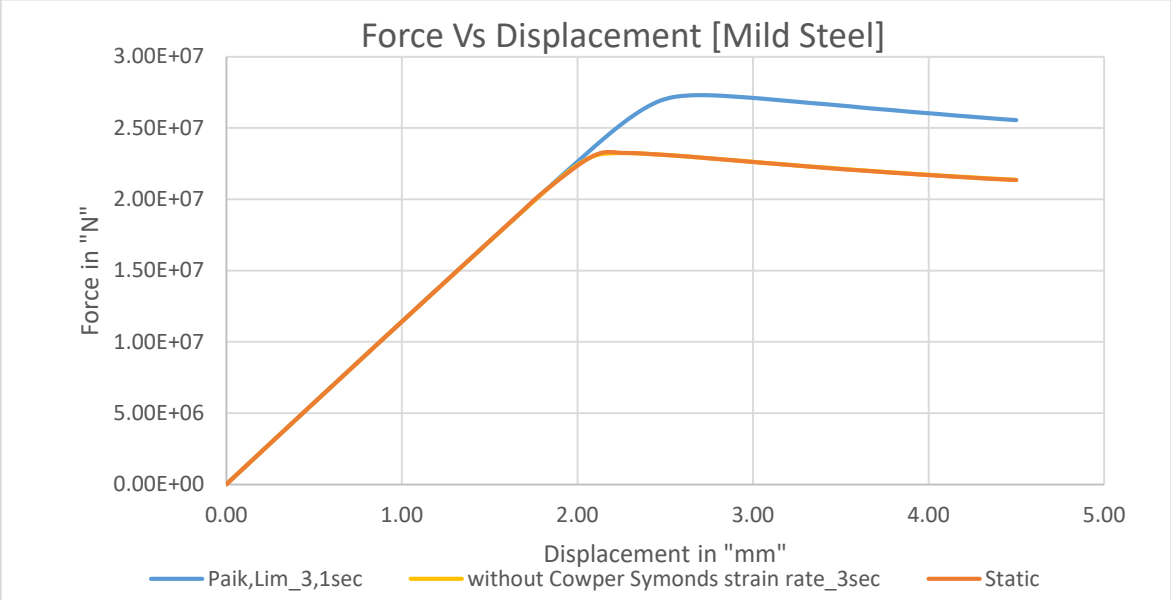


**Figure 24 Collapse Force Curve**

Figure 24 shows the influence of the strain rate on the stiffened panel analysis for the desired collapse mode of frequency of 0.54 Hz. When the model is imposed with the strain rate recommended by the researchers, Paik and Lim, the dynamic collapse force goes up significantly while the case without strain rate is almost same with the static model analysis. It indicates that the strain rate the key parameter in the dynamic analysis. Here, we can see clearly the dynamic and static behaviour of the model.

#### 4.2.3.2 Simulation Result of the Stiffened Panel with High Tensile Steel

For High Tensile Steel,
By using the Cowper-Symonds constants of **Lim 2005**, the model is imposed with **C= 24806, P=5** and performed the desired simulations.
The simulations results can also be summarized in Table 8 and the behaviour of the force with respect to the displacement for all simulation times can be seen in Figure 25.

| Simulation Time | Collapse Time[sec] | Collapse Frequency [Hz] | Dynamic Collapse force [MN] | Stress [MPa] | Force Ratio | Stress Ratio | Strain Rate | Displacement [mm] |
|---|---|---|---|---|---|---|---|---|
| 0,1sec | 0,07 | 14,29 | 31,66 | 355 | 1,08 | 1,11 | 3,75E-02 | 3,15 |
| 1sec | 0,65 | 1,54 | 31,07 | 348 | 1,06 | 1,09 | 2,61E-03 | 2,92 |
| 2sec | 1,3 | 0,77 | 30,9 | 346 | 1,05 | 1,08 | 1,36E-03 | 2,92 |
| 2,8sec | 1,85 | 0,54 | 30,81 | 345 | 1,05 | 1,08 | 9,22E-04 | 2,97 |
| 5sec | 3,25 | 0,31 | 30,7 | 344 | 1,04 | 1,08 | 5,80E-04 | 2,92 |
| 10sec | 6,5 | 0,15 | 30,57 | 343 | 1,04 | 1,07 | 2,57E-04 | 2,9 |

**Table 8 Summary of Simulation Result**

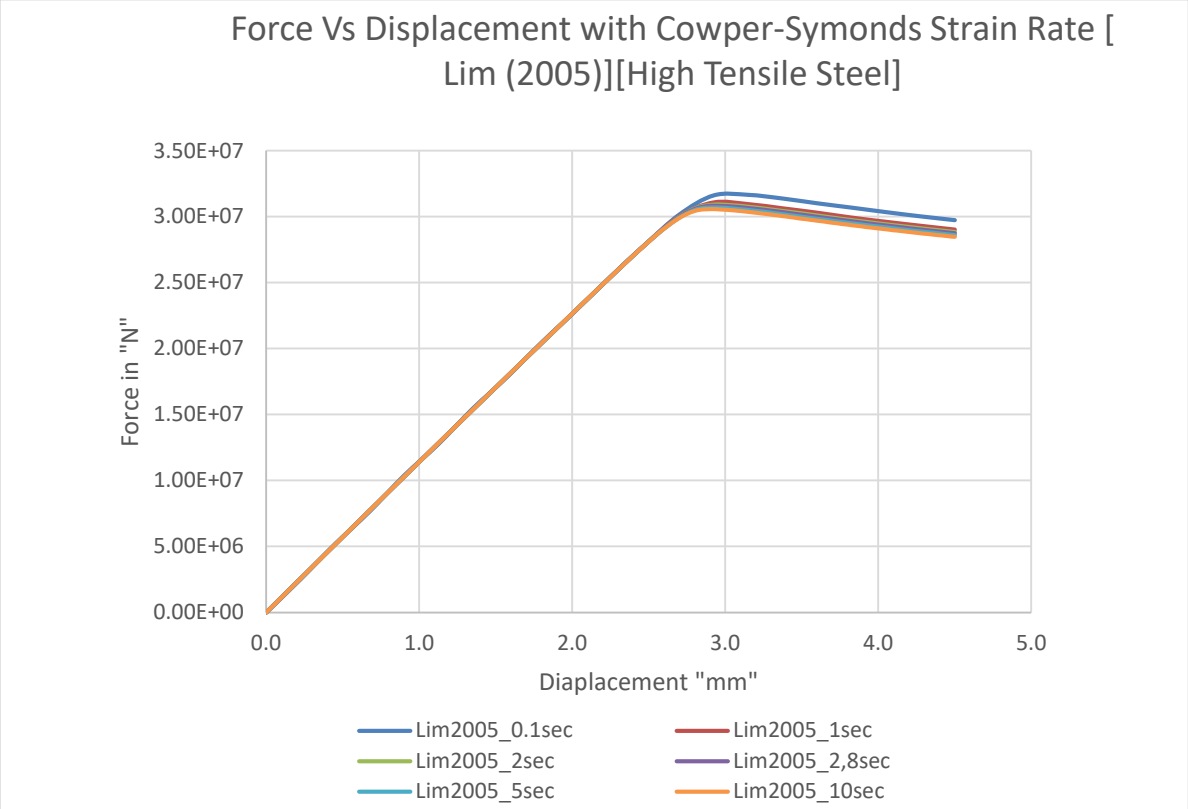


**Figure 25 Collapse Force Curve**

For the Cowper-Symonds constants of Paik,
All simulations are performed by using C= 3200 and P=5 and the result are read similarly as before and can be described as in **Table 9** and **Figure 26**.
.

| Simulation Time | Collapse Time[MN] | Collapse Frequency [Hz] | Dynamic Collapse force [MN] | Stress [MPa] | Force Ratio | Stress Ratio | Strain Rate | Displacement [mm] |
|---|---|---|---|---|---|---|---|---|
| 0,1sec | 0,07 | 14,29 | 33,01 | 369 | 1,12 | 1,16 | 2,66E-02 | 3,15 |
| 1sec | 0,7 | 1,43 | 31,89 | 345,5 | 1,09 | 1,08 | 2,66E-03 | 3,15 |
| 2sec | 1,35 | 0,74 | 31,68 | 343 | 1,08 | 1,07 | 1,32E-03 | 3,04 |
| 2,8sec | 1,85 | 0,54 | 31,55 | 342,2 | 1,07 | 1,07 | 9,45E-04 | 2,97 |
| 5sec | 3,3 | 0,30 | 31,37 | 340,38 | 1,07 | 1,07 | 5,10E-04 | 2,97 |
| 10sec | 6,65 | 0,15 | 31,17 | 338,75 | 1,06 | 1,06 | 2,54E-04 | 2,99 |

**Table 9 Summary of Simulation Result**

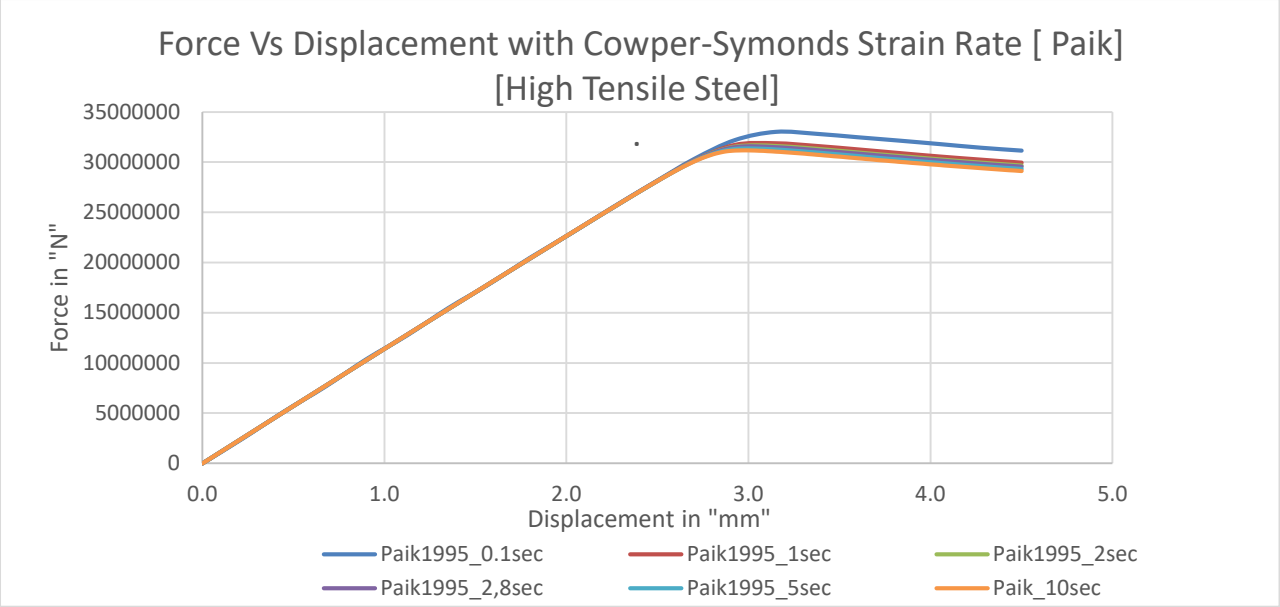


**Figure 26 Collapse Force Curve**

Then, we can summarize the results of all simulations of the model with high tensile steel considering the material strain rate. In Table 8 and Table 9, the results at the design frequency of the model are highlighted in green and the force ratio with respect to the static condition are highlighted in blue and we can see that the force ratio using Paik's recommendation is greater than that using Lim's. When we imposed the displacement to the model within very short time, the force ratio is obviously increased. And the collapse force and displace curves showing for the different simulation times can be described as shown in Figure 25 and Figure 26. And overview of the collapse force and displacement of at the desired frequency of 0.54 Hz is shown in Figure 27.

.

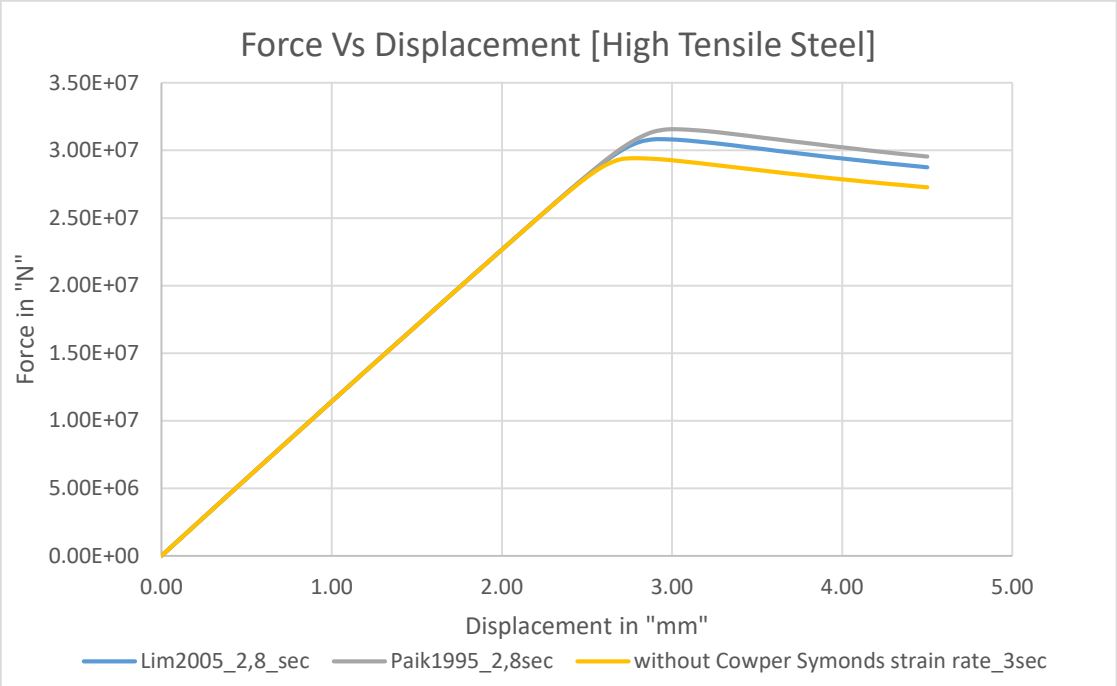


**Figure 27 Collapse Force Curve**

When we overview all analysis of the stiffened panel, Implicit and Explicit finite element analysis are almost same if we not considered the material strain rate imposed with Cowper-Symonds constants in the analysis. It means that time doesn't influence the analysis of the model if we don't consider the strain rate. When we consider the material strain rate in the model, the collapse force increases with respect to the time. When the simulation time decreases (it means that we impose the displacement within the short time), the collapse force increases and the material strain rate also increase. Therefore, we can see obviously that time influences the material strain rate and material strain rate influences the collapse force of the model. Moreover, it is clear that the strain rate is the one of key parameters that we should consider in the dynamic analysis.

## 4.3 Validation of the Strain Rate

Many researchers have verified that small change in strain rate caused relatively large changes of the dynamic yield stress ratio. For the material strain rate behaviour of ship's shell structure, some researchers for instant Paik, Lim (2005) have suggested to use the Cowper-Symonds constants. Figure 28 shows the behaviour of the strain rate and the dynamic yield stress ratio for mild steel and high tensile steel and this is from many experimental results. Here, we can see clearly mild steel is more sensitive than the high tensile steel.

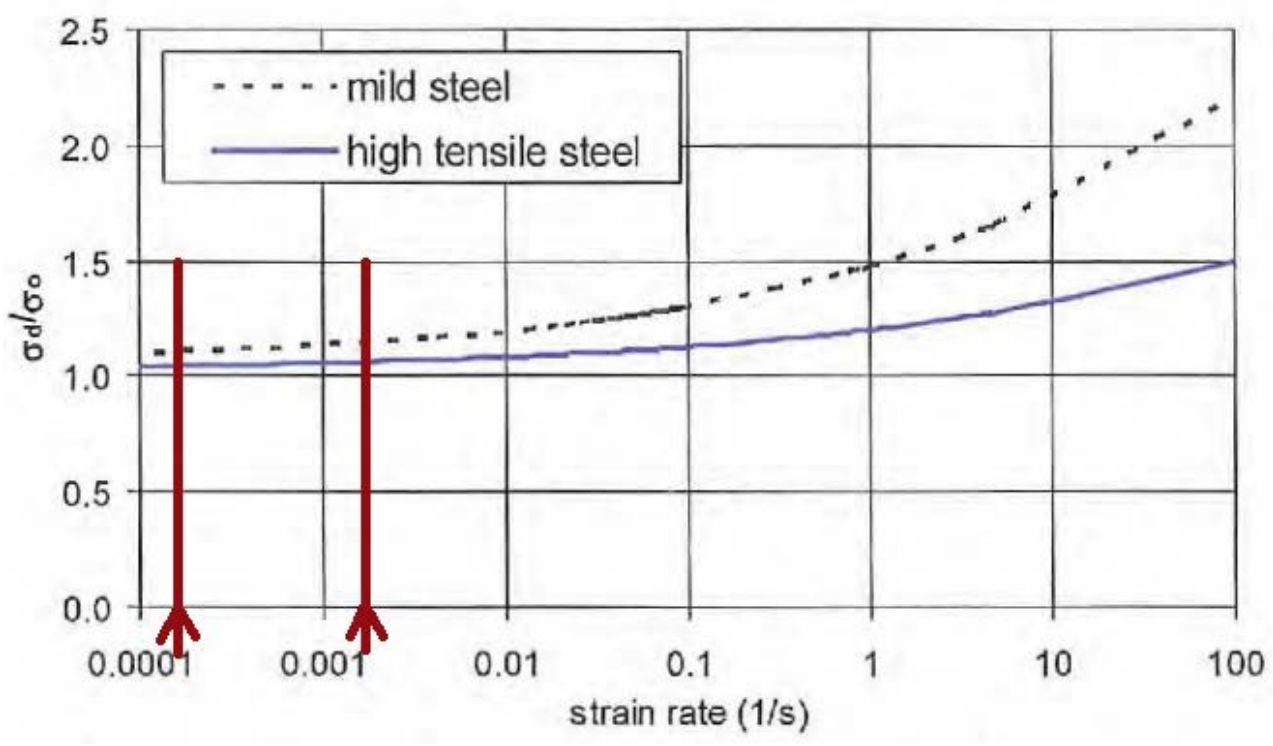


**Figure 28 Strain Rate Vs Stress Ratio**
**[Figure from [25]]**

From the simulation results, we can plot the curves for both Paik's and Lim's Cowper-Symonds constants as in Figure 29 and Figure 30.

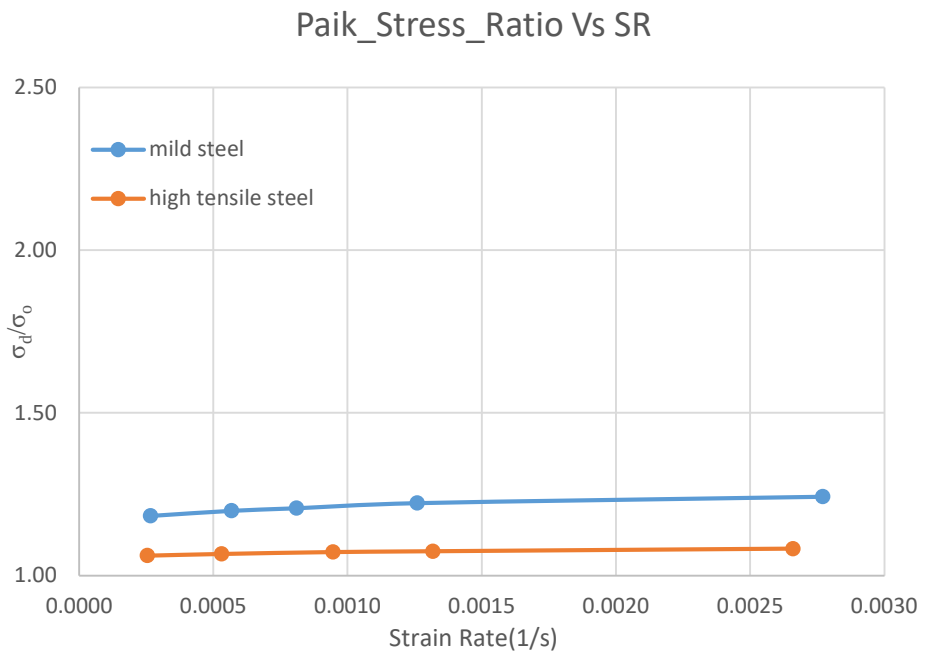


**Figure 29 Strain Rate Vs Stress Ratio**

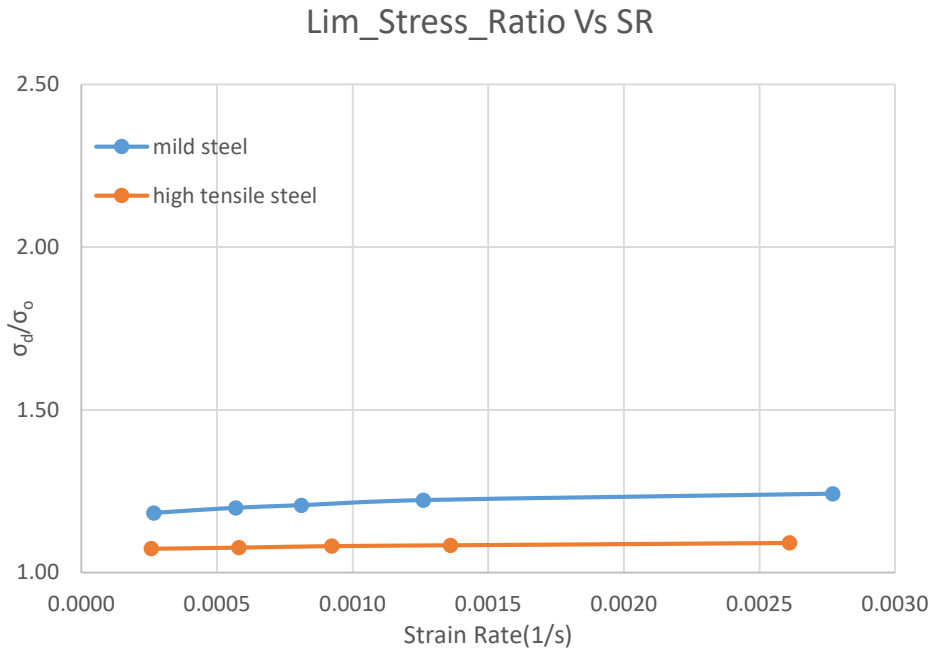


**Figure 30 Strain Rate Vs Stress Ratio**

Strain Rate from Measurements on Mild Steel Containership [26]

For Whipping, 50’ seas, hove-to $= 1.1 \times 10^{-3}$

Forward hatch corner, wave-induced 50’ seas, hove-to $= 3.0 \times 10^{-4}$

Deck or bottom of ship hull due to wave induced loads $= \sim \sim \times 10^{-4}$ (order of $10^{-4}$)

Inner hull of ship due to sloshing or slamming $= \sim \sim \times 10^{-3}$ (order of $10^{-3}$)

For our model analysis, the strain rates are approximately in the range between two red strips in Figure 28 Strain Rate Vs Stress Ratio. When we compare our result in Figure 29 and Figure 30 with the experimental result in Figure 28, we can see that the behaviour of the curves are almost same. Moreover, the strain rate from our model analysis are also approximately in the range of the strain rate from the measurements on Mild steel Containership. Cowper-Symonds constants that we use in our analysis is acceptable reliable to use in further analysis. However, we will choose only one researcher’s C and P values for future study

For further study, we will choose and use only Lim’s Cowper-Symonds Constant for those reason:

- Detail formulation for all type of ship structural steel
- Force increment ratio is within the acceptable range of 10 % [less than that using Paik’s constants]
- Strain rate is also valid with the measurement values

# 5 SIMULATION RESULTS WITH DOUBLE BOTTOM MODEL

After the analysis of the stiffened panel, we will analysis the double bottom structure of the 14000 TEU container ship.

In double bottom model, there are different colours in the model for different properties of the parts of the model. Double bottom model is created from the cargo hold model. It is cut between two bulkheads from the cargo hold FE model as shown in Figure 31. And then, perturbation and initial deflection are updated with for the double bottom model by removing the nodes not in this model.

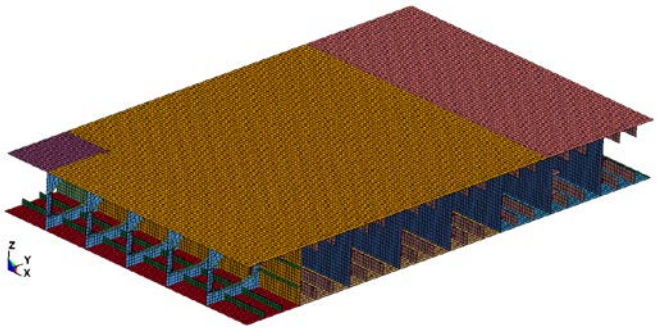

**Figure 31 Model of Double Bottom**

And boundary conditions are applied as in the stiffened panel. Two ends of the double bottom model are fixed in **y and z translational** and also in **x and z rotational DOFs** as shown in Figure 32.

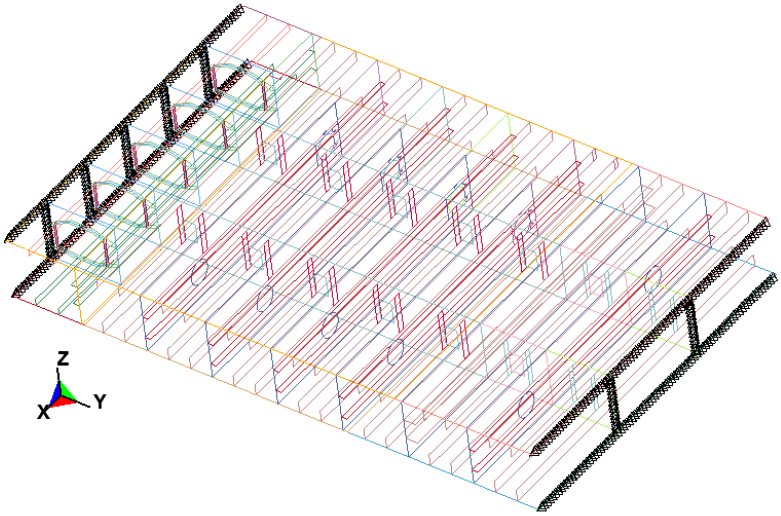


**Figure 32 : Application of Symmetric Boundary Conditions**

One side of the stiffened panel is fixed in **all six degree of freedom (6 DOFs)** as shown in Figure 33. And The other side of the model is imposed with the displacement in x direction and fixed in y and z translational DOFs and also y rotational DOF as in Figure 34.

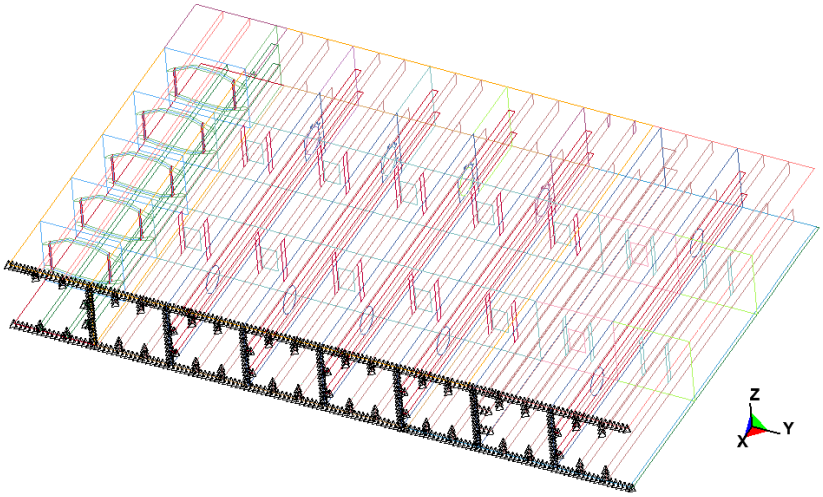


**Figure 33 : Application of fixed boundary condition**

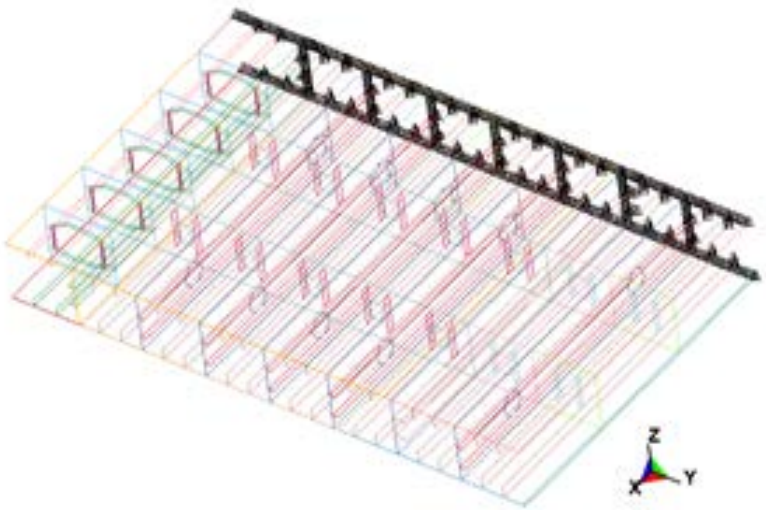


**Figure 34 : Double Bottom Model imposed with displacement as load**

## 5.1 Static Condition

Static model analysis of the model is performed by using the FE Implicit code of LS-DYNA on the double bottom using the material of high tensile steel (initial yield strength of 315MPa) and the mixture of different type of steel (original material of the cargo hold model of the container ship).

### 5.1.1 Static Condition with High Tensile Steel

For the double bottom model with high tensile steel, implicit simulation is performed and the collapse force and the displacement are directly read from the simulation results. The behaviour of the collapse force with respect to the displacement can be plotted as in Figure 35. Then take the element (element number 285753) that may be experienced the high stress and then read the strain rate and stress directly from the results of that element. The result can be summarized as in Table 10.

| Items | Value | Unit |
|---|---|---|
| Collapse Force | 290,506 | MN |
| Stress | 341,557 | MPa |
| Collapse time | 0,616 | sec |
| Collapse displacement | 17,73 | mm |

**Table 10 Summary of Simulation Result**

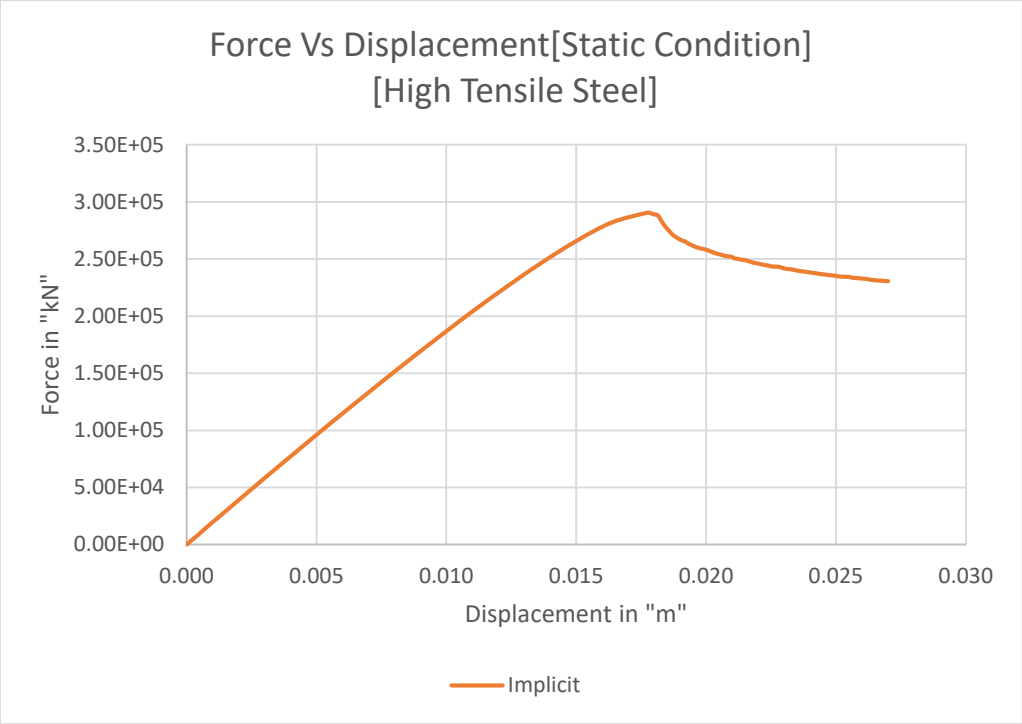


**Figure 35 Collapse Force Curve**

### 5.1.2 Static Condition with Mixture of Different Strength of Steel

Double bottom model consists of the mixture of initial yield strength of 235MPa, 315MPa, and 355MPa steel. The simulation is performed and the result are read as in sec 5.1.1.The simulation results of static condition can be summarized as in Table 11. The behaviour of the collapse force with respect to the displacement is shown as in Figure 36.

| Items | Value | Unit |
|---|---|---|
| Collapse Force | 295,406 | MN |
| Stress | 341,761 | MPa |
| Collapse time | 0,673 | sec |
| Collapse displacement | 18,19 | mm |

**Table 11 Summary of Simulation Result**

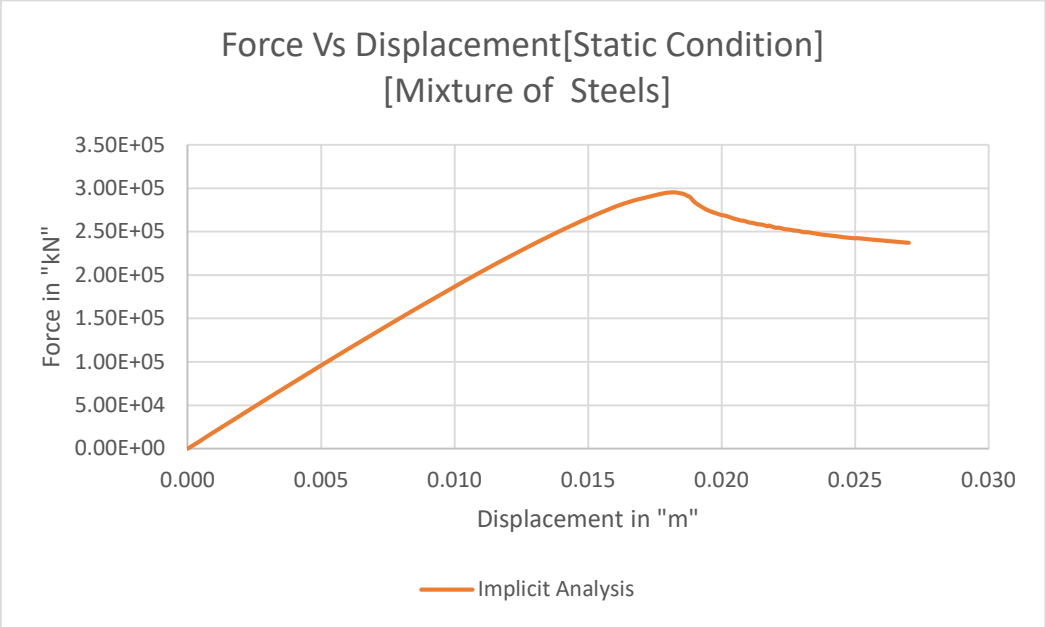


**Figure 36 Collapse Force Curve**

Figure 37 shows the overview of static analysis of the influence of materials. In double bottom model using the mixture of steel, most part are high tensile steel of initial strength of 315 MPa and some parts are used with the steels of initial strength of 355 MPa and 235MPa. It is obvious that the collapse force of double bottom model using the mixture of different strength of steel is approximately 2% greater than that of the model using only high tensile steel because the model with the mixture of steel consist of higher strength of steel.

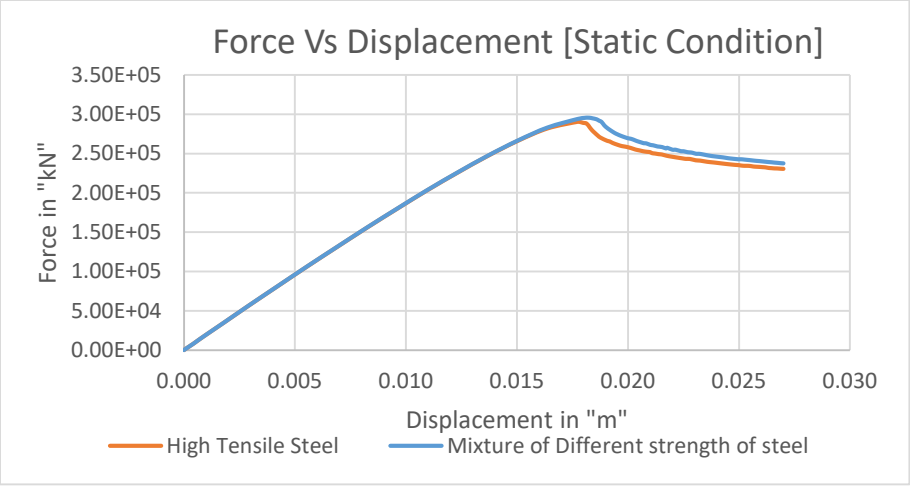


**Figure 37 Collapse Force Curve**

## 5.2 Dynamic Condition without Strain Rate Imposed with Cowper-Symonds Constants

In this section we will analyse the dynamic collapse of the double bottom by using the high tensile steel (initial yield strength of 315MPa) and the mixture of different type of steel (original materials of the cargo hold model of the container ship).

Finite element explicit code of the LS_DYNA is applied to the double bottom model and dynamic analysis is performed without considering the material strain rate imposed with Cowper-Symonds constants.

### 5.2.1 Dynamic Condition without Strain Rate Imposed with Cowper-Symonds Constants (Model with High Tensile Steel)

Simulations of the double bottom model with **high tensile steel** (initial yield strength of 315 MPa) are performed without considering the material strain rate imposed with Cowper-Symonds constants. For each simulation, collapse time, collapse force and collapse displacement are directly read from the simulation results. And take the same element (element number 285753) as in static condition and stress and strain rate are directly read from that element. Then, collapse force and stress resulted from this simulation are compared to those from the results of static condition (force ratio and stress ratio). The results can be summarized as shown in Table 12 and Figure 38.

| Simulation Time | Collapse Time[sec] | Collapse Frequency [Hz] | Dynamic Collapse force [MN] | Stress [MPa] | Force Ratio | Stress Ratio | Strain Rate | Displacement [mm] |
|---|---|---|---|---|---|---|---|---|
| 0,1sec | 0,07 | 14,29 | 293,11 | 344 | 1,01 | 1,01 | 5,54E-02 | 18,91 |
| 1sec | 0,66 | 1,52 | 291,21 | 343 | 1,00 | 1,00 | 1,99E-03 | 17,82 |
| 2sec | 1,325 | 0,75 | 291,01 | 343 | 1,00 | 1,00 | 1,20E-03 | 17,90 |
| 2,8sec | 1,85 | 0,54 | 291,01 | 343 | 1,00 | 1,00 | 6,59E-04 | 17,82 |
| 5sec | 3,31 | 0,30 | 291,01 | 342 | 1,00 | 1,00 | 4,23E-04 | 17,88 |

**Table 12 Summary of Simulation Result**

When we see force ratio of the highlighted part of the table, there is no significant change in dynamic collapse force compared to the static force when we don't consider the material strain rate imposed with Cowper-Symonds constants in our model. The behaviour of the collapse force with respect to displacement is still same as in the stiffened panel explained as in 4.2.2. However, collapse force Vs displacement curve for this model of the simulation time of 0.1 sec is little bit different. When the load is applied within very short time (it means the model in high dynamic condition), we can see that the behaviour of the force for the simulation time of 0.1 sec is slightly different from those of the other simulation times after the collapse occurs as in Figure 38.

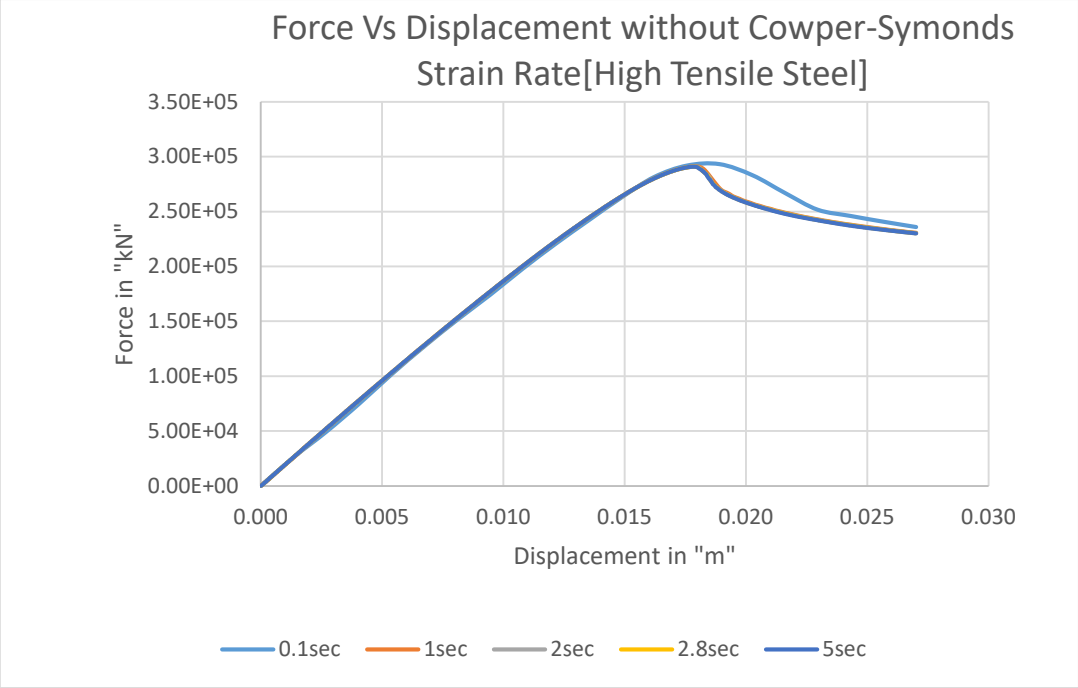


**Figure 38 Collapse Force Curve**

### 5.2.2 Dynamic Condition without Strain Rate Imposed with Cowper-Symonds Constants (Model with Mixture of Different Strengths of Steel)

Simulations of double bottom model with mixture of different strengths of steel are performed considering the material strain rate for different frequencies. Double bottom model consists of initial strengths of 235MPa, 315MPa and 355MPa steel. Simulation results are read as in sec 5.2.1 and can be summarized as shown in Table 13 and the collapse force can be plotted with respect to the displacement as shown in Figure 39.

| Simulation Time | Collapse Time[sec] | Collapse Frequency [Hz] | Dynamic Collapse force [MN] | Stress [MPa] | Force Ratio | Stress Ratio | Strain Rate | Displacement [mm] |
|---|---|---|---|---|---|---|---|---|
| 0,1sec | 0,07 | 14,29 | 298,81 | 345 | 1,01 | 1,01 | 6,50E-02 | 18,91 |
| 1sec | 0,68 | 1,47 | 295,81 | 343 | 1,00 | 1,00 | 1,23E-03 | 18,37 |
| 2sec | 1,355 | 0,74 | 295,71 | 343 | 1,00 | 1,00 | 6,53E-04 | 18,30 |
| 2,73sec | 1,85 | 0,54 | 295,61 | 343 | 1,00 | 1,00 | 8,01E-04 | 18,31 |

**Table 13 Summary of Simulation Result**

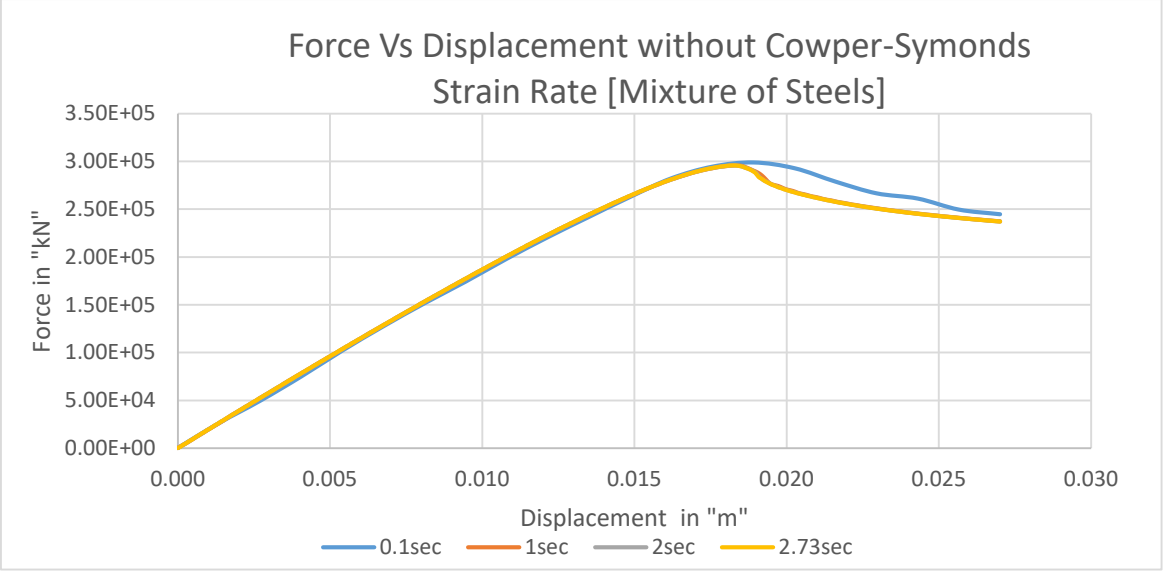


**Figure 39 Collapse Force Curve**

Here, the ratio of the collapse force is almost same as in static collapse force in sec 5.1.2 when we don't consider the material strain rate imposed with Cowper-Symonds constants. And we can see that the behaviour of the force with respect to the displacement is also still same as in sec 5.2.1.

## 5.3 Dynamic Condition with Strain Rate Imposed with Cowper-Symonds Constants

In this section, the simulation are performed for different simulation times( for different frequencies) considering the material strain rate imposed with Cowper-Symonds constants for the cargo hold model with high tensile steel and mixture of different strengths of steel .The procedures are same as in sec 5.2 .

### 5.3.1 Dynamic Condition with Strain Rate Imposed with Cowper-Symonds Constants (High Tensile Steel)

In this case, the model of double bottom uses only the material of high tensile steel. And the model is imposed with the material strain rate for high tensile steel of initial yield stress of 315MPa by using the Cowper-Symonds constants recommended by Lim (C= 24806,P=5). Simulations are performed for different frequencies. Collapse force and displacement are directly read from the simulation results of the model. And for the strain rate and stress, the same element is taken and read the results as in sec 5.2.1. The result can be summarized as in Table 14 and the collapse force Vs Displacement curve can be plotted as in Figure 40.When we overview the blue highlighted column of force ratio in Table 14, dynamic collapse force of the double bottom model used only high tensile steel with the consideration of material strain rate is 5 ~ 8 % greater than that of the same model without considering the Cowper-Symonds strain rate according to the simulation times.

| Simulation Time | Collapse Time[sec] | Collapse Frequency [Hz] | Dynamic Collapse force [MN] | Stress [MPa] | Force Ratio | Stress Ratio | Strain Rate | Displacement [mm] |
|---|---|---|---|---|---|---|---|---|
| 0,1sec | 0,08 | 13,33 | 313,31 | 363 | 1,08 | 1,062 | 7,00E-02 | 20,26 |
| 1sec | 0,72 | 1,39 | 307,71 | 363 | 1,06 | 1,063 | 2,04E-03 | 19,44 |
| 2sec | 1,43 | 0,70 | 306,91 | 362 | 1,06 | 1,059 | 1,44E-03 | 19,32 |
| 2,59sec | 1,85 | 0,54 | 306,60 | 361 | 1,06 | 1,058 | 1,05E-03 | 19,24 |
| 5sec | 3,57 | 0,28 | 306,00 | 363 | 1,05 | 1,064 | 4,36E-04 | 19,26 |

**Table 14 Summary of Simulation Result**

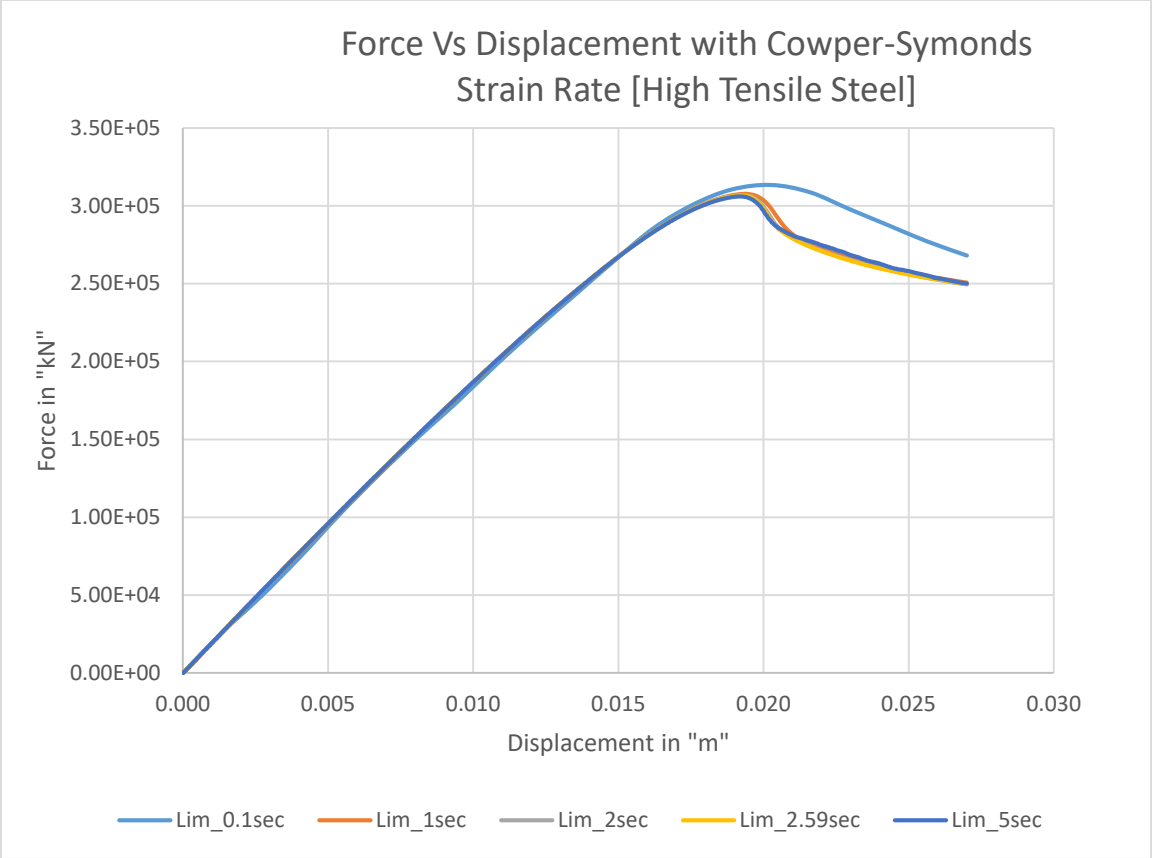


**Figure 40 Collapse Force Curve**

Here, we can clearly see the overview effect of strain rate of double bottom model at the desired frequency of 0.54Hz in Figure 41. When the dynamic simulation is performed without consideration of material strain rate, there is no significant change in the collapse force and collapse force Vs displacement curve is same as the static analysis (implicit). When the simulation of this model is performed considering the strain rate imposed with Cowper-Symonds constants recommended by “Lim”, the dynamic collapse force is 6% greater than collapse force without whipping load.

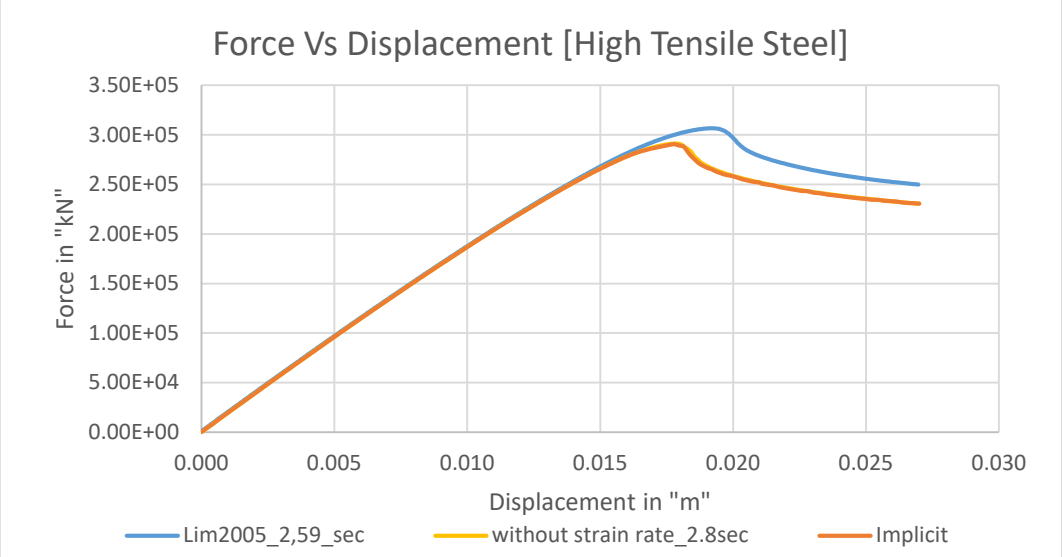


**Figure 41 Collapse Force Curve**

### 5.3.2 Dynamic Condition with Strain Rate Imposed with Cowper-Symonds Constants (Mixture of Different Strength of Steel)

Double bottom model consists of the mixture of initial yield strength of 235MPa, 315MPa, and 355MPa steel. And explicit code of LS-DYNA is applied and the Cowper-Symonds constants recommended by Lim 2005 for different steels are also applied to the model as in Table 15. Simulations are performed for different frequencies. The results are read as explained in sec 5.2.1 and can be summarized as in Figure 42 and Table 16.

| | Cowper-Symonds Constant | |
|---|---|---|
| Initial Yield Strength of Steel[MPa] | C | p |
| 235 | 40 | 5 |
| 315 | 24806 | 5 |
| 355 | 50195 | 5 |

**Table 15 Cowper-Symonds Constants Used in Analysis**

| Simulation Time | Collapse Time[sec] | Collapse Frequency [Hz] | Dynamic Collapse force [MN] | Stress [MPa] | Force Ratio | Stress Ratio | Strain Rate | Displacement [mm] |
|---|---|---|---|---|---|---|---|---|
| 0,1sec | 0,08 | 13,33 | 318,11 | 363 | 1,08 | 1,062 | 4,65E-02 | 20,26 |
| 1sec | 0,73 | 1,37 | 312,41 | 362 | 1,06 | 1,058 | 2,07E-03 | 19,71 |
| 2sec | 1,45 | 0,69 | 311,61 | 362 | 1,05 | 1,058 | 1,76E-03 | 19,58 |
| 2,55sec | 1,85 | 0,54 | 311,41 | 361 | 1,05 | 1,057 | 1,17E-03 | 19,59 |

**Table 16 Summary of Simulation Result**

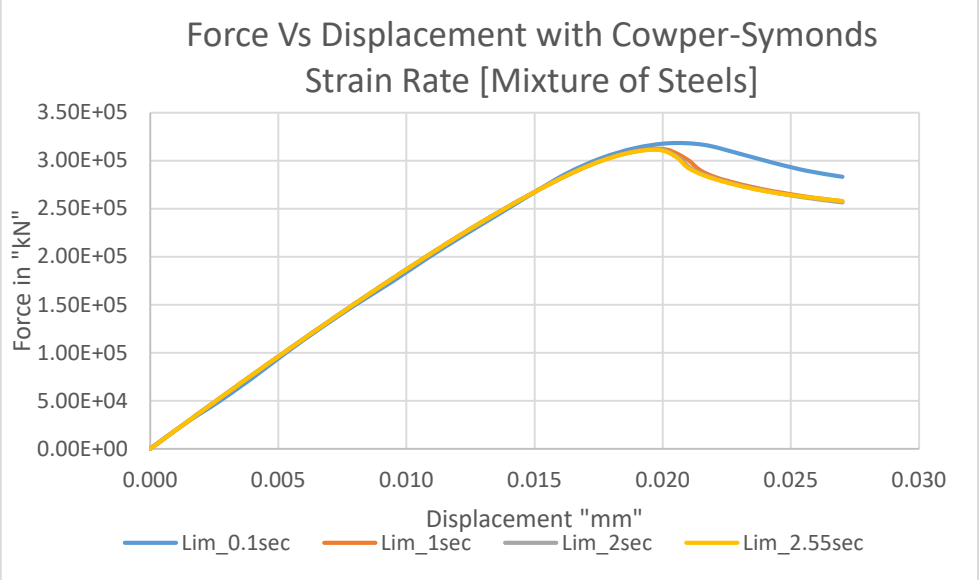


**Figure 42 Collapse Force Curve**

When we see the highlighted column of force ratio (dynamic collapse force/ static collapse force) in Table 13, dynamic collapse force is 5% greater than the static collapse force at the collapse frequency of 0.54 Hz. And the collapse force for different simulation times is slowly increased when the model is more dynamic (it means that the frequency of the model become high). In Figure 42, the collapse force Vs displacement curve for simulation time of 0.1 sec is slightly different from the others because when the displacement is imposed within 0.1 sec (very short time).

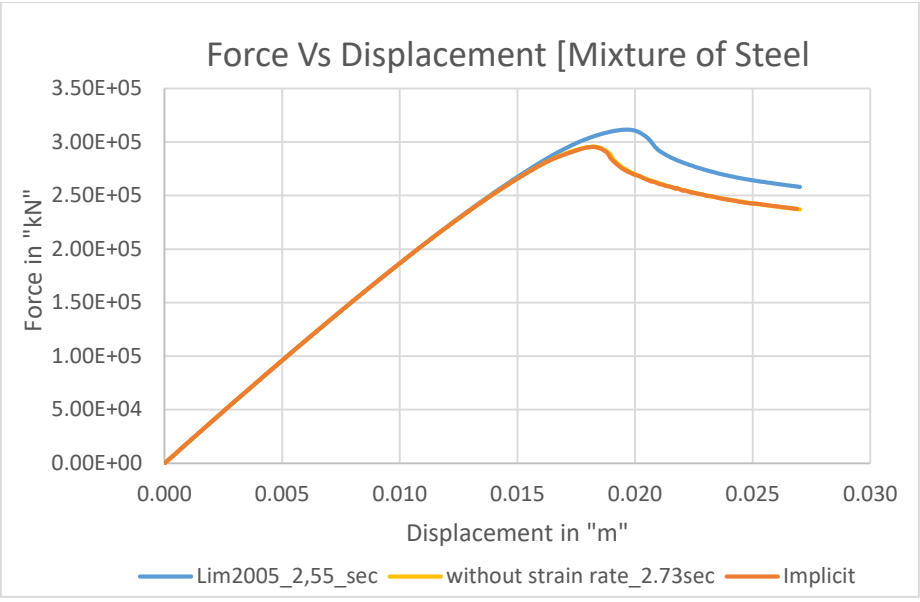


**Figure 43 Collapse Force Curve**

We can see the overview of the behaviour of the collapse force of the double bottom model used the mixture of steels at the model's collapse frequency of 0.54Hz in Figure 43. When the model is imposed with the strain rate recommended by Lim, the dynamic collapse force increases significantly compared to the static model analysis while the case without Cowper-Symonds strain rate is almost same with the static model analysis.

# 6 SIMULATION RESULTS OF CARGO HOLD MODEL

After analysing the stiffened panel and double bottom structure of the midship part of the container ship, dynamic analysis of the cargo hold model of the container ship(14000TEU container ship) is performed. From the previous analysis, we have already seen the nature and behaviour of the dynamic analysis including the influence of the material strain rate and influence of the strength of steels. The size of the cargo hold model is really large and the simulation for this model required too much time. Therefore, simulation will be performed only to get the results at the desired frequency of the collapse mode of the container ship. Ultimate hull girder strength of the container ship will be accessed from the simulation results.

HGUS FE model is available. Perturbation and imperfection are already imposed to the model. Material that we used in this model is the modified piecewise linear plasticity. Cargo hold model consists of different strengths of steel [initial yield strength of 235MPa, 315MPa, 355MPa, 390MPa, 460MPa]. We play and increase the y-moment until the model collapse. When the collapse of the model occurs, this y-moment is used for all simulations. And cargo hold model is imposed with this y-moment on the constrained nodal rigid body which consists of the nodes on one side of the cargo hold model as shown in **Figure 44**. And y-translation and x, z rotations are kept fixed on the constrained nodal rigid body. One side of the model keep fixed in 6 DOFs and can be shown in **Figure 45**.

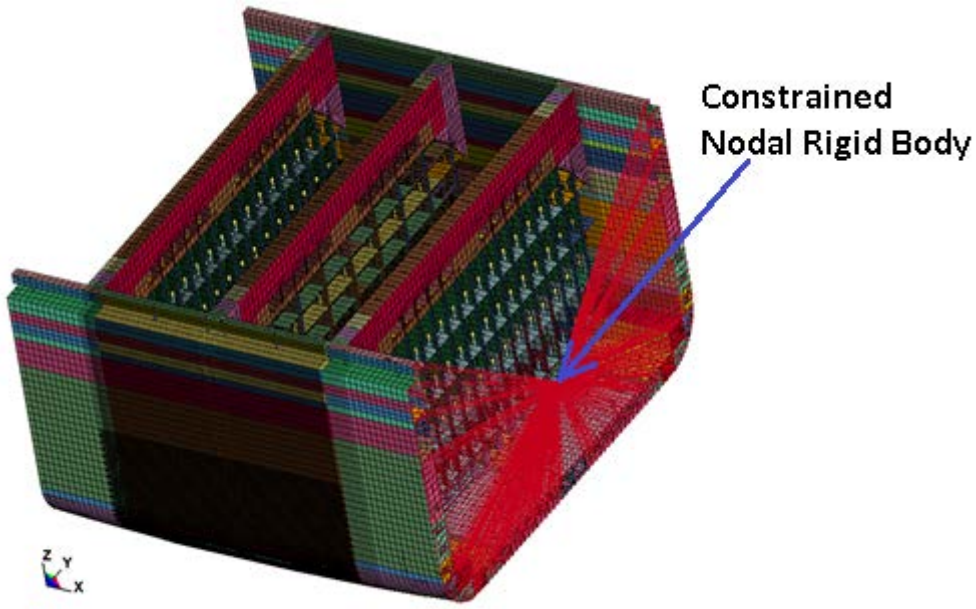


**Figure 44 Cargo Hold Model showing the constraint nodal rigid body**

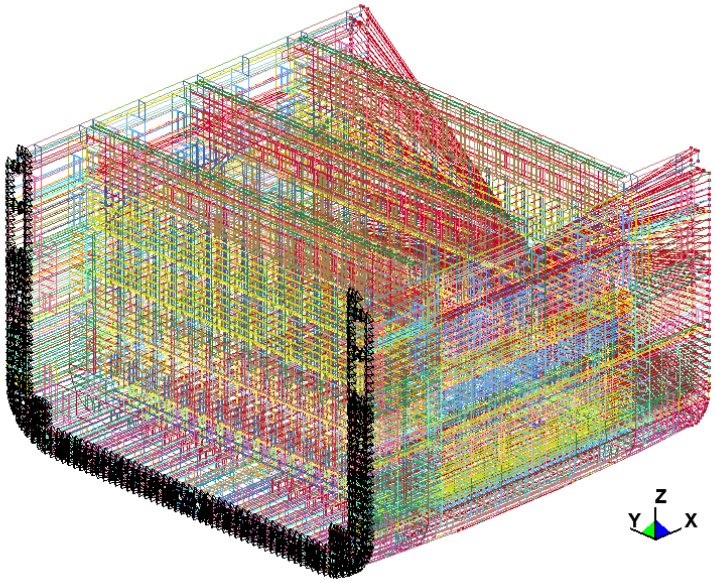


**Figure 45 Application of fixed boundary condition to Cargo Hold Model**

## 6.1 Static Condition

Static model analysis of cargo hold model is performed by using the implicit code of LS-DYNA. Then collapse moment and collapse rotational displacement are read from the simulation result and Collapse moment Vs Rotational Displacement curve can be plotted as shown in Figure 46. And one element (element no. 593939) is taken and read the results and can be summarized as in **Table 17**. From the Collapse Moment Vs Rotational Displacement curve (Figure 46), cargo hold model will be collapsed when the maximum moment reaches to 22.38 GN-m and maximum y-rotational displacement to 0.0048 rad.

| Items | Value | Unit |
|---|---|---|
| Collapse Moment | 22.38 | GN-m |
| Stress | 229.29 | MPa |
| Collapse time | 0.482 | s |
| Collapse rot_ displacement | 0.0048 | rad |

**Table 17 Summary of Simulation Result**

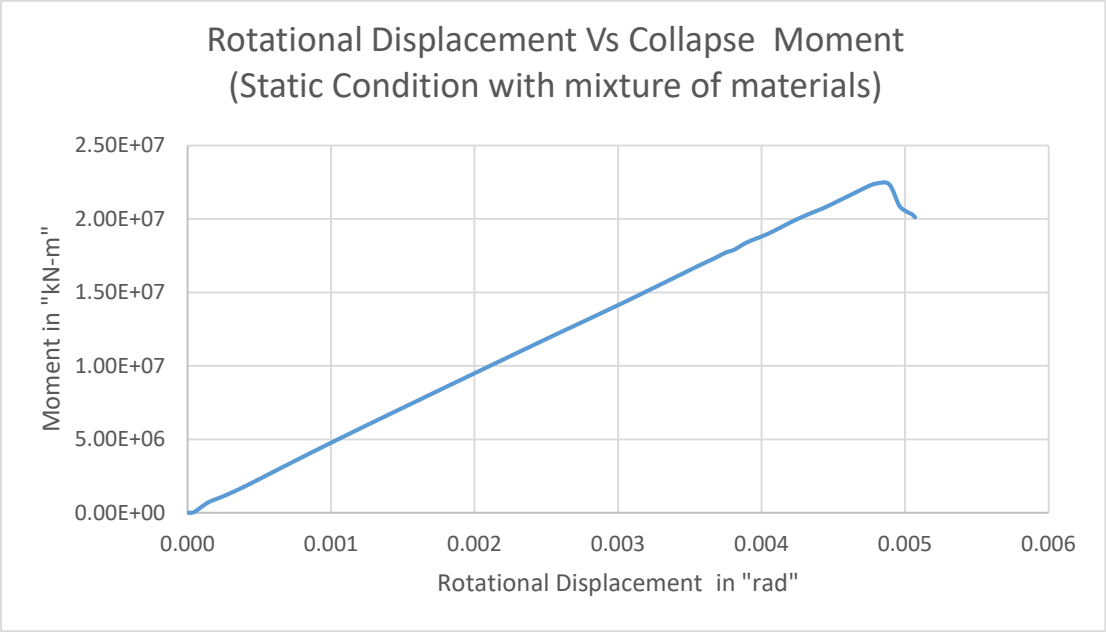


**Figure 46 Collapse Moment Curve**

## 6.2 Dynamic Condition with Strain Rate Imposed with Cowper-Symonds Constants (Mixture of Different Strength of Steel)

Cargo hold model is applied with the explicit code of LS-DYNA and the simulation of the model with the whipping load considering the strain rate of the materials imposed by Cowper-Symonds constants is performed. To consider the strain rate of the materials in the model, Cowper-Symonds constants recommended by Lim [as explained in Table 1] are used for different strengths of steel as in Table 18 Collapse moment and collapse rotational displacement are directly read from the simulation results and are plotted as shown in Figure 47. And then take the same element as in section 6.1 (element no. 593939) and read the results directly from the simulation as shown in Table 19.

| | Cowper-Symonds Constant | |
|---|---|---|
| Initial Yield Strength of Steel[MPa] | C | p |
| 235 | 40 | 5 |
| 315 | 24806 | 5 |
| 355 | 50195 | 5 |
| 390 | 74819 | 5 |
| 460 | 131774 | 5 |

**Table 18 Cowper-Symonds Constants Used in Analysis**

| Simulation Time | Collapse Time [sec] | Collapse Frequency [Hz] | Dynamic Collapse Moment [GN-m] | Stress [MPa] | Moment Ratio | Stress Ratio | Strain Rate | Rotational Displacement [radian] |
|---|---|---|---|---|---|---|---|---|
| 1 sec | 0,54 | 1,86 | 24,21 | 249 | 1,08 | 1,09 | 1,83E-02 | 0,0054 |
| 3 sec | 1,68 | 0,59 | 23,84 | 247 | 1,07 | 1,08 | 5,03E-03 | 0,0053 |

**Table 19 Summary of Simulation Result**

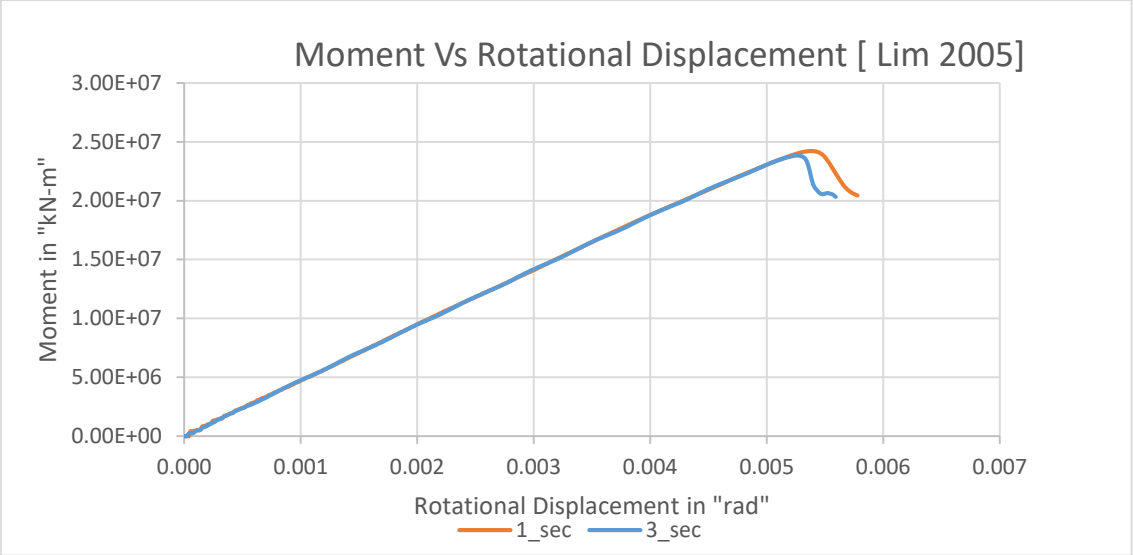


**Figure 47 Collapse Moment Curve**

Figure 47 show the dynamic analyses of the cargo hold model for the simulation time of 1 sec and 3 sec. We can see the time influence on the strength capacity of the model. It means the collapse moment increases when we imposed moment in y-axis to collapse within short time (high frequency). And we can make the comparison of the results of dynamic analysis to the static model analysis as shown in Figure 48.

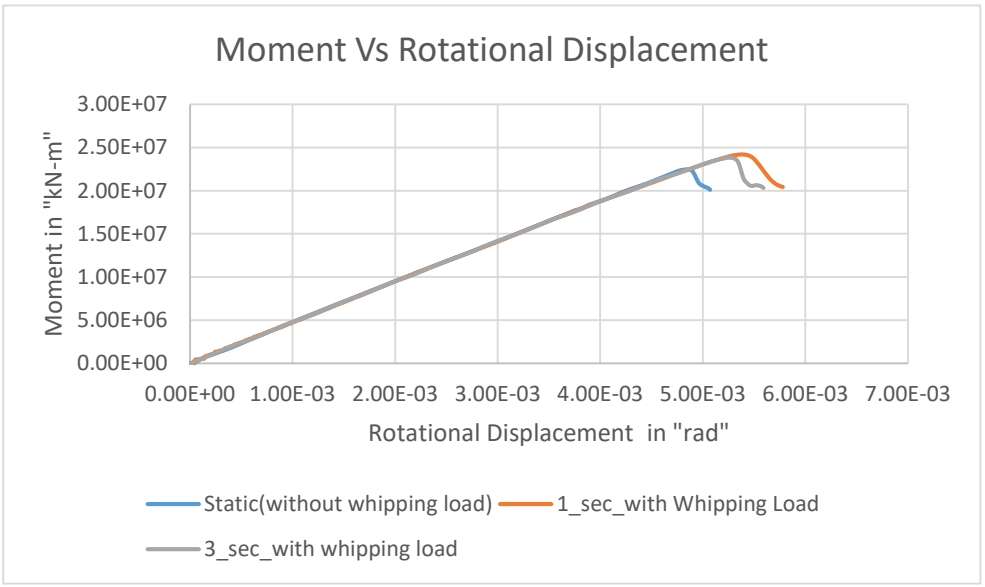


**Figure 48 Collapse Moment Curve**

# 7 COMPARISON AND ANALYSIS

In this section, we will analysis and compare the results for the case with whipping load and without whipping load at the desired collapse mode frequency of **0.54Hz**.

## 7.1 Comparison and Analysis of Model of Stiffened Panel

All simulation results of model of stiffened panel can be described as in Figure 49.

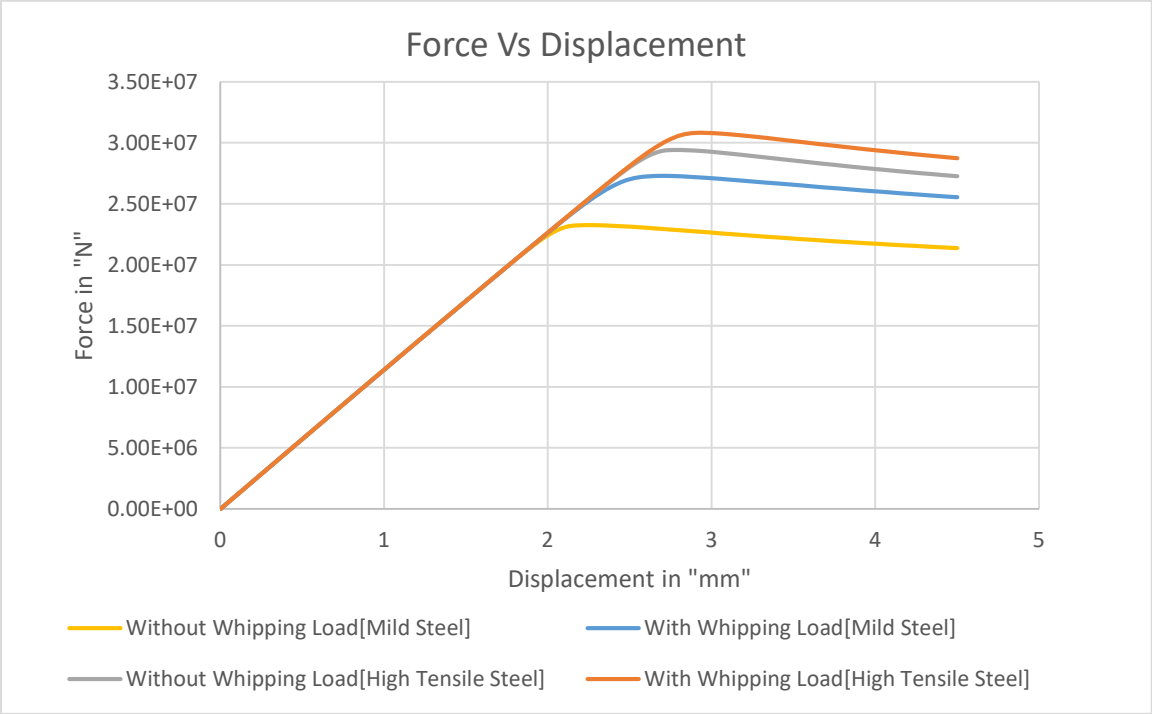


**Figure 49 Collapse Force Curve**

When the stiffened panel model using the material of **mild steel** is **not subjected to the whipping load**, collapse occurs when the resultant force reaches the maximum of 23.26MN and the displacement of 2.27mm. When the stiffened panel model using the material of **high tensile steel** is not subjected to whipping load, collapse occurs when the resultant force reaches the maximum of 29.38MN and displacement of 2.71mm. When the model is not subjected to the whipping load, the collapse forces of the stiffened panel model using the material of **high tensile steel** is approximately **26 % greater** than that of **mild steel**.

When the stiffened panel model using the material of **mild steel** is **subjected to the whipping load**, collapse occurs when the resultant force reaches the maximum of 27.3 MN and the displacement of 2.69 mm. When the stiffened panel model using the material of **high tensile steel** is subjected to whipping load, collapse occurs when the resultant force reaches the maximum of 30.81MN and displacement of 2.97mm. When the model is subjected to the whipping load, the collapse forces of the stiffened panel model using the material of **high tensile steel** is approximately **13 % greater** than that of **mild steel**.

For the stiffened panel model using the material of **mild steel**, the collapse force for the case **subjected to the whipping load** is approximately **17 % greater** than that for the case w**ithout**

**whipping load.** For the stiffened panel model using the material of **high tensile steel**, the collapse force for the case **subjected to the whipping load** is approximately **5 % greater** than that for the case **without whipping load**.

When we compare the collapse force considering the case with whipping load and without whipping load, the percent of difference of the collapse force of the stiffened panel using mild steel between the case with whipping load and without whipping load (17%) is greater than that of the stiffened panel using high tensile steel between the case with whipping load and without whipping load (5%). It means the model using mild steel is more sensitive to the whipping load compare to the model using high tensile steel.

## 7.2 Comparison and Analysis of Double Bottom Model

All simulation results of Double Bottom Model can be described in Figure 50.

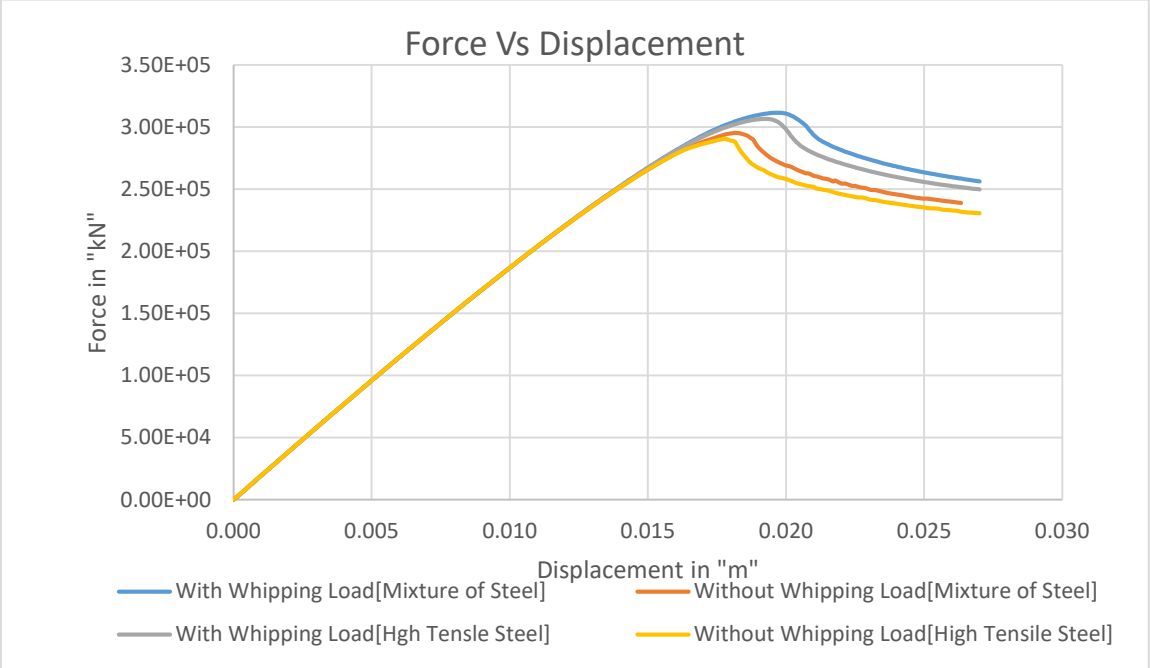


**Figure 50 Collapse Force Curve**

When the double bottom model using the material of **high tensile steel** is **not subjected to the whipping load**, collapse occurs when the collapse force reaches the maximum of 290.5MN and the displacement of 17.73mm. When the double bottom model using the material of **mixture of steel** is **not subjected to the whipping load**, collapse occurs when the collapse force reaches the maximum of 295.4MN and the displacement of 18.19mm. When the model is not subjected to the whipping load, the collapse forces of the stiffened panel model using the material of **mixture of steels** is approximately **2 % greater** than that of **high tensile steel** because the model with the mixture of steel consist of higher strength of steel than high tensile steel.

When the double bottom model using the material of **mixture of steel** is **subjected to the whipping load**, collapse occurs when the collapse force reaches the maximum of 306.6 MN and the displacement of 19.24mm. When the double bottom model using the material of

**mixture of steel** is **subjected to the whipping load**, collapse occurs when the collapse force reaches the maximum of 311.41MN and the displacement of 19.59mm. When the model is subjected to the whipping load, the collapse forces of the stiffened panel model using the material of **mixture of steel** is approximately **2 % greater** than that of **high tensile steel**.

For the double bottom model using the material of **high tensile steel**, the collapse force for the case **subjected to the whipping load** is approximately **6 % greater** than that for the case **without whipping load.** For the double bottom model using the material of **mixture of steel**, the collapse force for the case **subjected to the whipping load** is approximately **5 % greater** than that for the case **without whipping load**.

When we compare the collapse force considering the case with whipping load and without whipping load, the percent of difference of the collapse force of the double bottom model using the material of **high tensile steel** between the case with whipping load and without whipping load (6%) is almost close compared to that of the double bottom model using the material of **mixture of steels** between the case with whipping load and without whipping load (5%).

## 7.3 Comparison and Analysis of Cargo Hold Model

All simulation results of Cargo Hold Model can be described as in Figure 51.

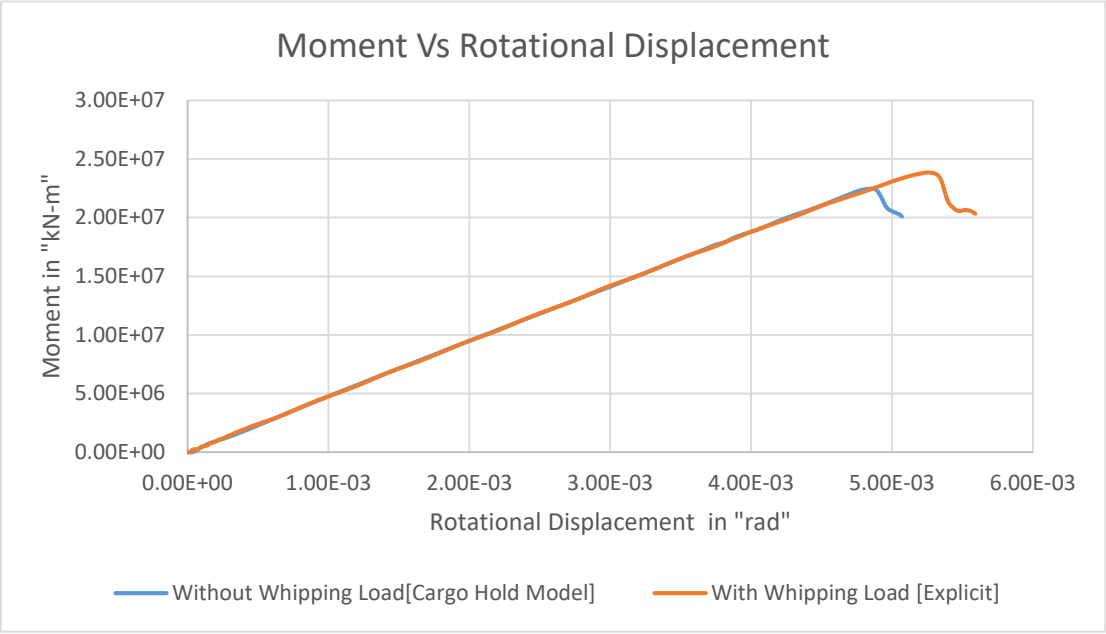


**Figure 51 Collapse Moment Curve**

For the cargo hold model of 14000TEU container ship,

The collapse occurs when the frequency of the cargo hold model for simulation time of 3 sec reaches to 0.59Hz. When we overview the dynamic analysis from the stiffened panel and double bottom, there is no significant change in collapse force up to the frequency difference of 0.15 Hz. Therefore, we will use the results from the dynamic analysis of simulation time of 3 sec subjected to whipping load for the analysis of the collapse frequency mode of the model of 0.54Hz.

When the cargo hold model of the container ship is not subjected to the whipping load, collapse occurs at the maximum moment of 22.38GN-m and rotational displacement of 0.0048rad.When the cargo hold model is subjected to the whipping load, collapse occurs at the maximum moment of 23.84GN-m and rotational displacement of 0.0053rad and we can see that the collapse moment increases by 7 % compared to the case without whipping load as in Figure 51.From the simulation result, we got $\Upsilon_{dU}$ of 0.93 ,partial safety factor reducing the effectiveness of whipping during collapse and $M_{u\ (static)}$ of 22.38GN-m and $M_{u\ (with\ whipping\ load)}$ of 23.84GN-m.

Using the result from cargo hold model analysis of 14000 TEU container ship, we will analysis and check the hull girder ultimate strength including the effect of whipping using DNV GL class guideline code-0153 described in sec 1.3.

For hull girder ultimate strength check including the effect of whipping,

$$\Upsilon_S M_{SW} + M_{WV} (\Upsilon_W + (\Upsilon_{WH} - \Upsilon_W) \Upsilon_{dU}) \leq M_U/\Upsilon_R \quad (1)$$

Load = $\Upsilon_S M_{SW} + M_{WV} (\Upsilon_W + (\Upsilon_{WH} - \Upsilon_W) \Upsilon_{dU})$ , Strength= $M_U/\Upsilon_R$

For hull girder ultimate strength check including the effect of whipping [5],

$$M_{SW} + M_{WV} \Upsilon_W \leq M_U/\Upsilon_R \quad (8)$$

Safety factors can be defined as follows:

$\Upsilon_W$ = 1.2

$\Upsilon_S$ = 1.0

$\Upsilon_{WH}$ = 1.4 [1.2 ~ 1.6]

$\Upsilon_{dU}$ = 0.9 [recommended by DNV-GL]

$\Upsilon_R$ = $\Upsilon_M$ * $\Upsilon_{DB}$

$\Upsilon_M$ = 1.05

$\Upsilon_{DB}$ = 1.15

From Analysis,

$\Upsilon_{dU}$ = 0.93

$M_{u(static)}$ = 22.38GN-m

$M_{u(whipping)}$ = 23.84GN-m

And then we can check the ultimate hull girder strength of 14000 TEU container using the still water bending moment and vertical wave bending moment.

For instance, use $M_{sw}$ = 8.5GN-m and $M_{wv}$ = 8GN-m and then we calculate using $\Upsilon_{dU}$ value from DNV GL class guideline and $\Upsilon_{dU}$ value from analysis result and summarized as inTable 20.

| | DNV GL | Analysis | Unit |
|---|---|---|---|
| Load (with whipping) | 19,54 | 19,59 | GN-m |
| Strength(with whipping) | 19,74 | 19,74 | GN-m |
| UF (with whipping)[UF=load/strength] | 0.990 | 0.992 | - |
| Load(Static) | 18,10 | - | GN-m |
| Strength(Static) | 18.53 | - | GN-m |
| UF (Static)[UF=load/strength][w/o whipping] | 0.977 | - | - |

**Table 20 Summary of Results**

Seeing the results in Table 18, the load subjected to whipping calculated using the $\Upsilon_{dU}$ = 0.93 resulted from analysis is slightly greater than the load subjected to whipping calculated using the $\Upsilon_{dU}$ =0.9 from DNV GL class guideline. And the strength is greater than the load. Therefore, the results we got from the dynamic collapse analysis are acceptable and reliable. And we can see that the usage factor for the container ship subjected to whipping load for the ultimate hull girder strength check is approximately 2% greater than the usage factor for static condition because the load is higher when the ship is subjected to whipping.

And we can summarize for all models at frequency of 0.54 Hz as in Table 21.

| Analysed Model | Increment of Ultimate Strength Capacity due to Strain Rate Effect | | |
|---|---|---|---|
| | Mild steel | High Tensile Steel | Mixture of Steel |
| Stiffened Panel | 17% | 5% | - |
| Double Bottom | - | 6% | 5% |
| Cargo Hold | - | - | 7% |

**Table 21 Summary of Results**

# 8 CONCLUSION AND RECOMMENDATION

In this master thesis, the dynamic collapse analysis of the container ship are performed by using the non-linear finite element explicit code of LS-DYNA. Simulations are performed for three types of models (stiffened panel model, double bottom model and cargo hold model of 14000TEU container ship).

Using the stiffened panel, we choose the strain rate parameters (Cowper-Symonds constants) that will give the acceptable and reliable results for the dynamic collapse analysis from the Researchers' recommendations as in chapter 4.Using the double bottom model, we analyses the effect of strain rate and influence of the materials and behaviour of the dynamic condition of the container ship subjected to whipping load as in chapter 5.Then simulations for the dynamic collapse analysis for the cargo hold of the container s hip are performed and results are analysed as described in chapter 6.

In this thesis, we impose the strain rate using the Cowper-Symonds constants in LS-DYNA. We can get these constants by doing the tensile test for the materials that will use in our models. However, there are different values for Cowper-Symonds constants (C & P). The simulations are performed using different C and p values recommended by the researchers(Paik, Lim, Thamballi, ect) and choose the best one that is reliable and acceptable .In this thesis, Cowper-Symonds constants recommended by the researcher [Lim 2005] are used in this thesis to save time and money.

From the previous analysis results, the following conclusion and recommendation could be made:

Strain rate is one of the main parameters we should consider in the dynamic collapse analysis. Increasing the strain rate makes the ultimate capacity of the model increase. The percent increase in ultimate capacity of the model using mild steel (dynamic ultimate capacity/static ultimate capacity) is greater than that of the model using high tensile steel. And consequently the model using mild steel is more sensitive to the effect of whipping load when the model is subjected to whipping. And whipping load makes the ultimate capacity up to7 % increase at the collapse frequency of 0.59Hz.Therefore, for the design collapse frequency of 0.54Hz, whipping load may increase 7% of the ultimate capacity of the cargo hold model of the 14000TEU container ship compare to the case without whipping load. The usage factor of the hull girder ultimate strength including the whipping effect (0.992) is approximately 1.5 % greater than the usage factor without whipping effect (0.977).

For non-linear explicit calculations of the model of stiffened panel, it takes few hours (up to 4~5 hours) depending on the simulation times that we impose. For the model of the double bottom, it takes more time. It may take up to 3 to 4 days for each simulation depending on the simulation times. When there are some problems with FE model of double bottom model, sometimes it may take more time than as we expect to fix the model. Regarding to the cargo hold model of 14000TEU container ships, we need too much time and effort for this model. Simulation time for each explicit calculation of the cargo hold model may take over 5 days depending on the frequency that we impose. In this thesis, some simulations and implement of cargo hold model are still needed because it may take several days to perform all simulations and to implement the cargo hold model. Therefore, I would like to recommend to implement this model to get the accurate results of the future work although the results we got from the simulations of cargo hold model are acceptable and reliable

## ACKNOWLEDGEMENT

First of all, I would like to give my wholehearted thanks to my internship supervisor Mr. Ionel Darie Dipl.-Ing, DNV GL SE who gave me supports and precious advices and also guided in the right direction to complete and finish this thesis in time throughout this thesis work. And I would like to thank to the employee of DNV GL SE, Hamburg for giving me supports and creating the warm atmosphere with friendliness.

Secondly, I would like to express my sincere gratitude to Prof. Dr.-Ing. Thomas Lindemann for providing good advices and guidance throughout this thesis work.

Thirdly, I would like to deeply thank to Prof. Philippe Rigo, who helped me and gave me a chance to participate in this challenging EMSHIP program.

Moreover, I would like to say special thanks to all members of my family for always giving me love, care, encouragement and motivation throughout this EMSHIP program.

Last but not least, my deepest gratitude goes to all my friends and all the people, who gave me strength directly or indirectly throughout this thesis work.

This thesis was developed in the frame of the European Master Course in “Integrated Advanced Ship Design” named “EMSHIP” for “European Education in Advanced Ship Design”, Ref.:159652-1-2009-1-BE-ERA MUNDUS-EMMC.

## REFERENCES

(1) Tuitman J & Malenica, 2008. Some Aspects Of Whipping Response Of Container Ships.

(2) Toichifukasawa And Keiichimukai, Vol 6, 2014. On The Effects Of Hull-Girder Vibration Upon Fatigue Strength Of A Post-Panamax Container Ship Disaggregated By Short-Term Sea State.

(3) Mondher Barhoumi (Vestfold University College, Norway) And Gaute Storhaug (DNV-GL, Maritime, Norway), 2014. Assessment Of Whipping And Springing On A Large Container Vessels.

(4) DNVGL-CG-0153, Edition October 2015. Fatigue And Ultimate Strength Assessment Of Container Ships Including Whipping And Springing.

(5) Dnvgl-Ru-Ship-2016-2017.

(6) Full-Scale Measurements, DNV-GL.

(7) Hemanand Kalyanasundaram (Emship, 6th Cohort), 2016.Hull Girder Ultimate Strength Of A Ship Using Nonlinear Finite Element Method, Master Thesis.

(8) Rick Spilman, June 19, 2013. Why And How Did The MOL Comfort Break In Half? Structural Flaw Or Improper Loading?

(9) MSC Carla,Complete Hull Failure In A Lengthened Container Vessel.Ship Structure Committee, An Interagency Research And Development Committee For Safer Ship Structures, 2016(Updated).

(10) English Channel On 18 January 2007. Report On The Investigation Of The Structural Failure Of Msc Napoli.

(11) Tjark Tilman Schwebe, 2016. Dynamic Collapse Of The Hull Girder In A Container Ship In Waves, Master Thesis.

(12) Suri Bala , LSTC, Time Integration.

(13) F.J. Harewood, P.E. Mchugh , 2006. Comparison Of The Implicit And Explicit Finite Element Methods Using Crystal Plasticity.

(14) Bradley Klenow. Assessment Of LS-DYNA And Underwater Shock Analysis (USA) Tools For Modeling Far-Field Underwater Explosion Effects On Ships.

(15) Hyung Kyun Lim , Joo-Sung Lee, 2017. On The Structural Behavior Of Ship's Shell Structures Due To Impact Loading. International Journal Of Naval Architecture And Ocean Engineering xx(2017) 1-16.

(16) Ship Structural Analysis And Design, 2014. Lecture 26.Engi 6003.

(17) LS-DYNA, Keyword User's Manual ,Volume I R8.0.

(18) LS-DYNA, Keyword User's Manual, Volume II R8.0.

(19) LS-DYNA, Keyword User's Manual, Volume III R8.0.

(20) Getting Started With LS-DYNA.

(21) Jimmy Forsberg, Short Introduction To LS-DYNA And LS Prepost.

(22) LS-DYNA Theory Manual-2005-2006.

(23) LS-DYNA Examples Manual.

(24) LS-DYNA, User's Guide.

(25) Lei Jiang, Shengming Zhang And Nigel White, Hydroelasticity In Marine Technology 2012. Nonlinear Finite Element Dynamic Collapse Analyses Of Stiffened Panels.

(26) Offshore Technology Report- OTO 1999 018, The Behaviour Of Carbon Steels At High Strain Rates And Strain Limits.

(27) Gordon R. Johnson (Honeywell Inc., Defense Systems Division, Edina, Mn 55436, U.S.A) And William H. Cook(Air Force Armament Laboratory, Eghn Air Force Base, Fl 32542, U.S.A). Fracture Characteristics Of Three Metals Subjected To Arious Strains, Strain Rates, Temperature And Pressures. Engineering Fracture Mechanics Vol.21. No.1, Pp, 31-48, 1985.

(28) Kun Liu, Bin Liu , R. Villavicencio, Zili Wang And C. Guedes Soares. Assessment Of Material Strain Rate Effect On Square Steel Plate Under Lateral Dynamic Load, Ships And Offshore Structure 2017.

(29) Virginija Gyliene & Vytautas Ostasevicius. Cowper-Symonds Material Deformation Law Application In Material Cutting Process Using LS-DYNA FE Code: Turning And Milling. Department Of Engineering Design Faculty Of Mechanical Engineering And Mechatronics Kaunas, University Of Technology. 8th European LS-DYNA Users' Conference.

(30) M.A.G. Calle, R.E. Oshiro, L.M. Mazzariol And M. Alves. Structural Response Of Reduced Scale Naval Structures Under Impact Tests. MATEC Web Of Conferences 16, 07002, 2014.

(31) Buckling ,DNVGL-CG-0128 Edition October 2015,Amended April 2016.

(32) S. K. Hashemi & M. A. Bradford, 2014, Vol 141. The Strain-Rate Effects On The Numerical Simulation Of Steel Beams Under Blast Loads. Centre For Infrastructure Engineering And Safety,School Of Civil And Environmental Engineering, The University Of New South Wales, Australia.

(33) Ingrid Marie Vincent Andersen & J_Rgen Juncher Jensen. Measurements In A Container Ship Of Wave-Induced Hull Girder Stresses In Excess Of Design Values. Dtu Mechanical Engineering.

(34) Trondheim, June 2008. Experimental And Numerical Investigation Of Non-Linear Wave-Induced Load Effects In Containerships Considering Hydroelasticity. Thesis For The Philosophiae Doctor. Norwegian University Of Science And Technology, Faculty Of Engineering Science And Technology, Department Of Marine Technology.

# APPENDIX

The influence of Strain Rate imposed with Cowper-Symonds of different model for different frequencies can be described in this section.

**For Model of Stiffened Panel**,

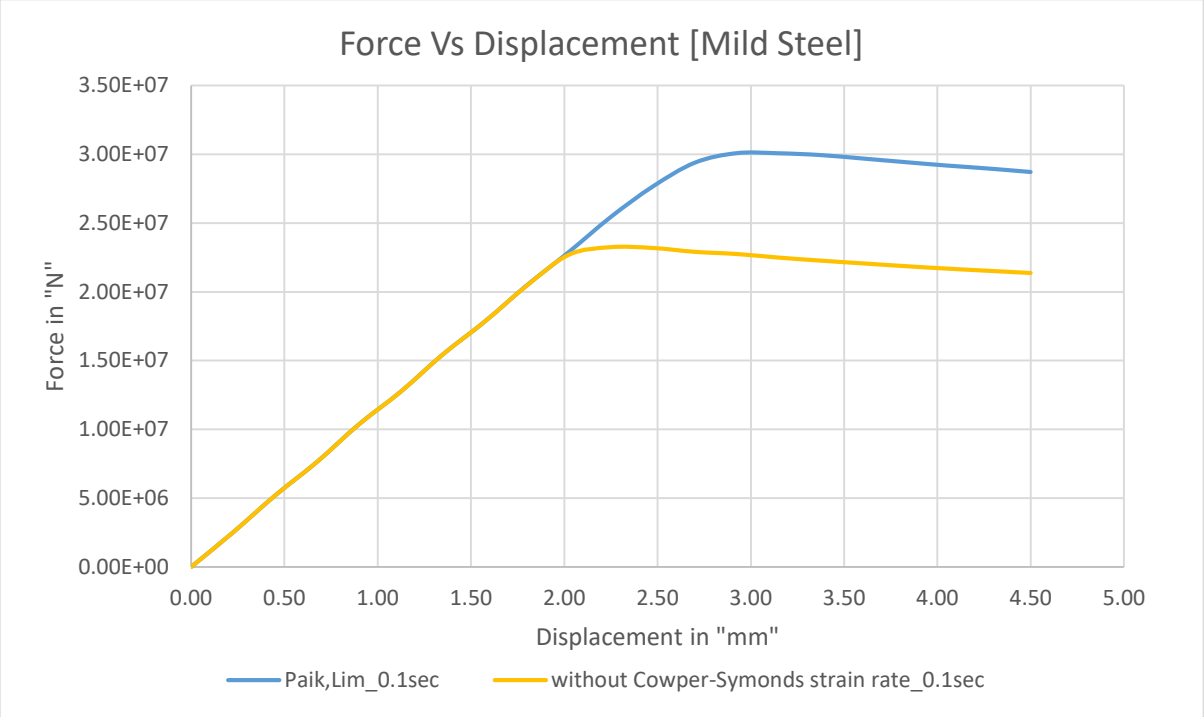


**Figure 52 Collapse Force Curve**

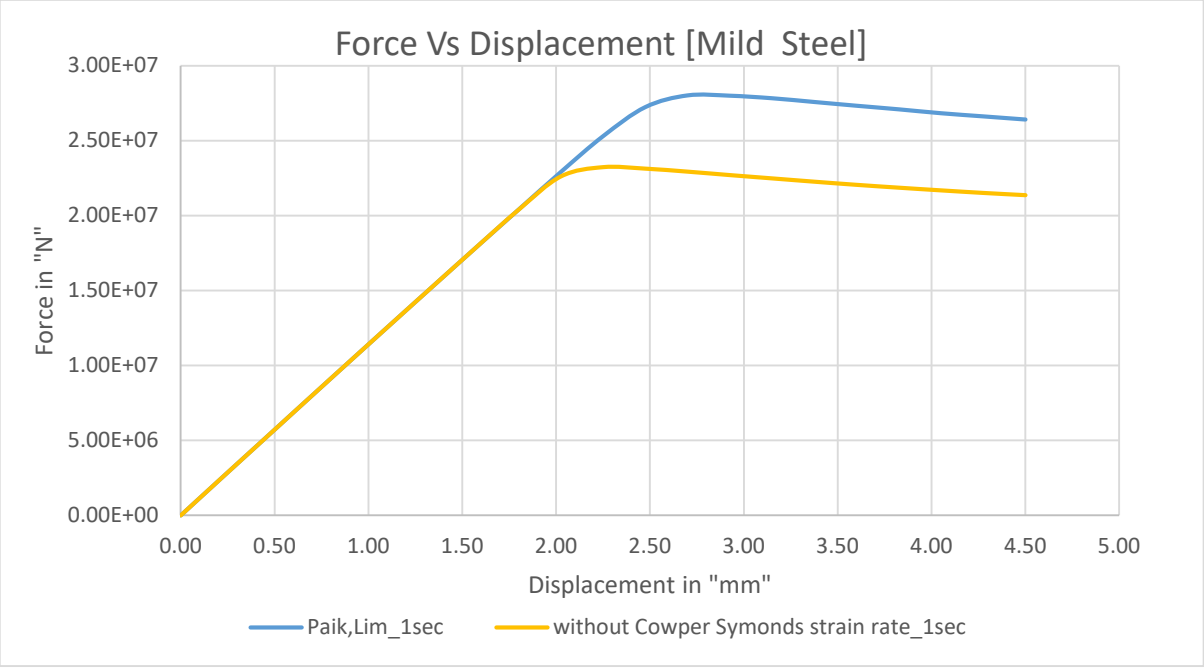


**Figure 53 Collapse Force Curve**

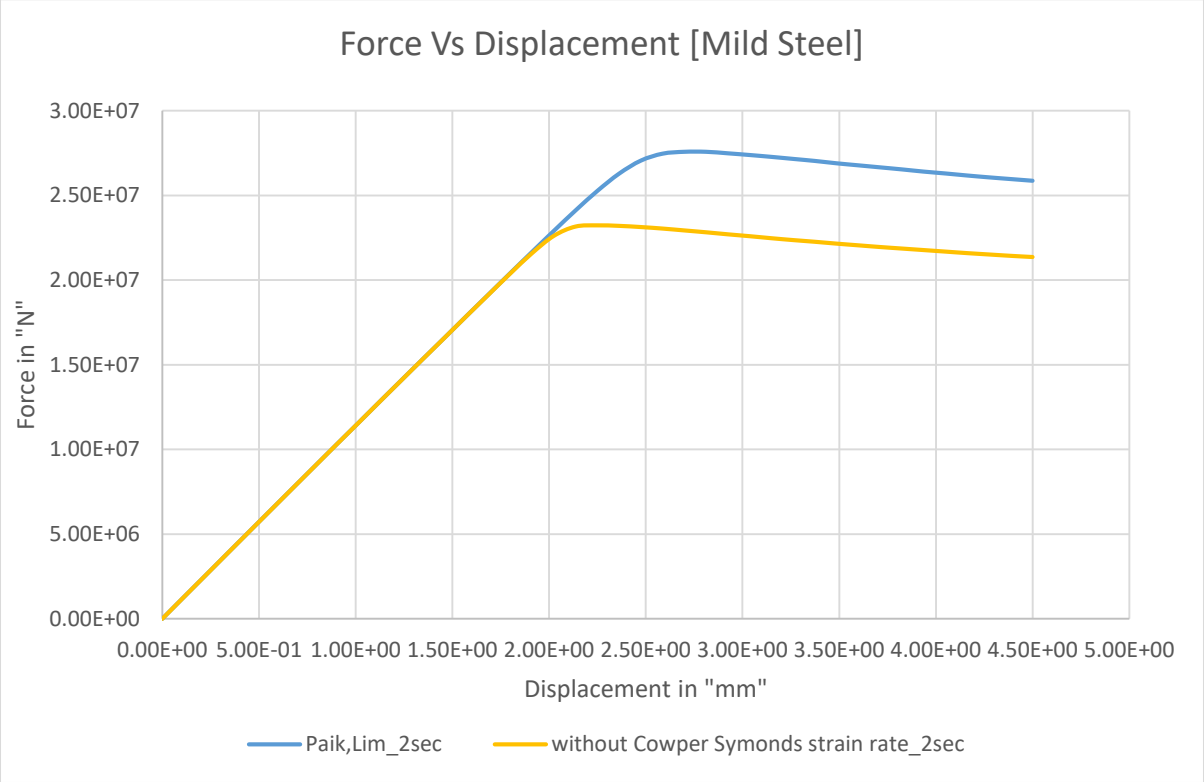


**Figure 54 Collapse Force Curve**

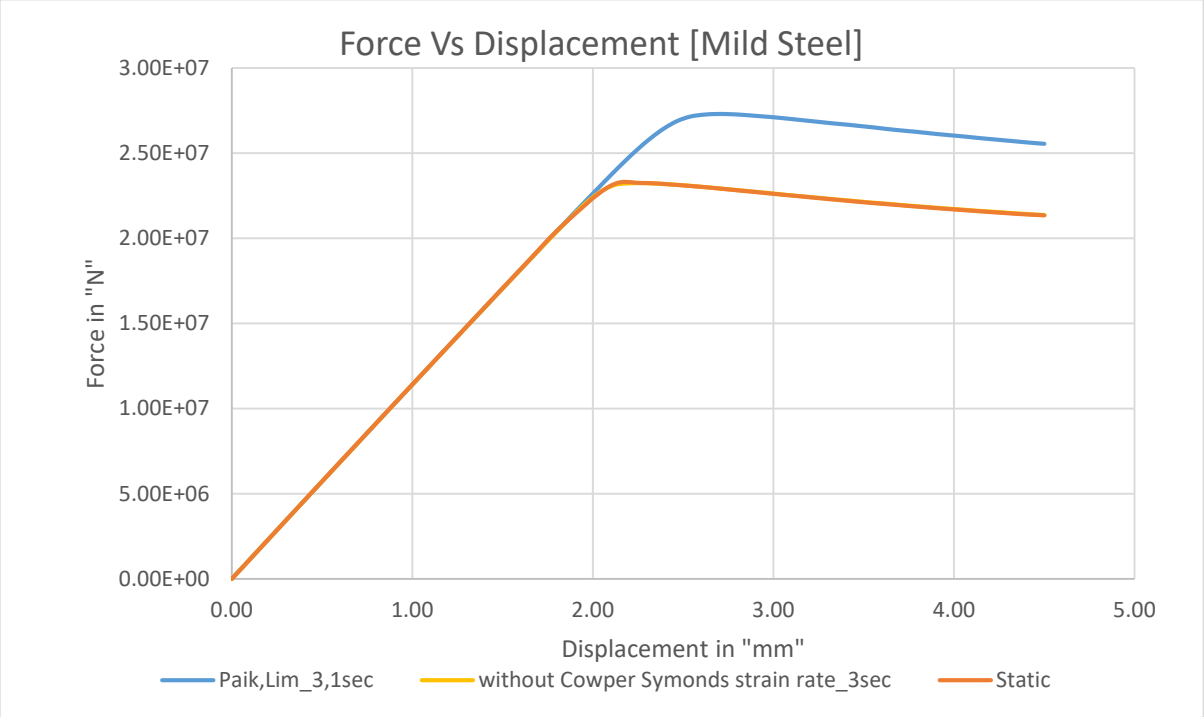


**Figure 55 Collapse Force Curve**

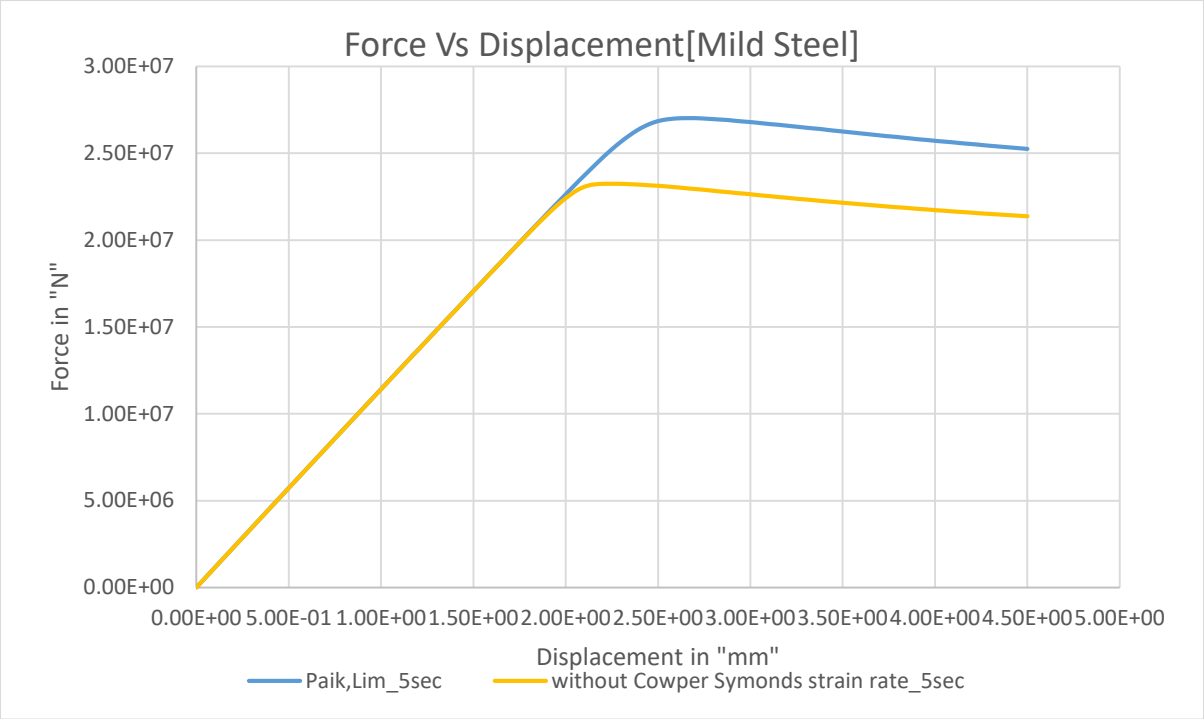


**Figure 56 Collapse Force Curve**

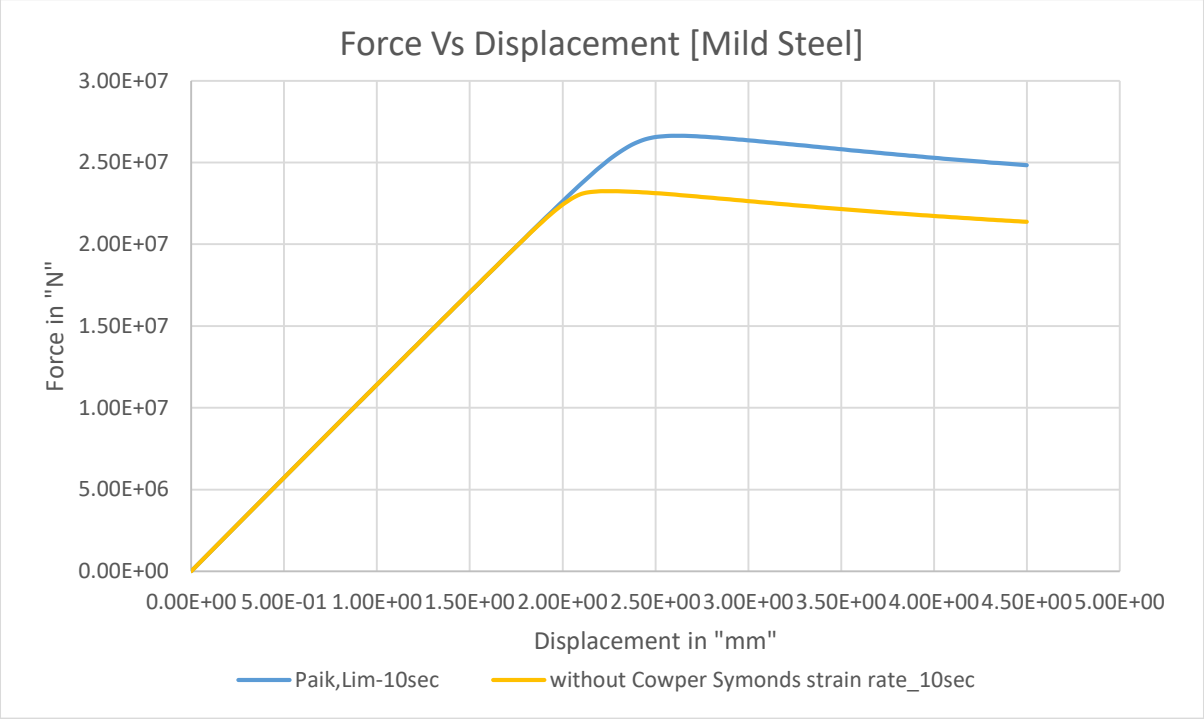


**Figure 57 Collapse Force Curve**

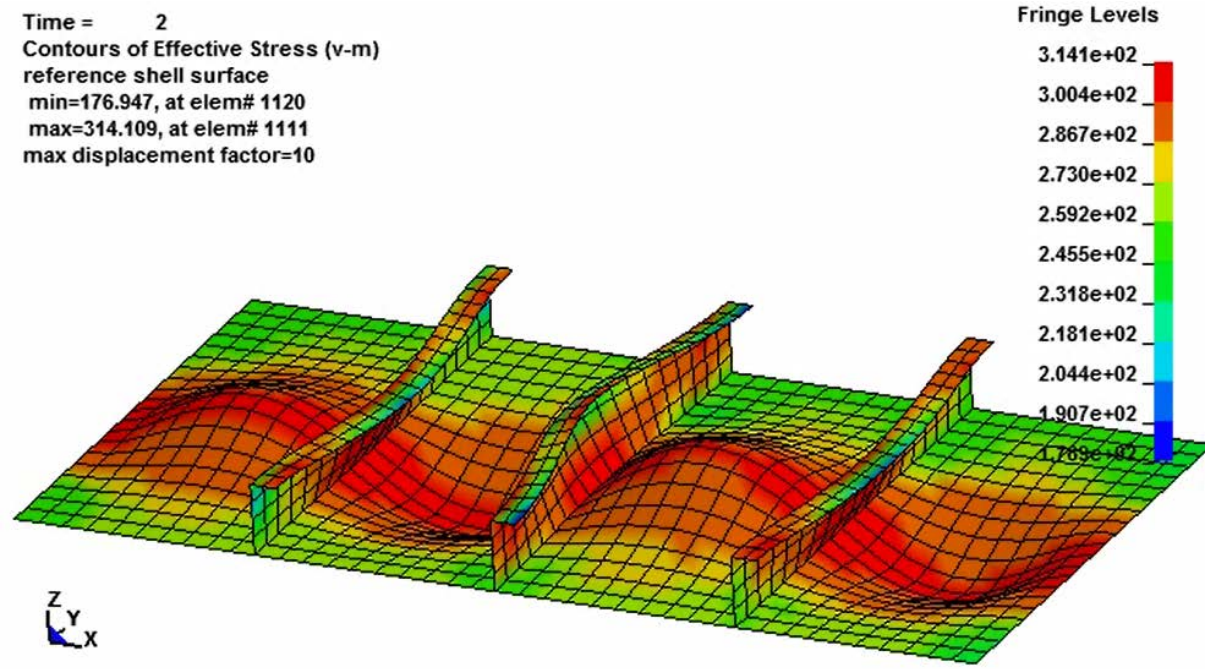


**Figure 58 Distribution of Von-mises Stress of the Stiffened Panel with Mild Steel**
(After collapse)

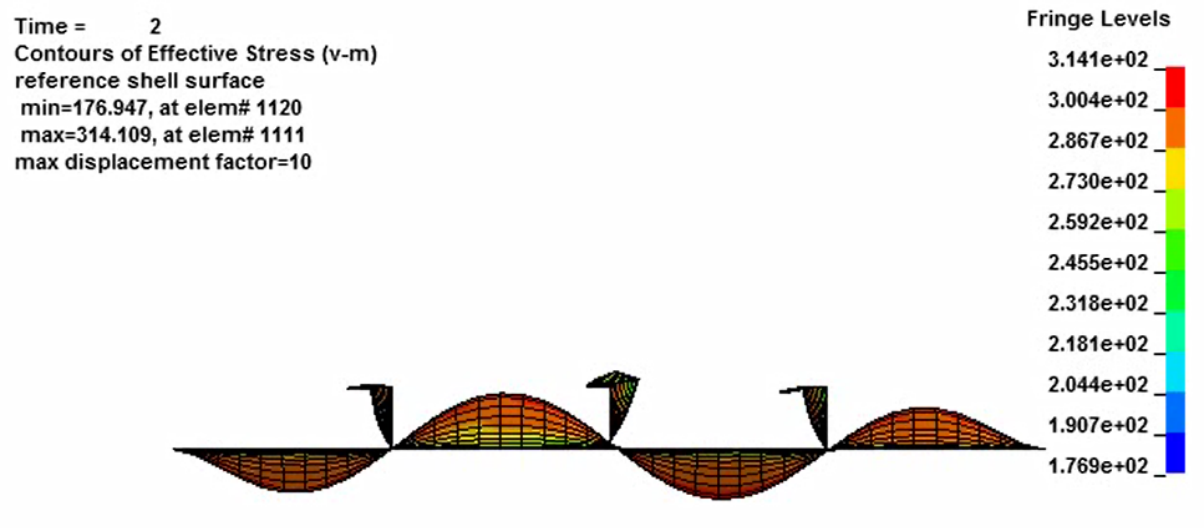


**Figure 59 Distribution of Von-mises Stress of the Stiffened Panel with Mild Steel**

(Right View: Scale Factor = 10)

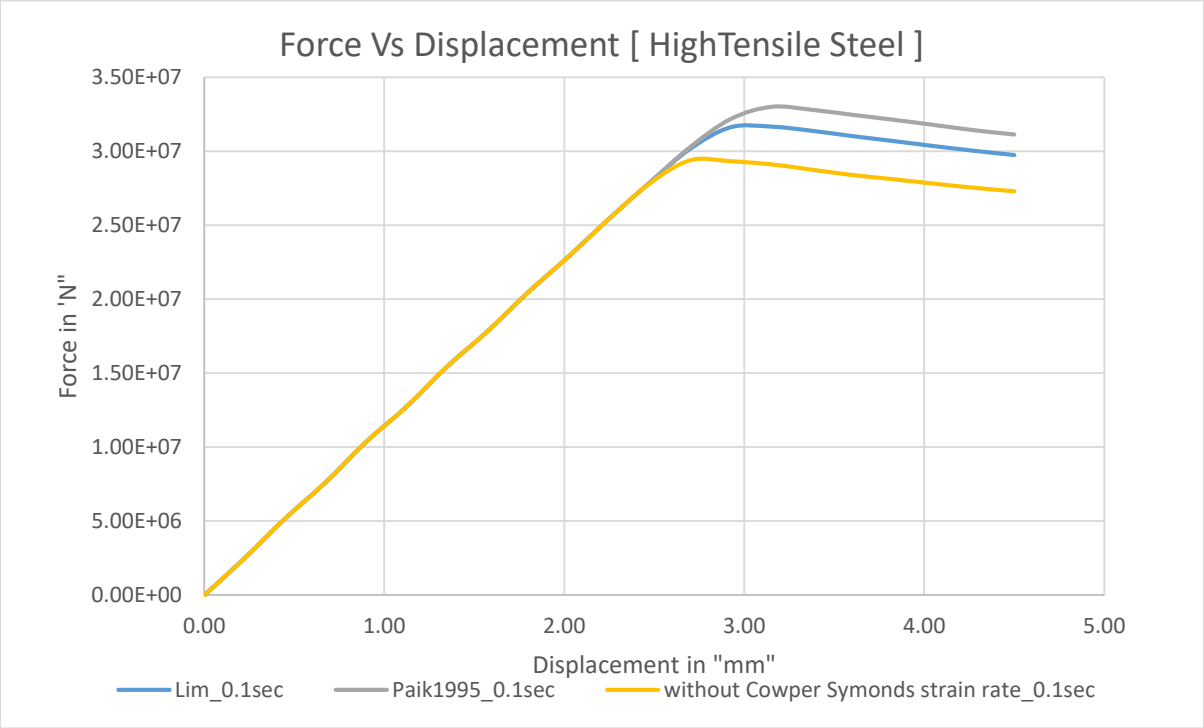


**Figure 60 Collapse Force Curve**

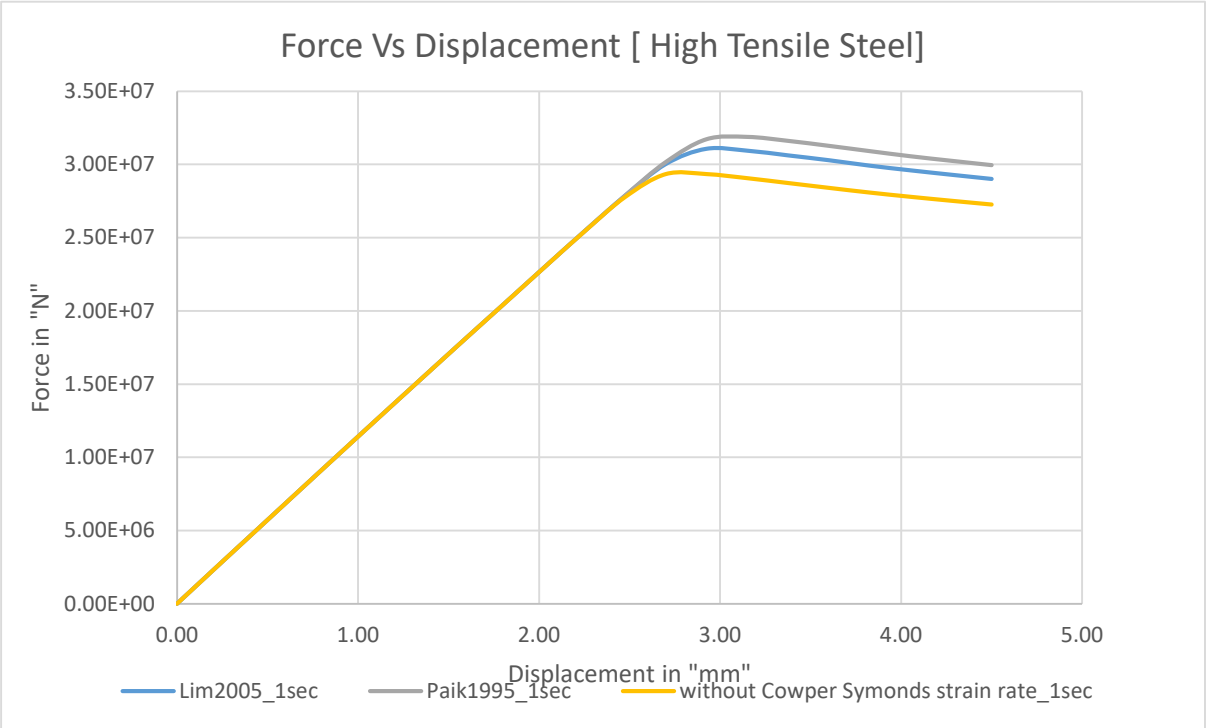


**Figure 61 Collapse Force Curve**

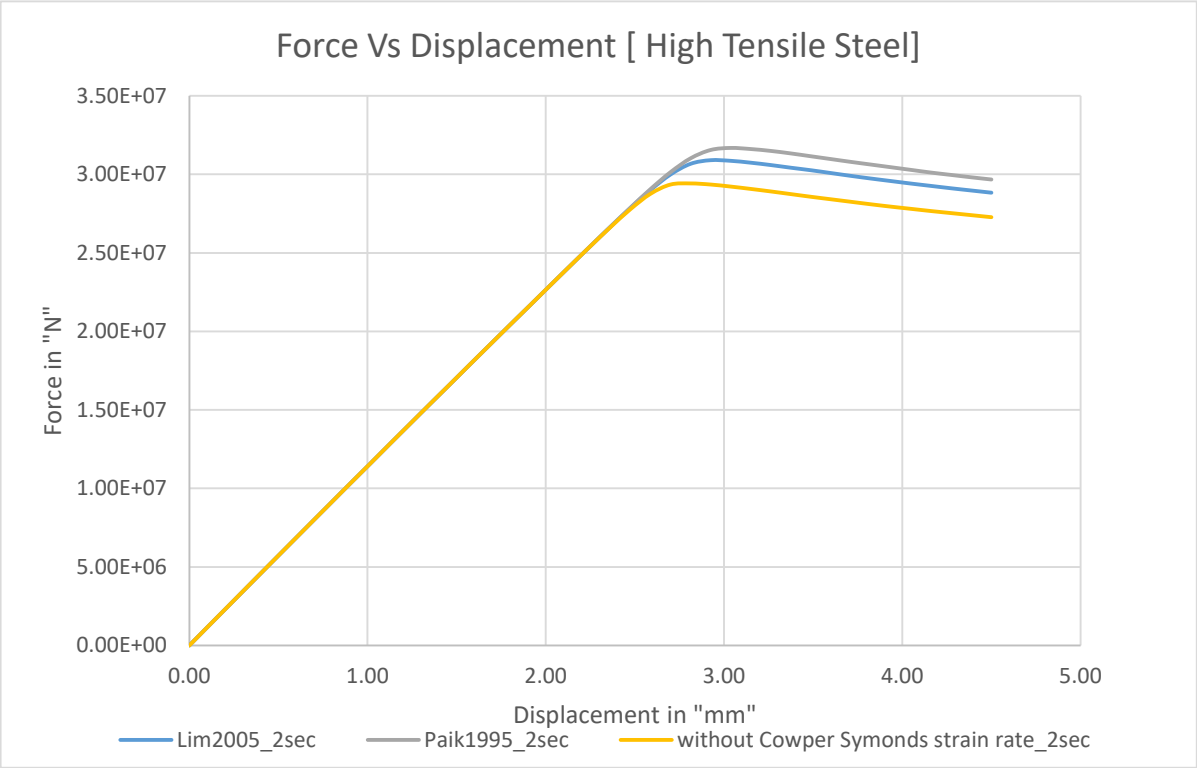


**Figure 62 Collapse Force Curve**

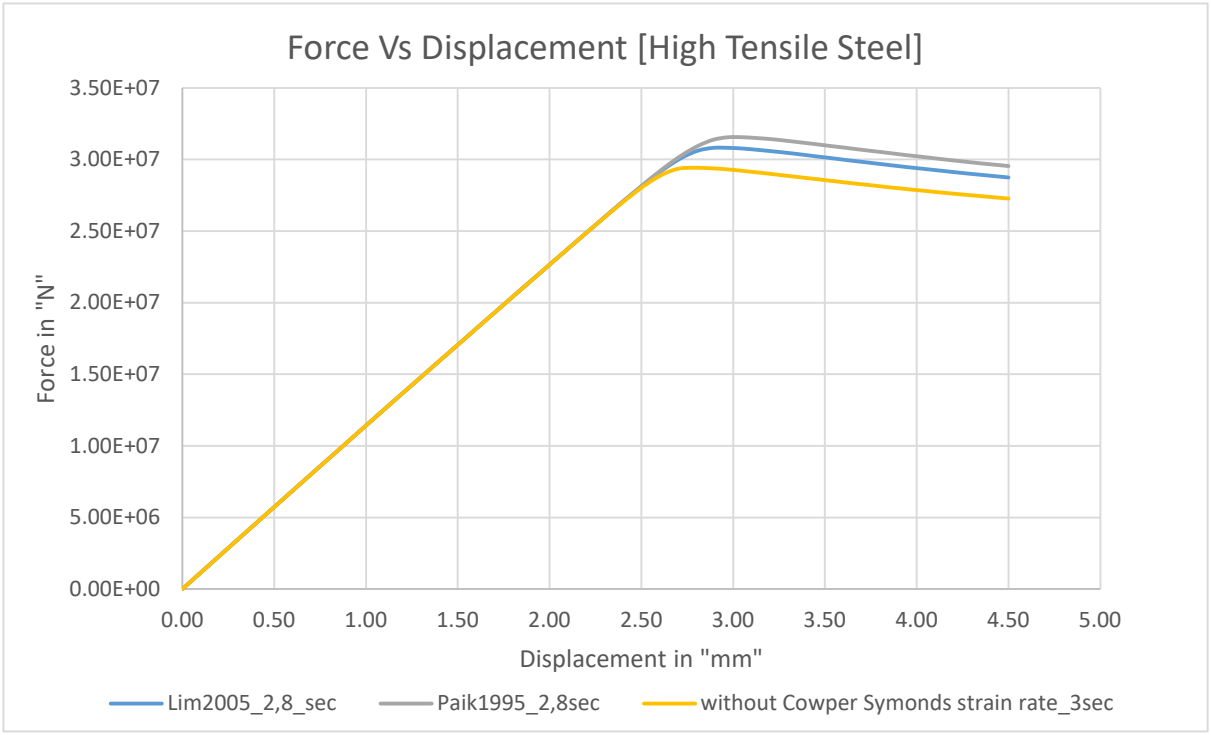


**Figure 63 Collapse Force Curve**

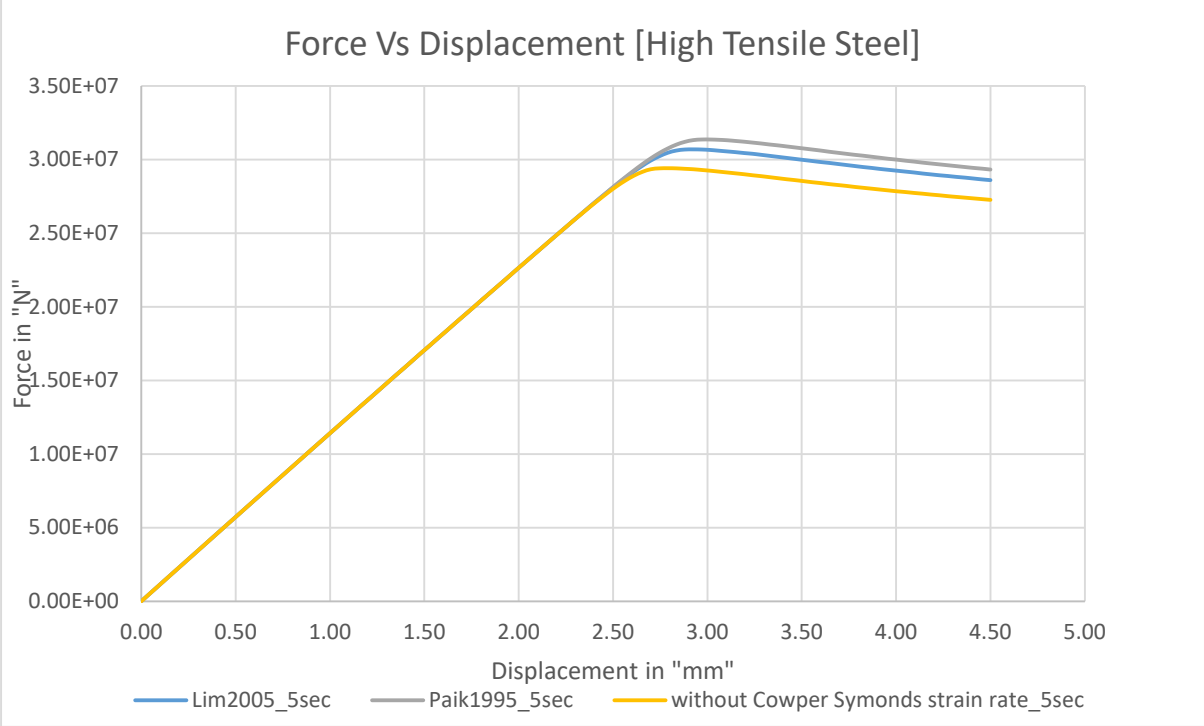


**Figure 64 Collapse Force Curve**

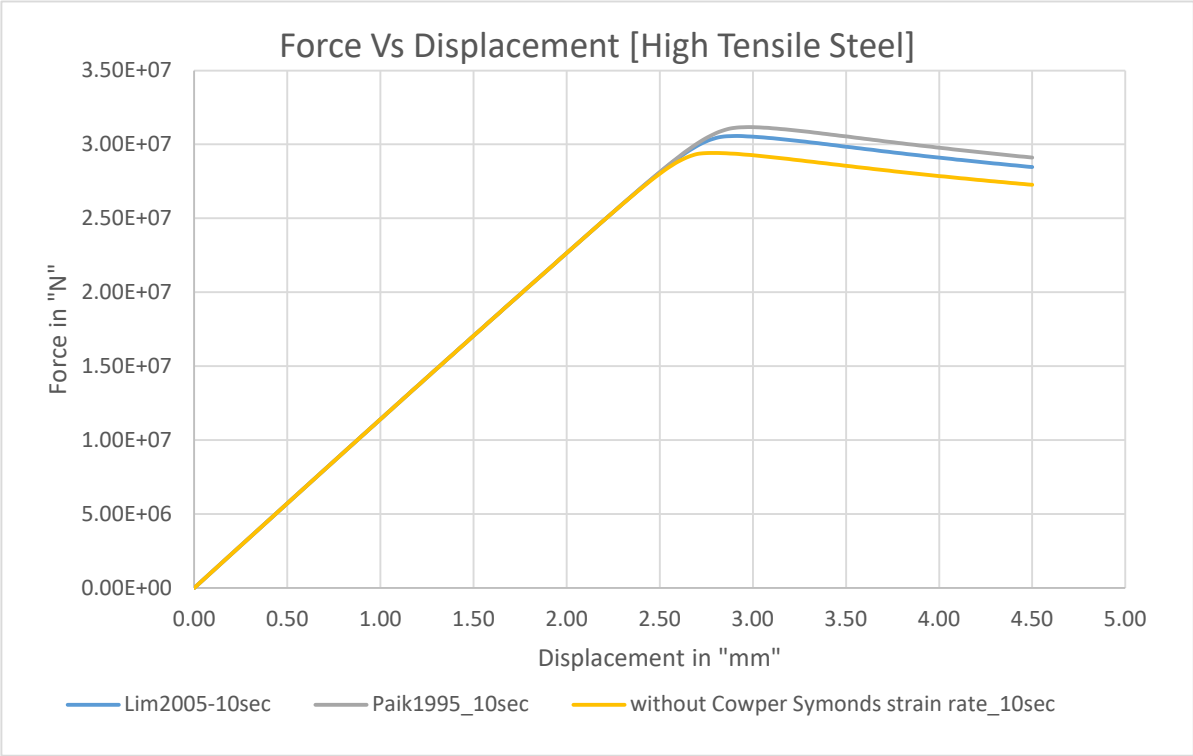


**Figure 65 Collapse Force Curve**

**For Double Bottom Model,**

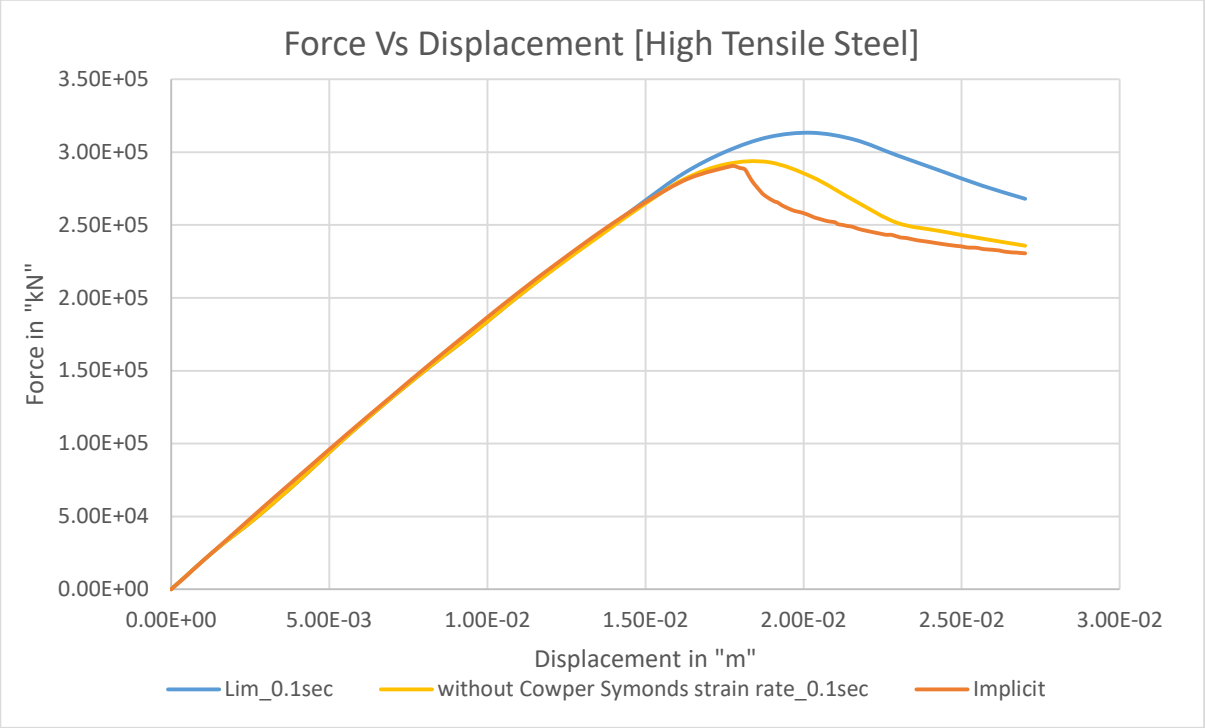


**Figure 66 Collapse Force Curve**

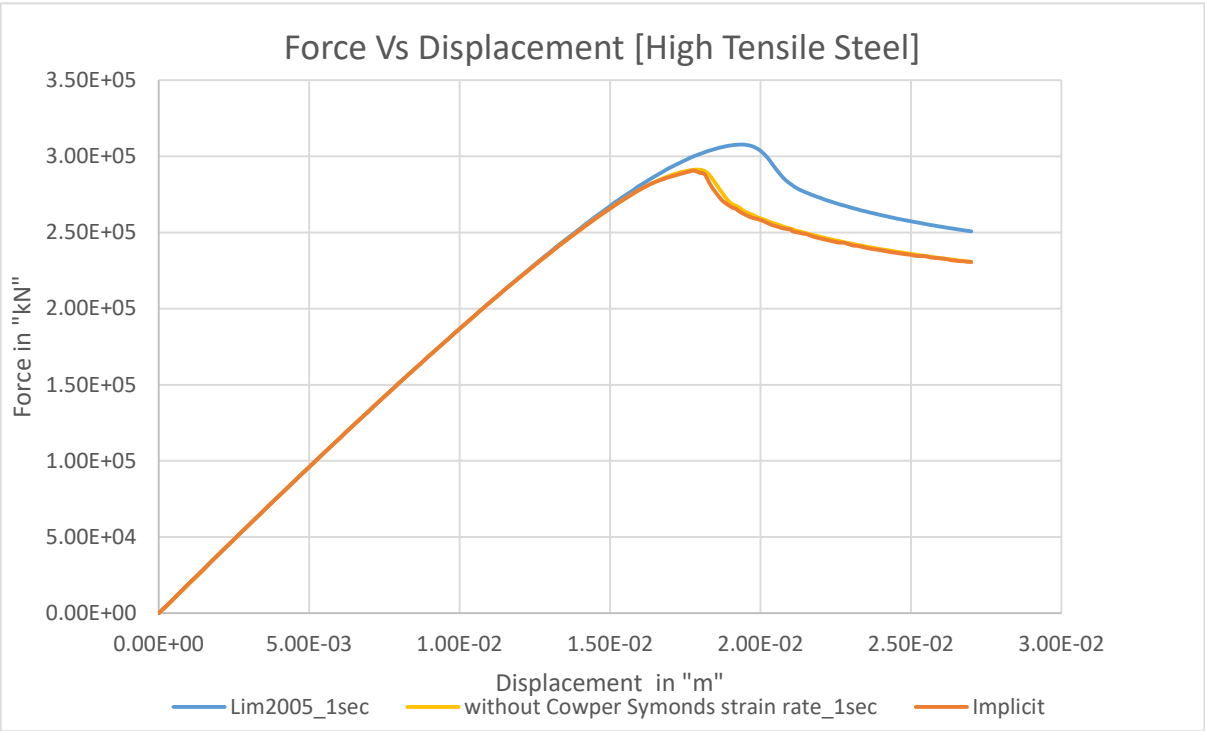


**Figure 67 Collapse Force Curve**

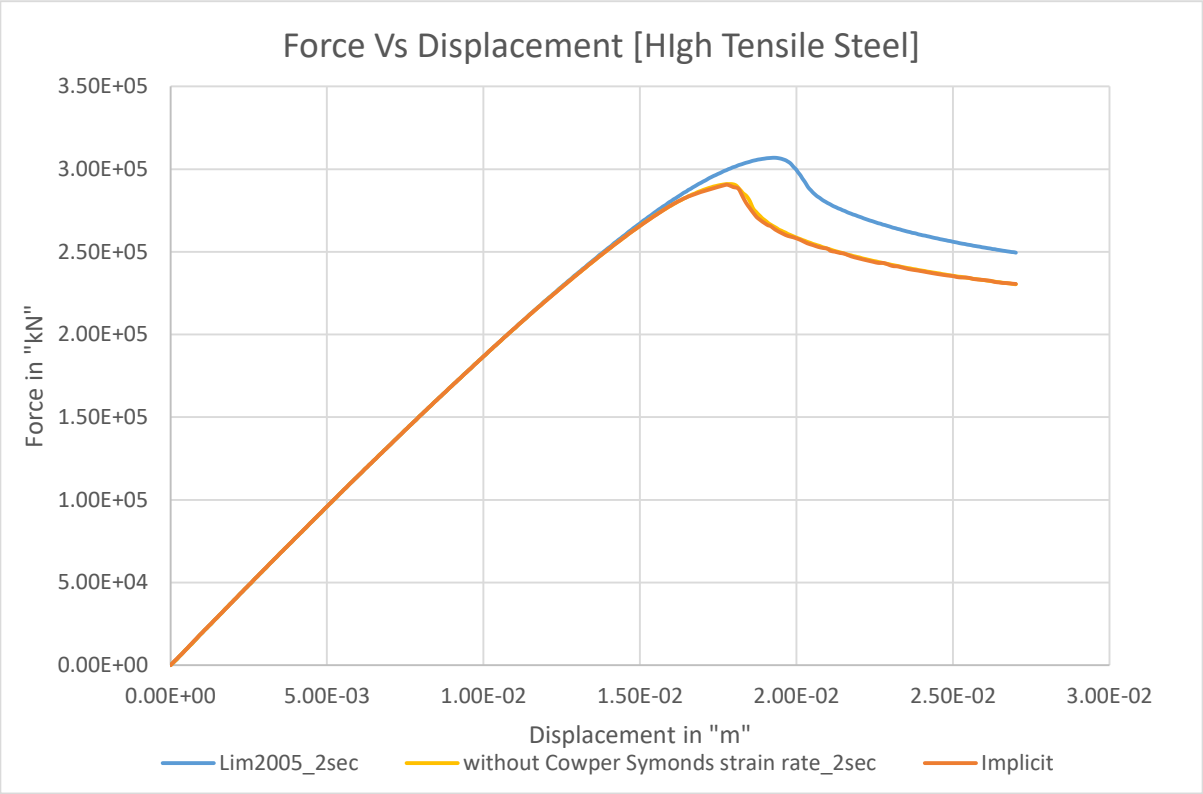


**Figure 68 Collapse Force Curve**

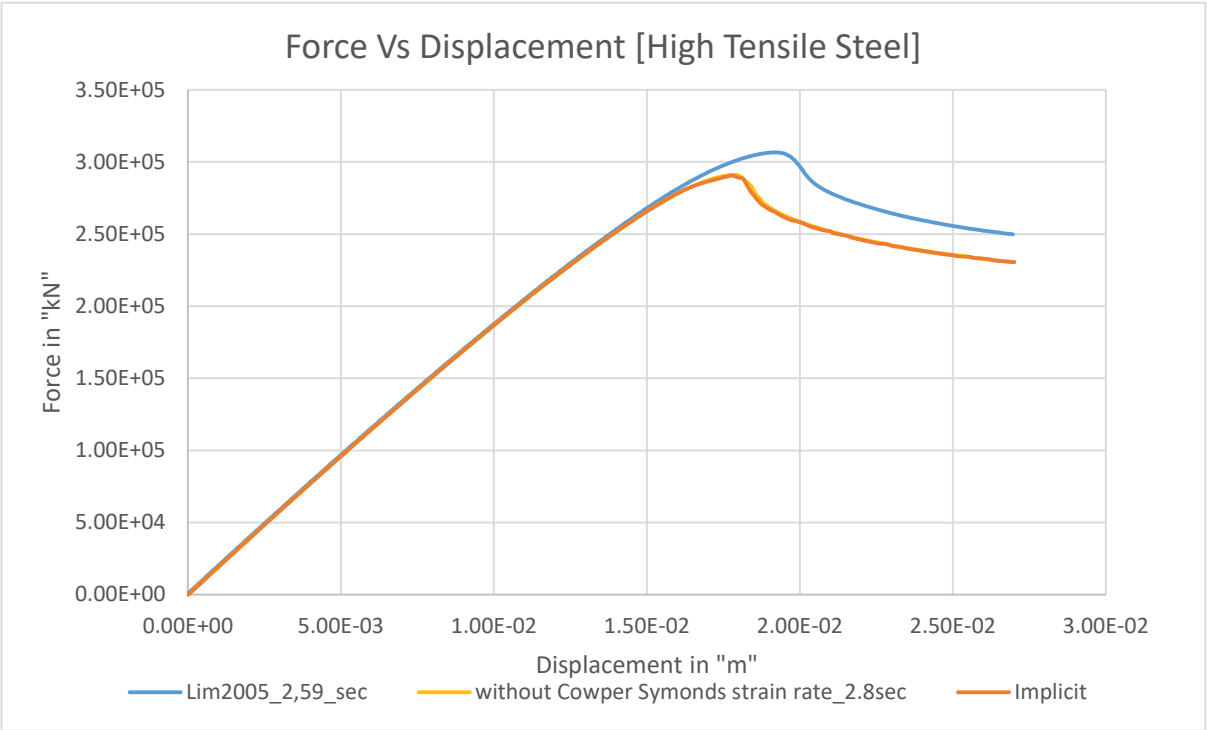


**Figure 69 Collapse Force Curve**

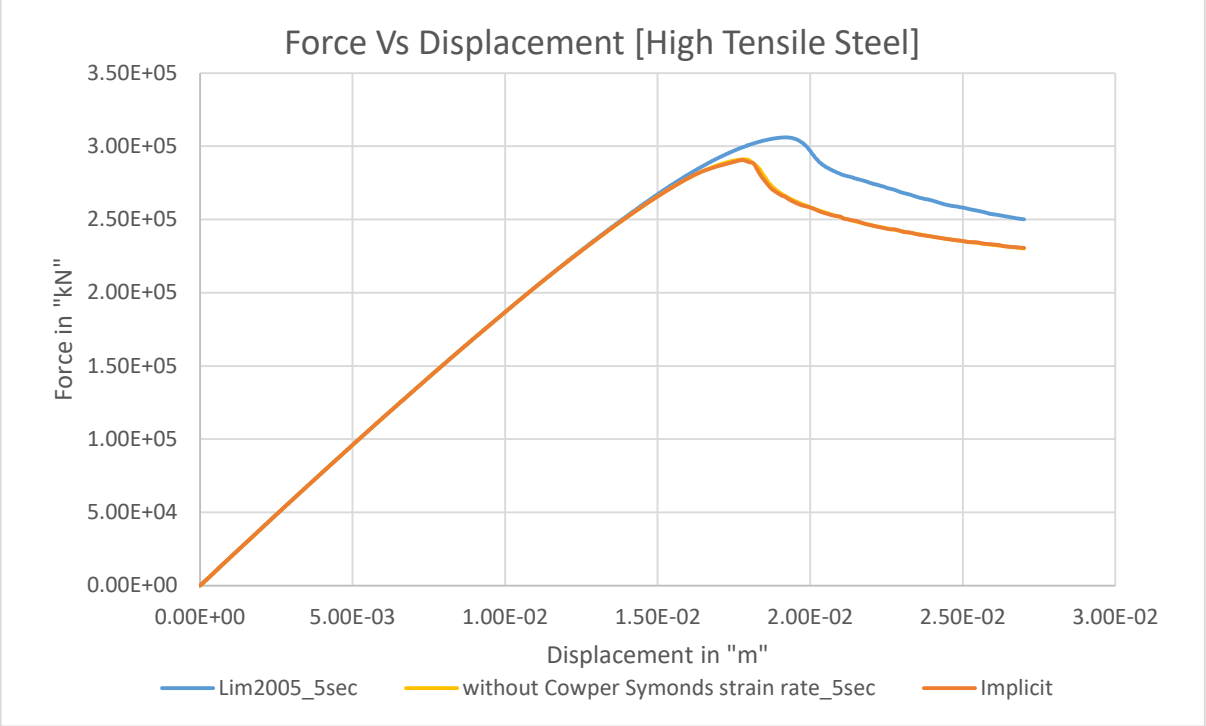


**Figure 70 Collapse Force Curve**

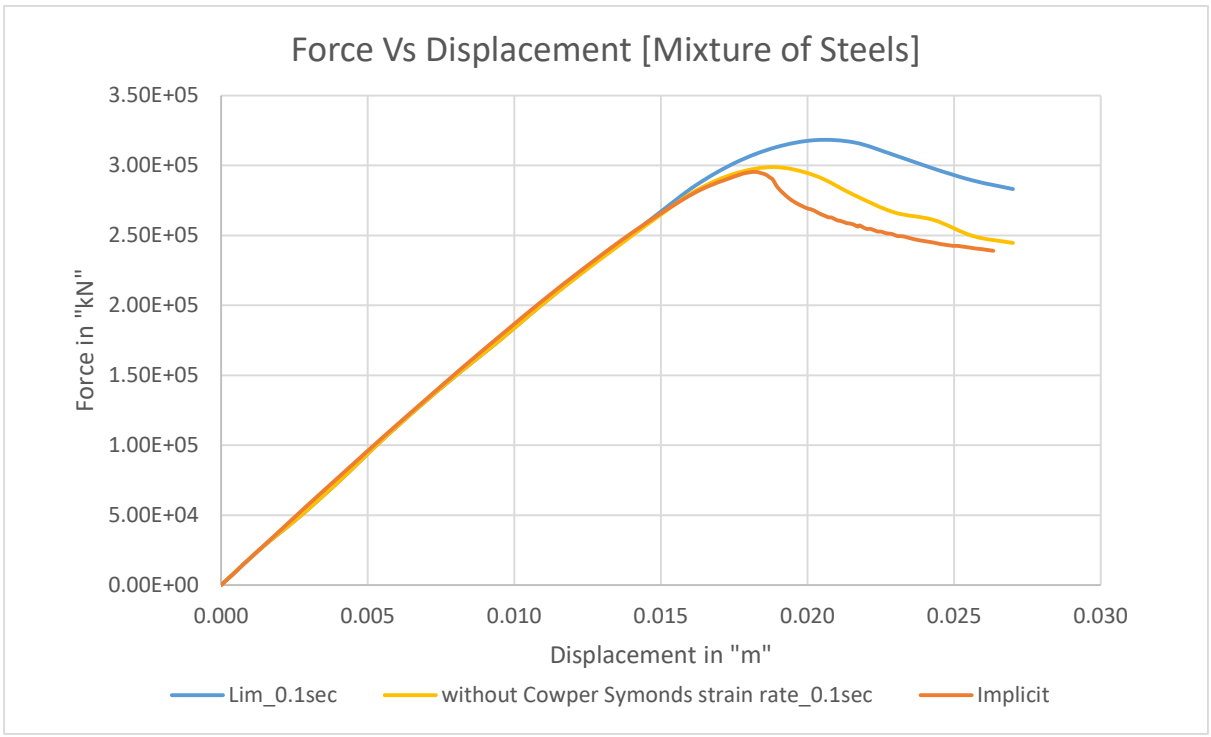


**Figure 71 Collapse Force Curve**

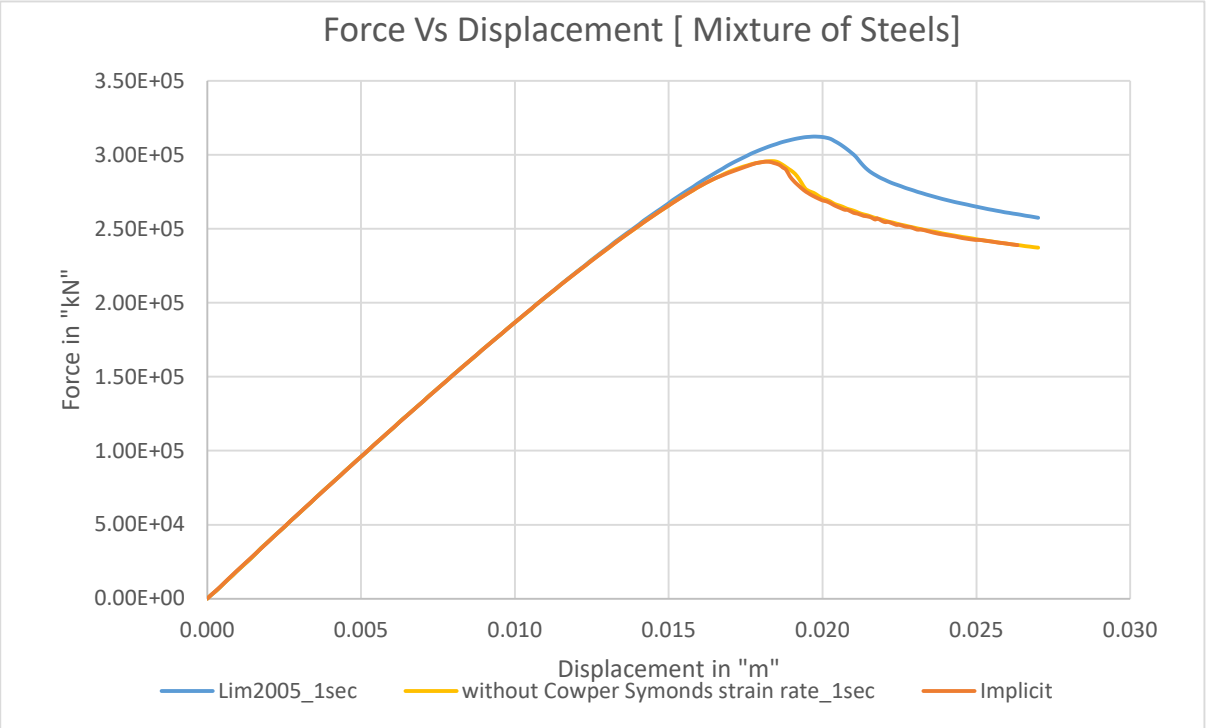


**Figure 72 Collapse Force Curve**

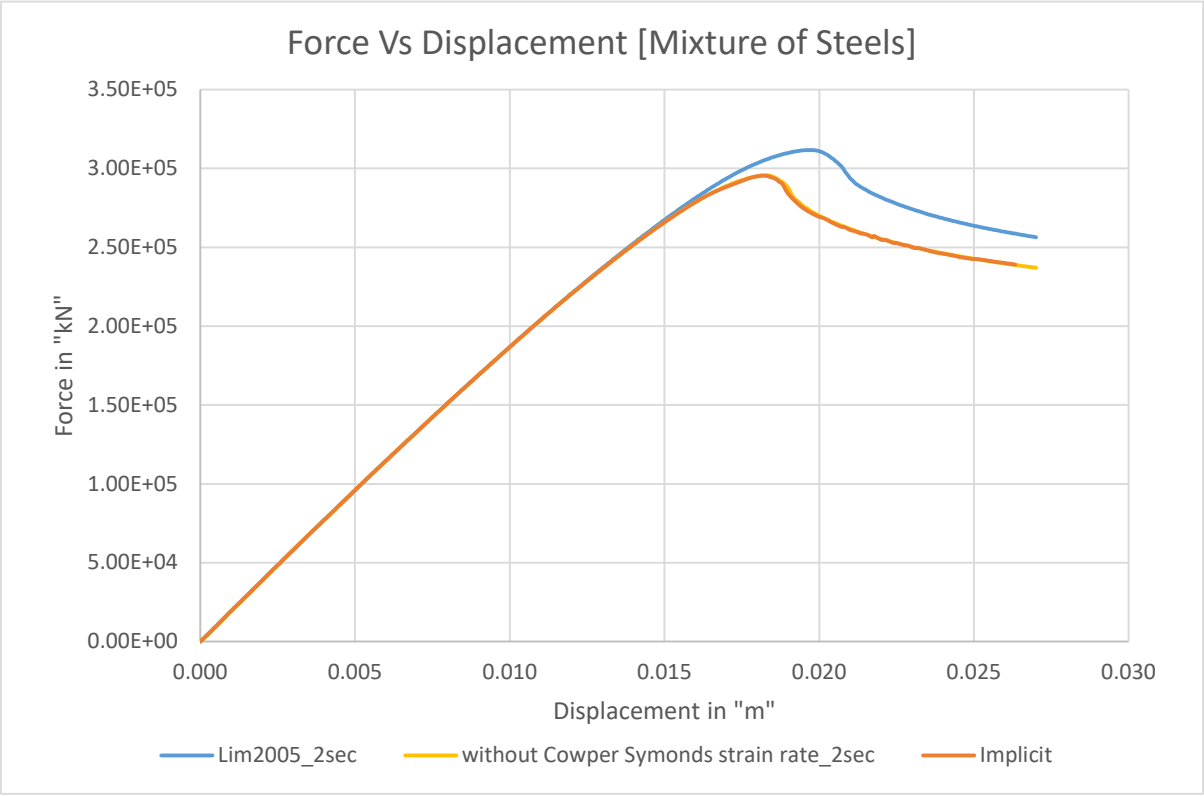


**Figure 73 Collapse Force Curve**

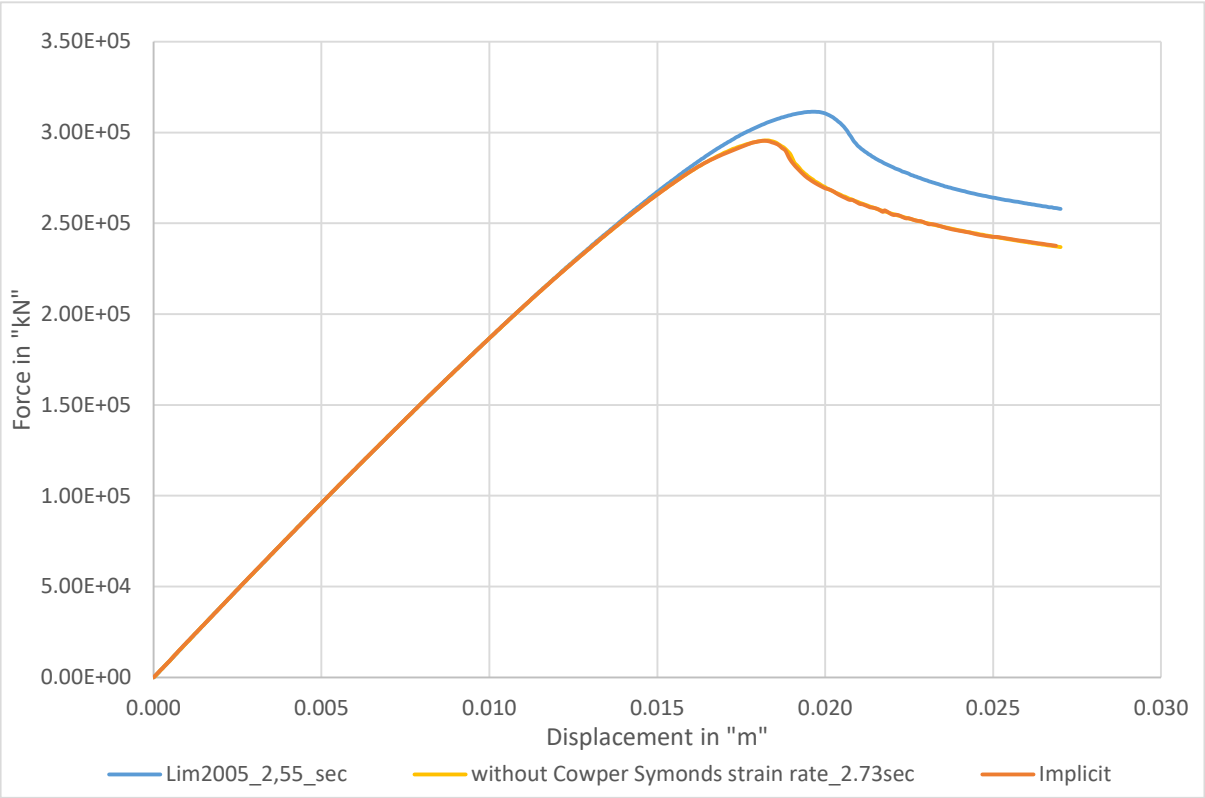


**Figure 74 Collapse Force Curve**

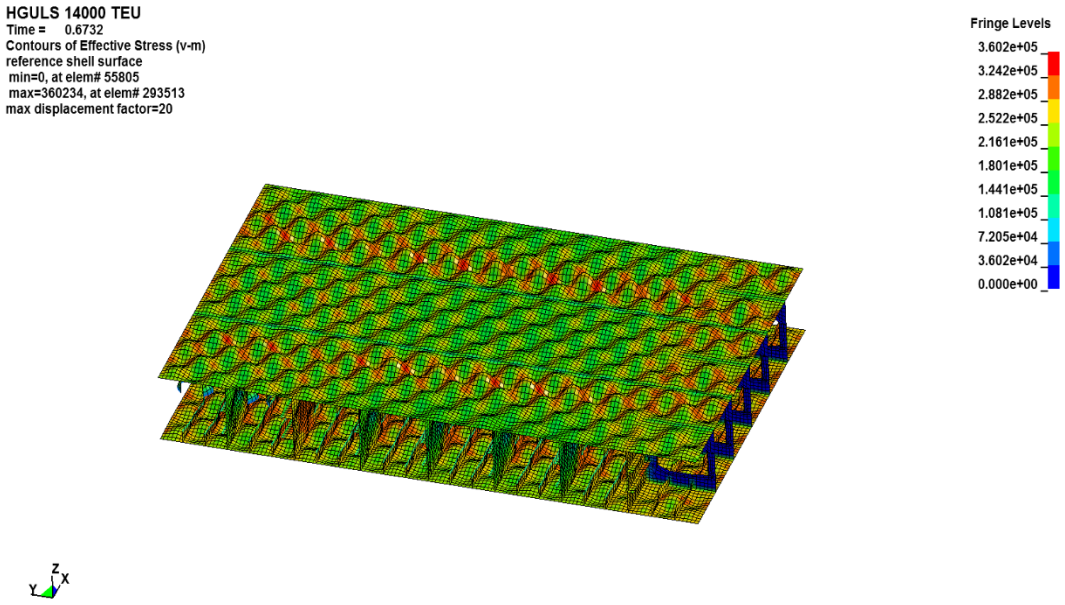


**Figure 75 Distribution of Von-mises Stress of Double Bottom Model (Displacement Scale factor=20)**

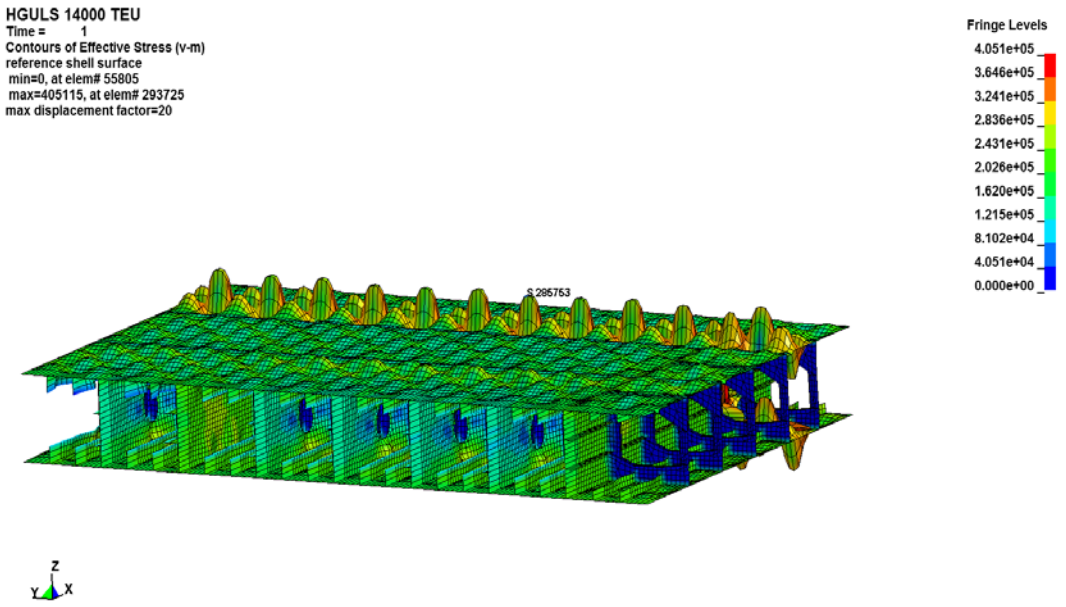


**Figure 76 Distribution of Von-mises Stress of Double Bottom Model (Displacement Scale factor=20)**

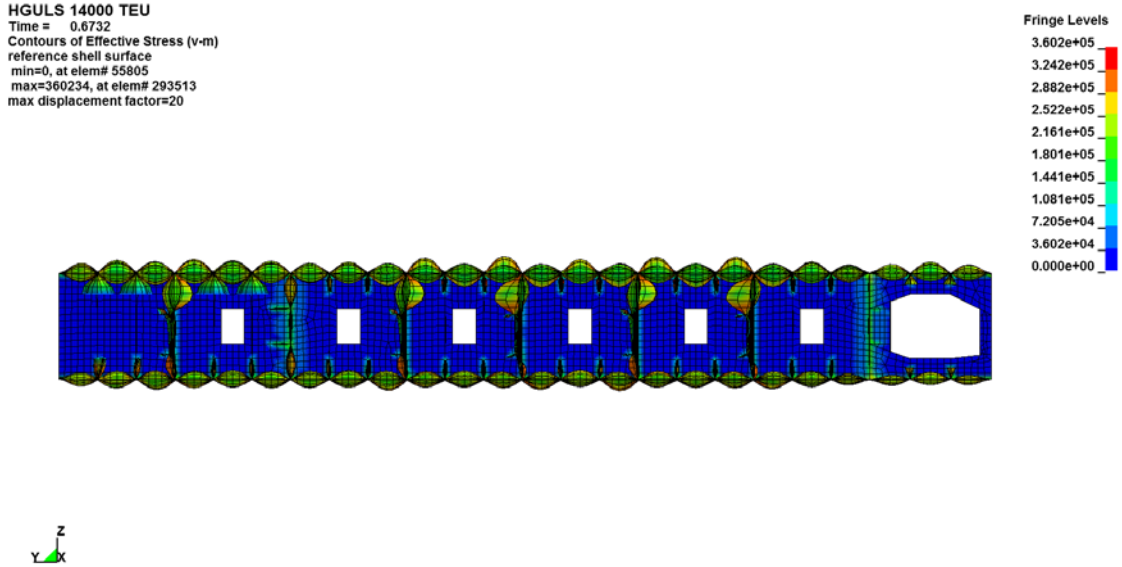


**Figure 77 Distribution of Von-mises Stress of Double Bottom Model (Front View: Displacement Scale factor=20)**